CHARACTERIZATION AND THERAPEUTIC EXPLOITATION OF THE VASCULAR PERMEABILITY INDUCED BY PHOTODYNAMIC THERAPY

THÈSE N^{O} 3887 (2007)

PRÉSENTÉE LE 28 SEPTEMBRE 2007

À LA FACULTÉ DE L'ENVIRONNEMENT NATUREL, ARCHITECTURAL ET CONSTRUIT
Laboratoire de pollution atmosphérique et du sol
SECTION DES SCIENCES ET INGÉNIERIE DE L'ENVIRONNEMENT

ÉCOLE POLYTECHNIQUE FÉDÉRALE DE LAUSANNE

POUR L'OBTENTION DU GRADE DE DOCTEUR ÈS SCIENCES

PAR

Elodie DEBEFVE

Licenciée en Sciences Biomédicales, Université de Liège, Belgique
et de nationalité belge

acceptée sur proposition du jury:

Prof. A. Barry, président du jury
Prof. H. van den Bergh , directeur de thèse
Prof. S. Brown, rapporteur
Prof. M. Swartz, rapporteur
Prof. S. Wolf, rapporteur

ÉCOLE POLYTECHNIQUE
FÉDÉRALE DE LAUSANNE

Lausanne, EPFL
2007

To my Grandfather,
Autodidact scientist
who left us in the beginning of this thesis

Abbreviations

List of abbreviations used throughout the text in alphabetic order:

AMD	Age-related macular degeneration
BPD-MA	Benzoporphyrin derivative monoacid ring
b.w.	Body weight
CAM	Chorioallantoic membrane
CCD	Charge-coupled device
CHUV	Centre Hospitalier Universitaire Vaudois
CNV	Chorioneoveascularisation
COX	Cyclo-oxygenase
DLI	Drug-light interval
DMLA	Dégénérescence maculaire liée à l'âge
Doxo-ILP	Isolated lung perfusion based on doxorubicin
EC	Endothelial cell
EDD	Embryo development day
EPFL	Ecole Polytechnique Fédérale de Lausanne
EPR	Enhanced Permeability and Retention effect
FA	Fluorescein angiography
FGF	Fibroblast growth factor
FITC	Fluorescein isothiocyanate dextran
Gp	Glycoprotein
HE	Hematoxylin-eosin
H-Meso-1	Human mesothelioma-1
HpD	Hematoporhyrin derivative
ICAM-1	Intercellular adhesion molecule-1
ICG	Indocyanine green
ILP	Isolated lung perfusion
IntFluo	Integrated fluorescence
ISC	Intersystem crossing
i.v.	Intravenous
IVM	Intravital microscopy
LDL	Low density lipoprotein
LTB4	Leucotriene
MCA	Methylcholanthrene-induced sarcoma
PBS	Phosphate buffered saline
PDT	Photodynamic therapy
PS	Photosensitizer
R101	Sulforhodamine 101
ROI	Region of interest
RPE	Retinal pigmented epithelium
VEGF	Vascular endothelial growth factor
vWF	von Willebrand factor

Abstract

Photodynamic therapy (PDT) can be used to cause vascular collapse and blood flow stasis of the irradiated pathological neovascularisation appearing in several diseases such as age-related macular degeneration (AMD) and cancer.

We hypothesized that this PDT-related interruption of vessel integrity may lead to an increased transvascular passage of drugs that could be used as a drug delivery pathway. Thus, preceding the occlusion of the pathological vasculature, PDT could be used for instance as a local drug delivery pathway to administrate an anti-angiogenic drug in the case of AMD or chemotherapy in the case of cancer, potentially improving combination therapies. In the case of chorioneovessels (CNV) due to AMD, the recurrence of the exudative AMD component of the weeks/months after PDT, due to the re-opening and/or re-growth of neovessels might be avoided by adding an anti-angiogenic factor such as anti-VEGF or anti-inflammatory drug before, during or shortly after PDT. In the case of cancer, the starvation of tumour cells induced by the PDT occlusion of blood vessels feeding the tumour might be combined with a chemotherapeutic agent for the direct kill of the cancer cells themselves. It has been reported that following the light application in PDT, a physiological cascade of responses on the one hand leads to vascular occlusion but may also induce a vascular permeability enhancement. The aim of this thesis is to find conditions where this increase in leakage due to PDT can be observed, to characterize it and to take advantage of this phenomenon to develop the basis of a novel combination therapy approach.

Hence in this thesis, pre-clinical experiments were performed in the vasculature of the chorioallantoic membrane model (CAM) of the chicken embryo and in the dorsal skinfold optical chamber of nude mice observed by intravital microscopy (IVM).

In the CAM, no PDT-induced leakage of a fluorescent dye (FITC-dextran) was observed unless an anti-aggregating factor, such as aspirin was added. In the chicken embryo model, delaying the blood clot appears to be an essential process to allow effective potential drug delivery.

In the dorsal skinfold of the nude mouse, the inflammatory response after PDT was observed and quantified. This revealed that PDT induces a time dependent acute inflammatory response as shown by increased number of leukocytes “rolling” along the vessel wall after treatment. This was observed over a 2 hour period following PDT. The quantification of the microvascular leakage showed a continuous FITC-dextran leakage from the vasculature treated by PDT to the interstitial space. This local leakage was clearly increased by the inflammatory status of the tissue (observed by quantifying the rolling leukocytes and by histology). This concept has the potential to improve the drug delivery of anti-angiogenic drugs in the eyes of patients treated for AMD and could also be applied to improve the uptake of cytostatic drugs in tumours.

Keywords: drug delivery, photodynamic therapy (PDT), Visudyne®, fluorescein isothiocyanate dextran (FITC-dextran), animal model, chorioallantoic membrane (CAM), dorsal skinfold chamber, intravital microscopy (IVM), vascular permeability, endothelial cells, age-related macular degeneration (AMD), cancer.

Résumé

La thérapie photodynamique (PDT) peut être utilisée pour induire un collapsus vasculaire et une stase du flux sanguin de la néovascularisation pathologique irradiée apparaissant dans certaines maladies comme la dégénérescence maculaire liée à l'âge (DMLA) et le cancer.
Nous émettons l'hypothèse selon laquelle l'interruption de l'intégrité vasculaire produite par PDT peut entraîner une augmentation du passage transvasculaire de drogues, phénomène qui pourrait être utilisé par exemple comme voie d'acheminement de la drogue. De cette façon, précédant l'occlusion des vaisseaux pathologiques, la PDT pourrait être utilisée comme un moyen d'acheminer localement la drogue et d'administrer un facteur anti-angiogénique dans le cas de la DMLA ou une chimiothérapie dans le cas du cancer, potentiellement améliorant les thérapies combinées. Dans le cas de chorio-néovascularisation (CNV) due à la DMLA, la récurrence de la forme exsudative de la DMLA dans les mois/semaines suivant la PDT, due à la réouverture des néovaisseaux et/ou la croissance de nouveaux néovaisseaux pourraient être évitées en ajoutant avant, pendant ou peu après la PDT une drogue anti-angiogénique telle que les facteurs anti-VEGF ou les drogues anti-inflammatoires. Dans le cas du cancer, la privation en nutriments des cellules tumorales, induite par l'occlusion par PDT des vaisseaux sanguins approvisionnant la tumeur pourrait être combinée avec un agent chimiothérapeutique tuant directement les cellules tumorales. Il a été reporté que suivant l'application de la lumière dans la PDT, une cascade de réponses physiologiques entraîne d'une part une occlusion vasculaire mais peut aussi induire une augmentation de la perméabilité vasculaire. Le but de cette thèse est de trouver des conditions dans lesquelles cette augmentation de perméabilité due à la PDT peut être observée, de la caractériser pour tirer profit de ce phénomène pour développer les bases d'une nouvelle approche de thérapie combinée.
Ainsi, dans cette thèse, des expériences pré-cliniques ont été effectuées dans la vascularisation du modèle de la membrane chorio-allantoïque (CAM) de l'embryon de poulet et dans la chambre optique du pli de peau dorsal de la souris nue observée par microscopie intravitale (IVM). Dans le CAM, aucune fuite vasculaire induite par PDT n'a pu être observée, à moins qu'un agent anti-agrégeant, tel que l'aspirine, ne soit ajouté. Dans le modèle d'embryon de poulet, retarder la formation du thrombus hémostatique se révèle être un processus essentiel pour permettre un acheminement de drogue efficace.
Dans le modèle du pli de peau de la souris nue, la réponse inflammatoire après PDT a été observée et quantifiée. Ceci a révélé que la PDT induit une réponse inflammatoire aiguë dépendante du temps, tel que montré par l'augmentation du nombre de leucocytes « roulant » le long de la paroi vasculaire après le traitement. Ceci a été observé pendant une période de 2h suivant la PDT. La quantification de la fuite microvasculaire a montré une fuite continue du FITC-dextran depuis les vaisseaux traités par PDT vers l'espace interstitiel. Cette fuite locale était clairement augmentée par le statut inflammatoire du tissu (observé par quantification des leucocytes roulant et par histologie). Ce concept a le potentiel d'améliorer l'acheminement de drogues anti-angiogéniques dans les yeux des patients traités pour la DMLA et pourrait aussi être appliqué pour améliorer la prise en charge de drogues cytostatiques par les tumeurs.

Mot-clés: acheminement de drogue, thérapie photodynamique (PDT), Visudyne®, fluorescein isothiocyanate dextran (FITC-dextran), modèle animal, membrane chorio-allantïque (CAM), pli de peau dorsale, microscopie intravitale (IVM), perméabilité vasculaire, cellules endothéliales, dégénérescence maculaire liée à l'âge (DMLA), cancer.

Table of Content

Chapitre 1
Introduction

Introduction

Photodynamic therapy

Once upon a time PDT…

Light has been employed in the treatment of diseases since antiquity. Ancient Egyptian, Indian and Chinese cultures (3000 BC- 1500 BC) used the therapeutic effect of the sun to treat a variety of diseases including, vitiligo, psoriasis, cancer and even psychosis [1]. The ancient Greeks employed whole-body sun exposure or heliotherapy in the treatment of disease, and even in the last century, lying nude in the sun was a popular pastime (Figure 1).

Figure 1: Children take sun at a sanatorium in the Swiss Alps, the region in which heliotherapy originated [2].

Around 500 BC, the famous Greek physician, Herodotus, who was regarded as the father of heliotherapy, emphasized the importance of sun exposure for the restoration of health [1]. However, only relatively recently the therapeutic effect of sunlight has been used to any significant degree in medicine and surgery. Phototherapy was further developed by the Danish physician Niels Finsen, who was awarded a Nobel Prize in 1903 for his work on bactericidal

effect of phototherapy having successfully treated smallpox using red light (in 1893) and lupus vulgaris (in 1895), a cutaneous tuberculosis, with ultraviolet light (generated by an arc lamp) [3]. Phototherapy describes the use of light in the treatment of disease; photochemotherapy, on the other hand, involves a combination of the administration of a photosensitising agent followed by the action of light on tissues in which the agent is localised [4]. The concept of cell death being induced by the interaction of light and chemicals has been recognized for 100 years. This was first reported by Oscar Raab, a medical student working for von Tappeiner in Munich. Famously he described the lethal effect of combining acridine red and light on Infusoria, species of paramecium responsible for a type of malaria [5]. This was an inadvertent discovery as the experiment was conducted during a thunderstorm, when the ambient lighting went out. In a series of successive experiments he established that this lethal effect on the paramecium occurred to a greater extent than with acridine alone, light alone or acridine exposed to light and then added to the paramecium. Raab had, therefore, discovered the optical property of fluorescence and concluded that it was not the light but rather some product of the fluorescence that induced *in vitro* toxicity. He postulated that this effect was caused by the transfer of energy from light to the chemical, similar to that seen in plants after the absorption of light by chlorophyll. Shortly afterwards, it was Raab's thesis director, von Tappeiner, in 1907 who coined the expression "photodynamic" therapy (PDT) (more or less mistakenly, because of the fluorescence of these substances), and who together with A. Jodlbauer reported the dependence of the photodynamic process on molecular oxygen (O_2). Von Tappeiner also concluded with a prediction of the potential future application of fluorescent substances in medicine [6-8].

At the same time as Raab's discovery, Prime, a French neurologist, reported photosensitive reactions in sun-exposed areas, in a patient who had been given parenteral eosin for the treatment of epilepsy [9]. In 1908, Haussmann took photochemotherapy in a new direction,

with his experiments of PDT with the blood derivative hematoporphyrin and tetrapyrrole chlorophyll on cell cultures and mice [10]. The first report of endogenous porphyrin photosensitisation was given in 1913 by Meyer-Betz [11]. After injecting himself 200mg of a hematoporphyrin, Meyer-Betz noted severe pain and swelling of that part of the body exposed to light, showing a massive phototoxic reaction. The pictures of him before and after treatment are shown in figure 2.

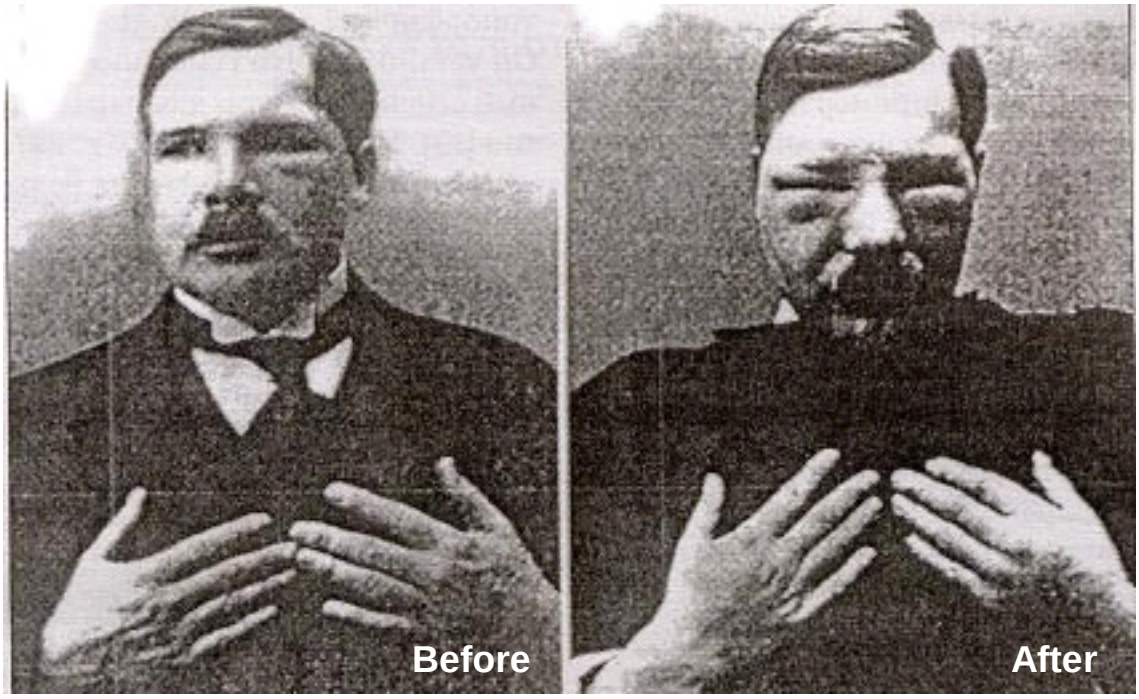

Figure 2 : First report of endogenous porphyrin photosensitisation. In 1913, after injecting himself 200mg of HpD, **Meyer-Betz** noted severe pain and swelling of the part of his body exposed to light, showing a massive phototoxic reaction. This illustration shows the pictures of him before and after treatment.

The first report of fluorescent porphyrin localisation in a malignant tumour appeared in 1924 when a Frenchman from Lyon, Policard, observed the characteristic red fluorescence of hematoporphyrin in an experimental rat sarcoma illuminated with ultraviolet light from a Wood's lamp [12]. Since then, porphyrins and hematoporphyrin derivatives (HpD) have been studied and used for diagnosis. In the 1970's, Diamond [13], Dougherty [14], Kelly and Snell [15, 16] performed the first systematic human trials of PDT after intravenous injection of

HpD, selectively destroying tumours. From these humble origins, photodynamic therapy (PDT) has been increasingly adopted throughout the world over the last few decades and many new photosensitisers and light delivery systems have been developed [17].

Basic principle

Photodynamic Therapy (PDT) is a medical technology that has been developed mainly to treat cancer [18, 19]. It consists in the systemic or topical application of a substance (a dye or a dye precursor), called photosensitiser (PS), that localises more or less selectively in the target tissue at concentrations at which this substance is not toxic.

The principle is based on the capacity of these substances to be excited by the light and to restituate this energy [20, 21]. This light, at an appropriate wavelength depending on the PS to be excited, is applied at a controlled dose (fluence and fluence rate), which by itself is not harmful to the tissue, and which is absorbed by the dye.

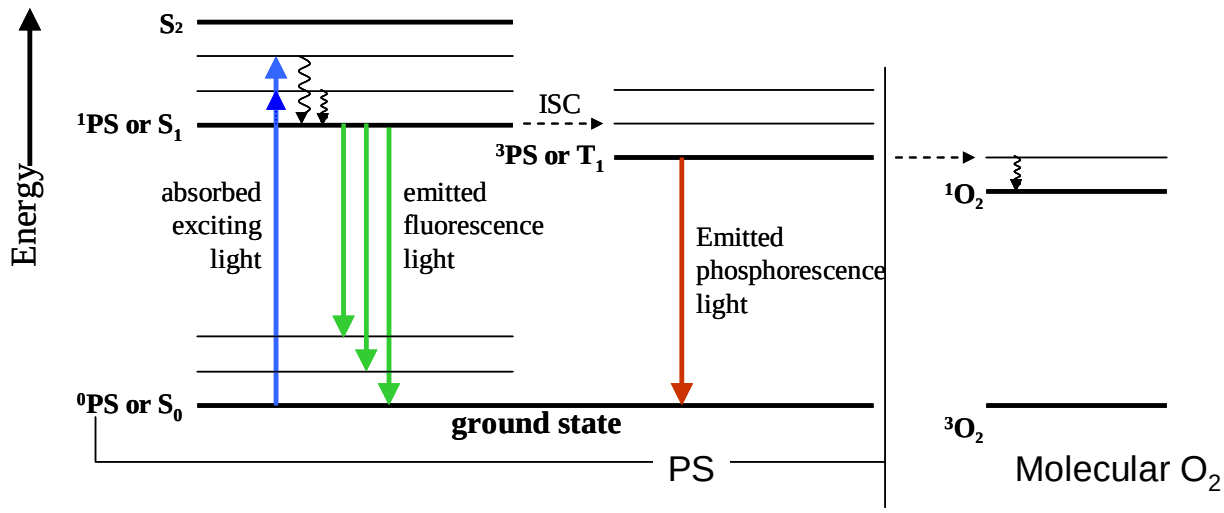

Figure 3: This Jablonski diagram schematically illustrates the pathway to the excited singlet oxygen state $^1O_2$, type II process that requires molecular oxygen in the first step of the photosensitisation.

The light absorbed by the PS brings it to excited singlet state that efficiently (depending on the PS) interconverts to a triplet excited state, by the intersystem (singlet-triplet) crossing process (ISC). In other words, the photosensitisation implies good yield of production of

triplet state (T_1 or ^3PS) of the sensitiser. As shown in more details in Jablonski diagram (Figure 3), ^3PS is formed from ^0PS after photo-absorption and ISC. The surrounding molecules, giving rise to two chemical mechanisms of photosensitisation, are called Type I and Type II reactions. In the Type I reactions, the ^3PS undergoes in a first step either electron transfer reactions with a substrate molecule (M) or hydrogen atom transfer giving rise to radical species which have one impaired electron, and are generally more reactive than molecules. If enough molecular oxygen (O_2) is present, it can lead in a second step to among others highly reactive peroxydes (H_2O_2), superoxyde radical anions (O_2^-) and hydroxyl radical (OH^-). The reactive intermediates then rapidly react with a multitude of surrounding biomolecules, potentially leading to tissue destruction. Type II reactions require ground state triplet state of molecular oxygen ($^3O_2$) in the tissue to interact in a first step reaction with the metastable excited triplet state of the PS. This leads to the formation of excited singlet oxygen ($^1O_2$) that can then either react with the PS itself (photobleaching) or with a biomolecular target located close to the PS. $^1O_2$ rapidly reacts or is quenched so that reactions take place at distances of only a few tens of nanometers from the PS, so that PS localisation determines essentially where PDT damage takes place [20-23]. The exact relative importance of Type I and Type II mechanisms is however not known. Whatever the nature of the intermediate (singlet oxygen or other reactive intermediate), biological damage caused by oxidation may be sufficient to kill cells. There are hundreds of natural and synthetic dyes that can function as PS for PDT, ranging from plant abstracts to complex synthetic macrocycles.

Photodynamic therapy can have three more-or-less distinct effects on the human body: (1) it can kill tumour cells by damaging plasma membrane, mitochondria, lysosomes and/or other organelles without in general significantly damaging the nucleus; (2) it can damage the vascular endothelium causing thrombosis and stasis; (3) it can modulate the immune system. Tissue localisation of PDT-induced damage is influenced by both the choice of sensitiser, the

choice of its formulation and/or vehicle used, and the experimental conditions. For instance, shortly after intravenous injection, Visudyne®, a benzoporphyrin derivative is localised mainly in the vasculature. Accordingly, in this case, destruction of the vasculature is the main result of Visudyne®-PDT in which light is applied shortly after injection.

Vascular effects of Photodynamic Therapy

The vascular effect induced by PDT was found quite early on in solid tumours. Vascular damage and blood flow stasis have become well-established phenomena in the PDT of cancer with many different PS [24-28]. Most of the PDT sensitisers show vascular damage during or shortly after light exposure of the tissue containing the PS, in particular if high enough serum levels of the PS are attained and if a high enough light dose is applied. The vascular PDT effects schematically presented in figure 4 are probably initiated to a large extent by damage to the endothelial cells, involving some of the usual PDT cellular targets (e.g., the plasma membrane, lysosomes, mitochondria or cytoskeleton) depending on the PS, its formulation and applied conditions [29]. Photodynamic therapy causes perturbation of the cytoskeleton [30-33] that can lead to alteration of cell shape. Both endothelial cell rounding [24, 34, 35] and contraction have been observed, as was the case in PDT-induced apoptosis. The change in shape of endothelial cells leads to the disruption of tight junctions between the endothelial cells and a decrease in inter-endothelial cell communication, and causes exposure of the sub-endothelial basement membrane proteins. These photodynamic damages to endothelial cells results in the release of von Willebrand factor and other blood clotting agents [36]. The released clotting factors such as thromboxane activate circulating platelets, among others [37]. Damaged endothelium results in calcium level modulation as well, which in turn can modulate the smooth muscle cell calcium balance, with vessel contraction as possible consequence [36, 38].

Some of the circulating platelets may also have been damaged themselves directly by PDT [34, 39, 40], although this probably does not play a major role in the blood clotting mechanism. The activated platelets now stick to the gaps between the damaged rounded endothelial cells, and further aggregation of platelets takes place at these sites [32, 33], thus starting to plug the vessel. Polymorphonuclear leukocytes start to adhere to the damaged vessel wall, and are probably also involved in increasing vascular permeability via their action on endothelial cells. In addition, increased vascular permeability may be expected following the release of histamine, which is vasodilator. The consequence of this scenario are vascular leakage and oedema [41-43]. Another part of the mechanism is associated with the PDT-induced damage to membrane lipids. This can cause the release of arachidonic acid that can react with cyclooxygenase in a cascade of processes, thus inducing the release of prostaglandin endoperoxydes and, in the end, producing the vasoconstrictor thromboxane, which acts on the surrounding smooth muscle cells. Consequently, the PDT-induced modulation of compounds among which eicosanoids, cytokines, clotting factors and histamine, causes an increase of aggregating and vasodilating compounds, thus destroying the normally existing balance between dilating and constricting agents and aggregating and disaggregating compounds among others [44].

The results of this are twofold: (a) a temporary increase in vessel permeability and leakage; followed by (b) vessel constriction and blood clotting with the consequent blood flow stasis. Smaller vessels can be closed by PDT more easily than larger vessels [45]. A final aspect that may play a role in the PDT of blood vessels is that the increased pressure in the perivascular region caused by PDT-induced leakage may also help to induce vasoconstriction.

The following summarizes the preceding discussion in the form of simplified mechanism for blood flow stasis induced by PDT [22, 46].

1. The injected photosensitiser arrives at the endothelial cells in which it is partially internalized.
2. Light application causes PDT-mediated damage to the endothelial cells.
3. Cytoskeletal changes and endothelial cell rounding are observed, which cause widening of junctions between endothelial cells. This leads to exposure of the vascular basement membrane, and/or the perivasculature.
4. Platelets are activated and start to aggregate at damaged site. This and other PDT-induced damage causes the release of eicosanoids that induce: (a) increased vascular permeability and leakage; and (b) clotting (thromboxane).
5. In parallel process, polymorphonuclear leukocytes start to adhere to the PDT-damaged surface, also helping platelet activation and inducing vascular permeability.

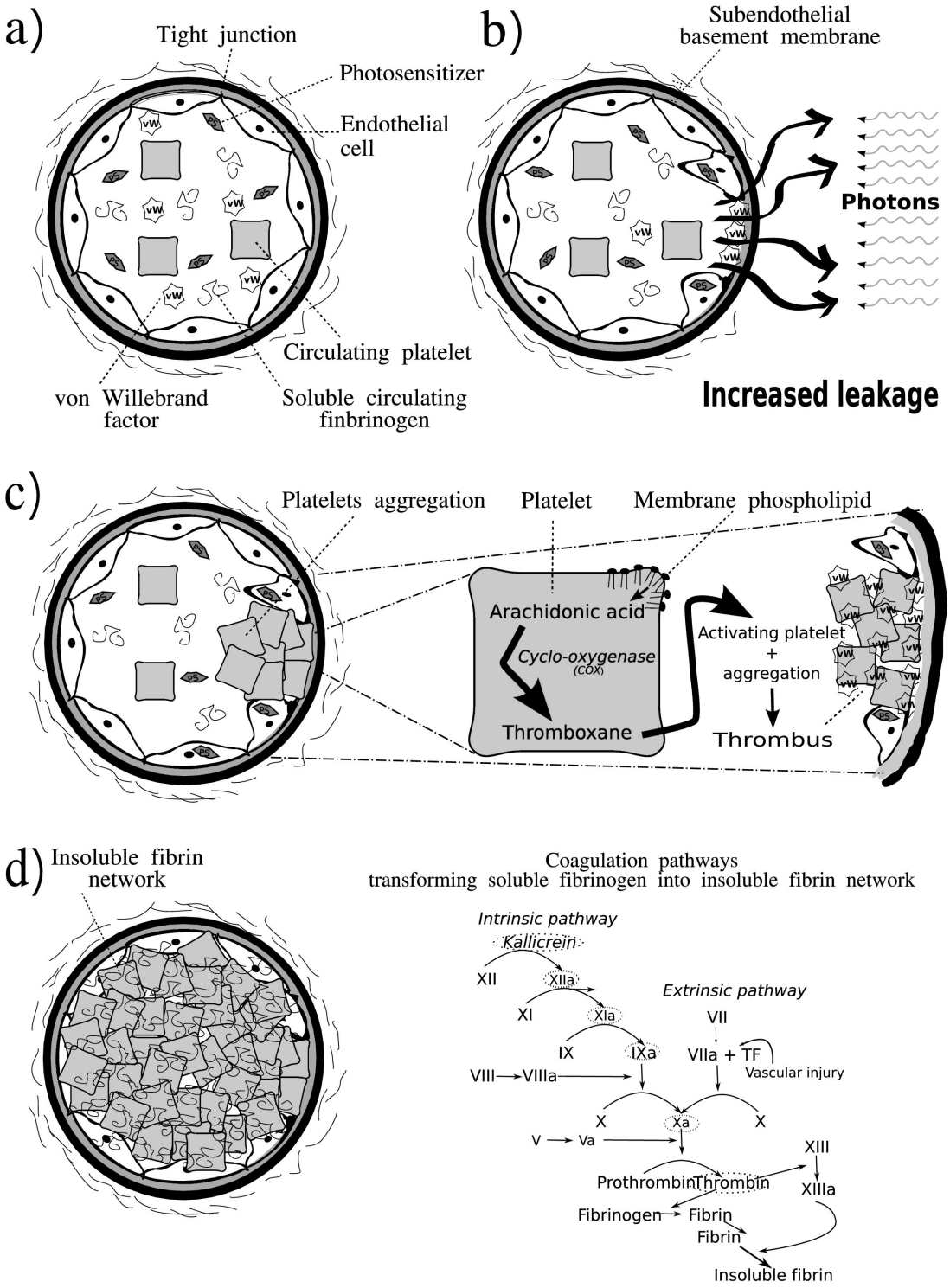

Figure 4 : Vascular effects of photodynamic therapy

Age-related Macular Degeneration and its Treatments

Age-related macular degeneration (AMD) is the major cause of vision loss in people over the age of 55 in industrialised countries. This disease takes its origin in a lack of oxygen and nutrients coming from the choroidal vasculature in the back of the eye, behind the retinal pigmented epithelium (RPE), to the photoreceptors, mostly cones, in the fovea, the central part of the retina. This lack, built up over years of inefficient elimination of debris coming from the high turn over of the photoreceptors outer segments. The evolution of the disease lets appear first “yellowish” fatty deposits (drusen), followed by signals to enhance oxygen and nutrients income by developing new vessels outside the blood brain barrier: choroidal neovessels (CNV). These CNV are normal leaky fenestrated vessels.

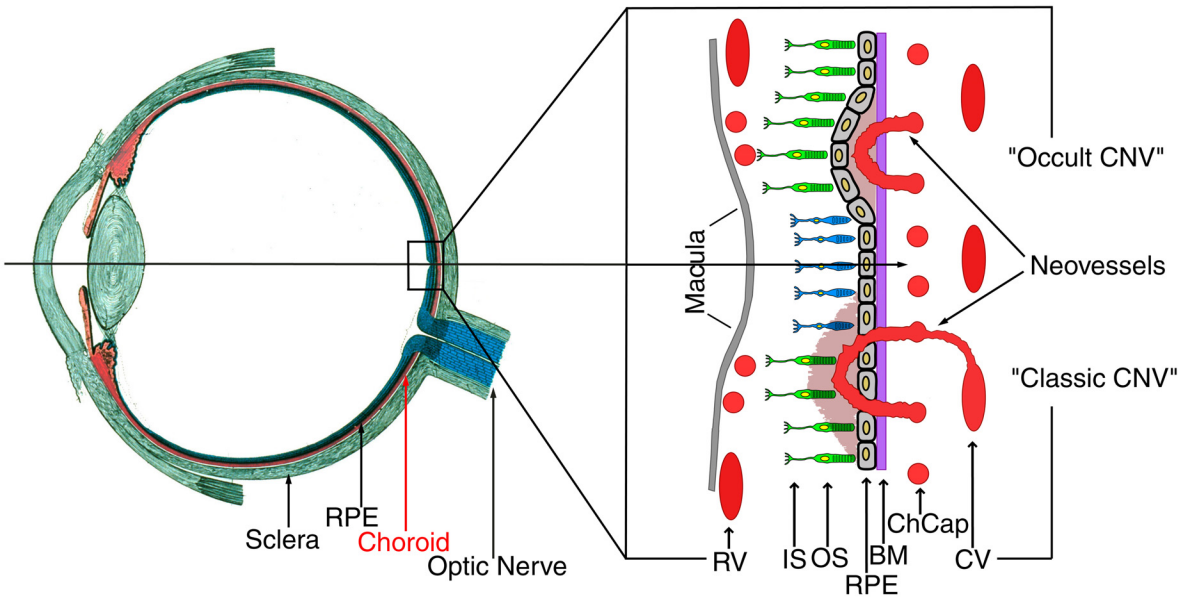

Figure 5 : Differences between occult and classic forms of AMD

Schematically, two kinds of AMD may occur, depending on the location where these CNV are and named “dry” or “wet”, coming from the way they are detected by fluorescein angiography (FA). FA consists in fluorescence images of the retina following i.v. injection of fluorescein, excited with a 488 nm light with fluorescence detection above 500 nm. These two wavelengths are strongly absorbed in the pigmentation of the RPE and of the choroids, then only leaking located before attaining the RPE, within the eye are clearly viewed in the first early pictures after i.v. injection, giving the name “wet” or “classic”. If the CNV are behind the RPE, this leaking of fluorescein is not visible while not absent, in these early pictures and we use then the name “dry” or “occult”. CNV due to AMD cause vision loss due to the death of photoreceptors with different degrees of blindness. Serious vision loss caused by dry AMD is less common, and appears slowly over years. Only about 10 to 20 percent of people with AMD have the "wet" type. Wet AMD strikes quickly, however, and can result in rapid vision loss in less than a year. This type of AMD is characterised by leaky CNV in the macula, which may create scar tissue, killing all further exchanges of oxygen and nutrients to photoreceptors causing permanent blind spots. Though less common than dry AMD, wet AMD is responsible for up to 90 percent of all cases of severe vision loss [47-50]. The differences between the two forms of AMD are schematically represented in Figure 5 [46].

In clinical trials, most vision loss due to wet AMD occurred within less than one year of diagnosis. The disease leads to a distortion of the straight lines and a severe reduction in quality of life for the patients, as they lose their ability to read, watch television, drive, and even see the faces of their beloved ones [51, 52], as illustrated in Figure 6.

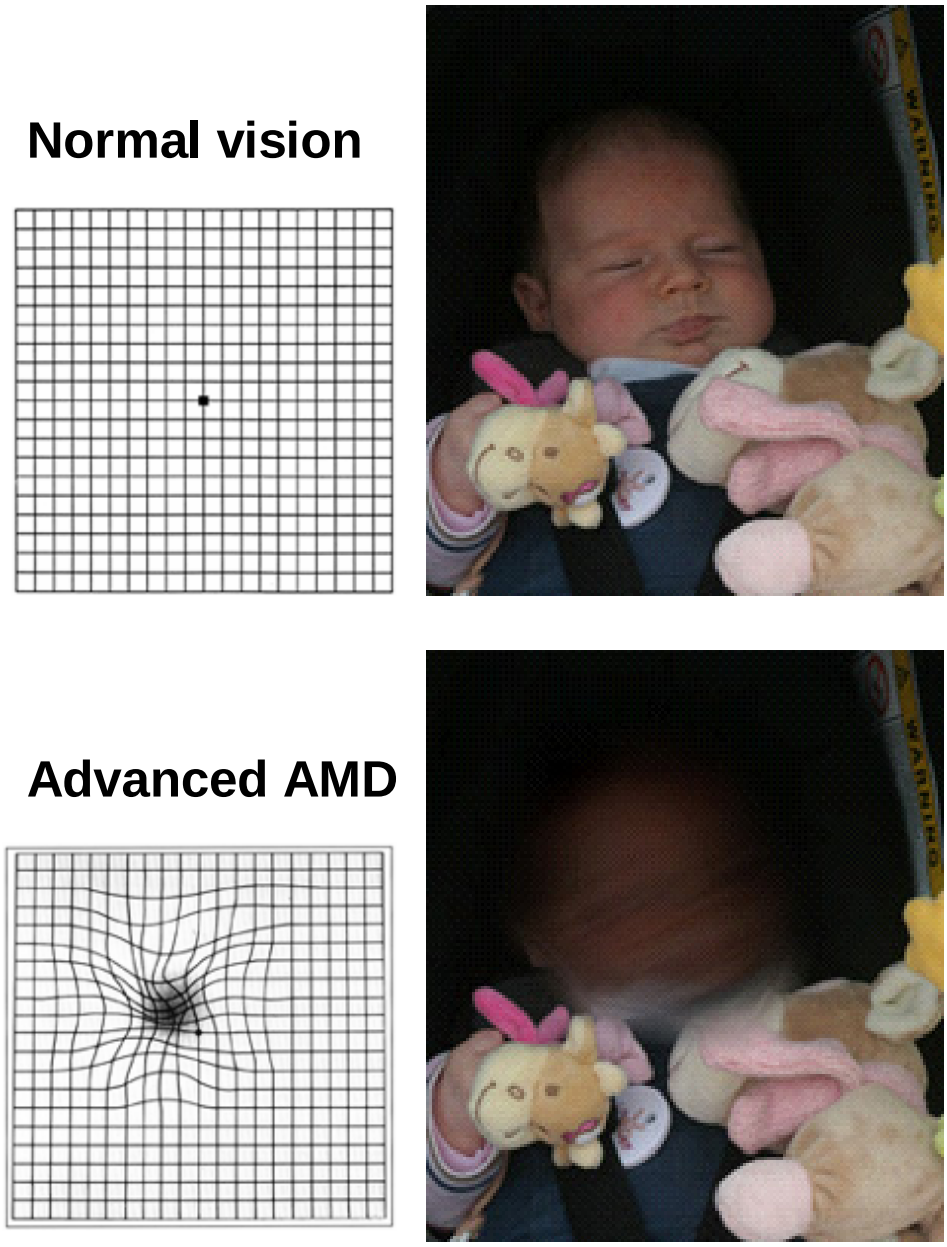

Figure 6 : Distortion of the straight lines and loss of the central vision characterizing a severe wet AMD

Only a few years ago, its diagnosis was the precursor sign of progressing blindness leading to severe loss of sight. The treatment of CNV due to AMD used to be one of the most frustrating problems for the vitro-retinal specialists. Despite intensive research, the aetiology of this disease remains poorly understood and consequently the treatments options are limited. During the last three decades, its diagnosis has become more accurate and several advances in epidemiology, genetics, and angiogenetics have increased our knowledge in understanding the physiopathology of this disorder [49]. Only a few years ago, thermal laser photocoagulation was the only available method of treatment and applicable to only 10-20% of patients with small, well-defined extra-foveal lesions [53]. However, this treatment is non-selective so that neighbouring normal retinal tissue including photoreceptor cells, retinal pigmented epithelium (RPE) and retinal blood vessels exposed to the laser light are thermally damaged, resulting in immediate and irreversible local vision loss. Patients undergo this procedure with the information that statistically it has been shown that the treatment will prevent the disease from progressing much and that the initial loss of vision resulting from the procedure is significantly less than the loss caused by the disease after several years of progression without treatment. Several new treatment strategies have revolutionised the potential successful management of neovascular wet AMD and hopefully will reduce the visual disability in this group of patients [54, 55]. At the present time, since the year 2000, the best available treatment of proven benefit for subfoveal neovascular wet AMD is photodynamic therapy (PDT) [56]. The rationale for using PDT to occlude pathologic neovascularisation arose from observations first recognised in treating tumors. Photodynamic therapy has been shown to be a relatively selective therapy for CNV, depending on the photosensitiser characteristics, formulation, packaging, drug dose, light dose, and timing of light application. Large-scale multicenter randomised Phase III clinical trials using PDT with verteporfin (Visudyne®), a benzoporphyrin derivative formulated in liposomes, have shown that this treatment is

effective in reducing visual loss in a large number of patients with subfoveal neovascular AMD [57-60]. This photosensitiser (Visudyne®) was approved by health authorities in many countries for clinical use in 2000, and remains the only photosensitiser approved for clinical use in ophthalmology to date. Currently, it is approved for treating choroidal neovascularization secondary to AMD as well as other disorders. Up to now, Visudyne® has limited the loss of sight of more than 500'000 people. Visudyne® is a benzoporphyrin, a type of coloured organic molecule that can interact with light. The chemical structure is presented in figure 7 [46].

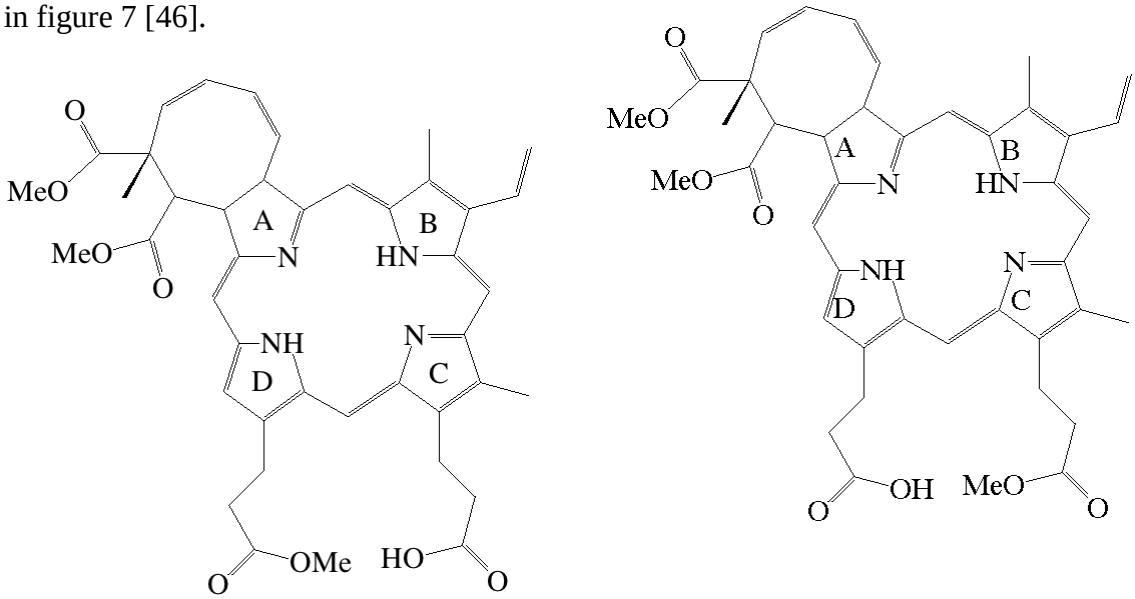

BPD-MA$_D$

Figure 7: Chemical structure of Verteporfin, also referred to as benzoporphyrin derivative monoacid ring (BPD-MA), consisting of a 1:1 mixture of the equally active structural isomers BPD-MA$_C$ and BPD-MA$_D$.

Many types of porphyrins exist [61]. The basic ring structure is composed of 20 carbons and 4 nitrogen atoms. These molecules are for many reasons a dream for the chemists. They are coloured and hence easy to see, stable, they can be centrally linked to almost all the metals. There are several well known porphyrins such as heme, which is part of the haemoglobin. This molecule gives the red colour to blood and contains Fe^{II+}. Chlorophyll is responsible for the green colour of plants and grass and contains mainly Magnesium in its central position.

Porphyrins were also found to have a good potential as PDT agents (see historical aspect of PDT in this chapter).

The research of Professors Dolphin, Levy and others at QLT Inc. [62, 63] on PDT with this substance demonstrated both a short half life in the body of animals and effective closure of blood vessels feeding tumours. This was a crucial step for the application of these molecules for the treatment of AMD. After more than 5 years of research and development, Visudyne® was ready to be approved by the FDA [64]. The therapeutic advantages of Visudyne® are its preferential accumulation in the new blood vessels as CNV, allowing the occlusion of choroidal neovessels but interestingly preserving the retinal vascularisation. Other advantages of this drug are its excitation with a visible light at 690 nm which is a wavelength not much absorbed by the blood components and the pigments of RPE and choroids. In PDT, Visudyne® is irradiated by a ray of light, which activates the oxygen to destroy the adjacent cellular machinery. When the light is turned off, and in all other protected parts of the body, Visudyne® becomes a not harmful molecule that the body can clear in a few days. Unfortunately, the PDT with Visudyne® has also 2 main drawbacks. The first possible drawback is the lack of selectivity for the CNV versus normal chorio-capillaries. Furthermore in a majority of cases, recurrence of the leaking CNV following treatment is observed by indocyanine green (ICG) and/or fluorescein angiographies. It has thus been reported that weeks/months after PDT, the re-opening and/or re-growth of neovessels is observed [46, 65, 66]. Thus the patients are retreated on the average 2-3 times per year over two years. This renewed observation of leaky chorio-neovessels may be attributed to local hypoxia combined with the release of angiogenic factors and/or inflammation following PDT.

Except for PDT and thermal laser treatment, alternative therapies also exist to treat AMD, such as transpupillary thermotherapy (TTT) [67] using a laser causing heat transmission to the retinal pigmented epithelium (RPE) and choroid studied by Reichel [68], radiation therapy

using low-dose ionizing radiation to prevent the proliferation of endothelial cells [69], submacular surgery removing the pathological chorio-capillaries, retinal translocation and pharmacologic intervention. Together with PDT, this last point is of great interest for this thesis. The pharmacotherapy is mainly based on either inhibition of vascular endothelial growth factor (VEGF) [70, 71] or use of various formulations of steroids to control the inflammatory response [72] associated with CNV. The most famous drugs used on this purpose are Avastin®, Macugen®, Lucentis®, Retaane® and Triamcinolone acetonide [73].

Cancer and its Treatments

Cancer occupies an increasingly important place in the load of world morbidity. Some 24,6 million people currently live with a diagnosed cancer; it is estimated that they will be 30 million in 2020. Until 2020, cancer could account for more than 10 million victims per year. If this tendency continues, one estimates that the annual number of new cases will pass from 10,9 million in 2002 to 16 million in 2020. Nearly 7 million people currently succumb each year to cancer. In the industrialised countries, cancer is located at the second rank of the causes of mortality after cardiovascular disease and, according to epidemiologic data this tendency is on its way to emerge in the least advanced countries. The lung cancer makes more victims than any other cancers. Certain cancers are more current in the industrialised countries: prostate, breast and colon cancers. Cancers of the liver, the stomach and the cervix are more current in the developing countries [74].

Nowadays, **surgery** remains the better classical method for removing a solid tumour with a slow evolution. If possible, the whole tumour is eliminated (e.g. cervix, breast, kidney, prostate, lung, gut…) [75 , 76, 77]. Surgery leads sometimes to success if the intervention occurs before the appearance of metastasis cells. However, ablation is often very badly accepted and sometimes refused, as the loss of an organ is a great trial for the patient.

Moreover it is not always sufficient and combination with the use of chemotherapy or radiotherapy are necessary to overcome metastasis developing cells [76, 77].

Surgery is often prescribed in combination with other techniques such as liquid nitrogen (cryotherapy) or radioactive needles (Curie therapy). The choice between these processes depends on the localisation of the tumour and its local extension degree. In the case of a fast evolving tumour leading to multiple metastasis where the more appropriated therapeutic indication is chemotherapy, the surgical act can be practised only to reduce the number of cancer cells (cyto-reductive surgery) in order to facilitate the activity of chemotherapy [78]. This process is used to treat for example ovarian cancer with peritoneal metastasis.

The second classical treatment is **radiotherapy** which is a therapeutic technique consisting of exposing a tumour to ionising radiation but preserving healthy cells. This treatment modality is often one of the treatments of choice following surgery. Almost sixty percent of the patients with a cancer have radiotherapy during their disease. Nevertheless, this therapy is complex, difficult to perform and induces many side effects in healthy tissues [79].

Another approach of medical treatment of cancer is to act directly on the cause itself of the disease by mean of natural substances already existing in the human organism, as it is the case for **hormonotherapy**. The main aim of this treatment is to limit the growth of hormone-dependant tumours or to induce their destruction. Orally or intravenously administered, these drugs are distributed to the organism according to their physico-chemical properties.

Beyond these treatments, **chemotherapy** keeps being the only recognised means to systemically treat cancer cells, wherever there are localised and particularly if there are metastases. The activity of these cytotoxic drugs used in chemotherapy is not specific and damage also occurs to the healthy cells characterised by a fast reproduction rate, inducing typical side effects such as vascular problems (leukopenia, thrombocytopenia), digestion

perturbations (diarrhea, nausea, vomiting) and alopecia. Furthermore, these cells can develop a resistance to the drug diminishing or even inhibiting the efficacy of the treatment.

Efficacy of chemotherapy, as for any drug treatment, depends on the ability of the therapeutic agent to reach the target cell. Delivery of therapeutics to the target after systemic intravenous injection is influenced by the blood supply to the region of interest, the drug transport through the vessel wall, and the drug diffusion through the interstitial space to the target cell [80-83]. Experimental approaches to improve delivery of therapeutic agents include the modification of the physicochemical properties of the drug, for example by formulating liposomes or nanoparticles or by grafting antibodies. Another possibility of improving the drug delivery to tumour is to modify the properties of the target area, such as the permeability of the tumour microvasculature [84].

Isolated organ perfusion is a strategy leading to a higher amount of drug accumulated in the organ containing the tumour tissue compared to systemic circulation, thus avoiding systemic side effects. However, space heterogeneity of the drug in the organ and a weak penetration of the substance in tumour cells can be observed. Although as observed in the isolated lung perfusion, one notes an accumulation of drug in the tumour vessel wall [85].

To overcome this inhomogeneous distribution of the cytostatic drug, its leakage from the vasculature should be locally enhanced. Tumour microvessels are leakier than normal vessels [86-88]. This leakiness of tumour vessels and the characteristic defective lymphatic drainage in solid tumours results in an enhanced accumulation of high-molecular-weight drugs in tumours as compared to normal tissue, due to an increased extravasation of the drug followed by a reduced clearance. This so-called enhanced permeability and retention effect (EPR) is limited by the increased fluid pressure in tumours [89]. It now becomes possible to modulate tumour-selective macromolecular drug delivery either by modulating vascular mediators or elevating the systemic blood pressure by infusing angiotensin II. Enhanced vascular

permeability of tumour and inflammatory tissue is the key to be considered for future more selective drug delivery. This should enhance the targeting to the desired tumours or inflammatory lesions, based on EPR effect using macromolecular drugs [90]. Different techniques have been proposed to increase this EPR effect by enhancing vessel permeability, e.g. by inducing a hyperthermia [91, 92], by pre-treating the tumour with radiation [93], by adding bradykinin antagonist HOE 140, protease inhibitors or inducible NOS inhibitors [89], vascular endothelial growth factor (VEGF) [94] or basic fibroblast growth factor (bFGF). However, these latter may not be ideal components of an anticancer treatment, since VEGF stimulates tumour growth and metastases, and bFGF induces tumour resistance to cytostatic drugs. Consequently, other innovating pre-treatments require to be explored to overcome the accumulation of drug in the vessel wall and to increase the tumour drug delivery of the cytostatic agent and its cellular uptake. **Photodynamic therapy** (PDT) is a good candidate for this purpose. PDT has been investigated as treatment for solid tumours. This treatment modality, described in the beginning if this chapter, is achieved by activating a photosensitizing agent, which generates oxygen species [20, 21]. It can act by direct phototoxicity [18, 19] or by indirect vascular-mediated effect by interruption of vessel integrity. More precisely, this treatment causes perturbation of the cytoskeleton [30-33] that can lead to alteration of cell shape [86, 87]. Both endothelial cell rounding [24, 34, 35] and contraction have been observed. We have hypothesized that the change in shape of the endothelial cell leading to an interruption of endothelial integrity may lead to an increased transvascular passage of high-molecular-weight drugs resulting in enhanced interstitial drug retention.

The advantages of PDT are linked to the low cytotoxicity of the substances. The cytotoxic effect is only obtained after the specific irradiation of the treated area. Post-therapeutic side effects are usually acceptable and consist mainly of a cutaneous sensitivity to sunlight. PDT

can be indicated when surgery is not possible because it can induce cell death without significantly destroying connective surrounding healthy tissue. Contrary to radiotherapy, PDT can be repeated many times, allowing treating the tumour until its complete clearance without any major risks for the patient.

Aim of the thesis

PDT can be used to cause vascular collapse and blood flow stasis leading to the temporary or permanent occlusion of the irradiated neovascularisation. This treatment can be used in many diseases associated to pathological neovasculature, for instance CNV due to AMD and cancer. As described above, these two diseases are of major interest as no "efficient well tolerated treatment" exists yet. Actually, CNV due to AMD still leads to severe loss of vision despite of the existing Visudyne®-PDT treatment and cancer is still one of the leading causes of death worldwide despite of the numerous oncological treatments that are being developed. The occlusion of the pathological neovessels characterizing these diseases can be achieved by PDT. The aim of this thesis is to explore in pre-clinical models, the possibility of improving the PDT treatment of these diseases by combining it with another classical therapy, the chemotherapy. In the case of CNV due to AMD, the recurrence of the weeks/months after PDT, the re-opening and/or re-growth of neovessels should be avoided by adding an anti-angiogenic drug such as anti-VEGF factor or anti-inflammatory drug during or shortly after PDT. In the case of cancer, the starvation of tumor cells induced by the PDT occlusion of blood vessels feeding the tumor should really be combined by a chemotherapeutic direct kill of the tumor cells themselves. The main question concerning the administration of these drugs potentially improving the treatments of AMD and cancer by PDT, is:

"How could we improve the drug delivery to reach the therapeutic dose locally?"

It has been reported that following the light application in PDT, a physiological cascade of responses in one hand leads to vascular occlusion but could also induce a vascular permeability enhancement. The aim of this thesis is to find conditions where this increase in leakage due to PDT can be observed, to characterize it and to take advantage of this phenomenon to develop in the future a novel combination therapy approach. Such enhanced vascular permeability in PDT could be used to release an anti-angiogenic or anti-

inflammatory factor to prevent recurrence of the neovasculature in the case of AMD or to selectively release chemotherapeutic agents in the case of PDT of a malignant tumour. These are schematically represented in figure 8.

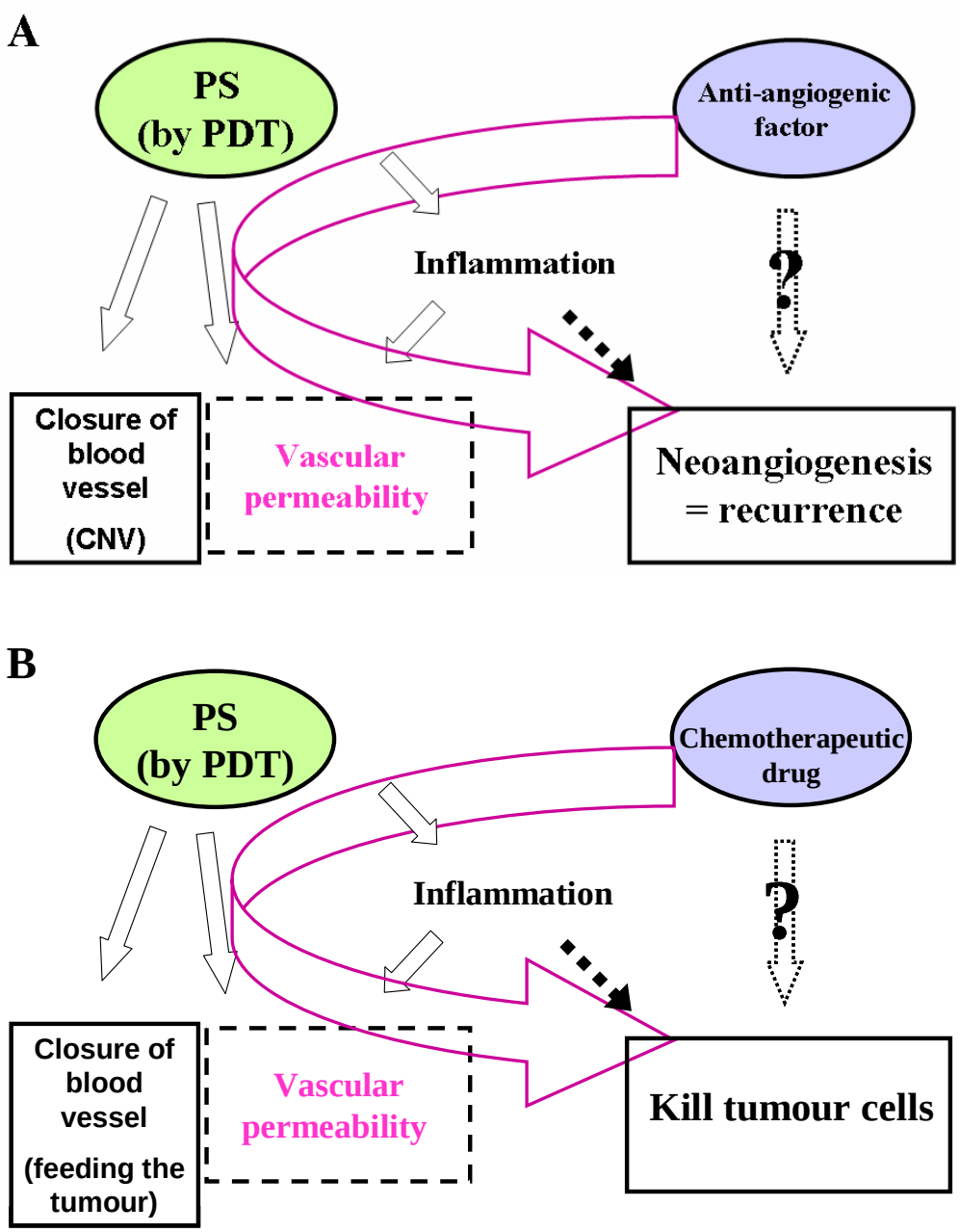

Figure 8: Photodynamic drug delivery pathway, for hypothetic improvement of the treatment of (A) age-related macular degeneration or (B) cancer.

Experimental models used in this thesis

1. Chorioallantoic membrane model (CAM)

The chorioallantoic membrane was the first model used for the study. This well vascularised membrane is a characteristic of avian and reptile eggs that is located in contact with the inner eggshell. Its role is to bring to the chicken embryo, the oxygen diffusing across the porous calcareous surface of the shell. It is composed of two extra-embryonic membranes: the allantoic membrane and the chorion, both growing during embryonic development, finally almost covering the entire inside of the eggshell with several blood vessels large enough (300 µm in diameter) to be intravenously injected by the 13th day of embryonic development [95-98]. See the illustration of figure 9.

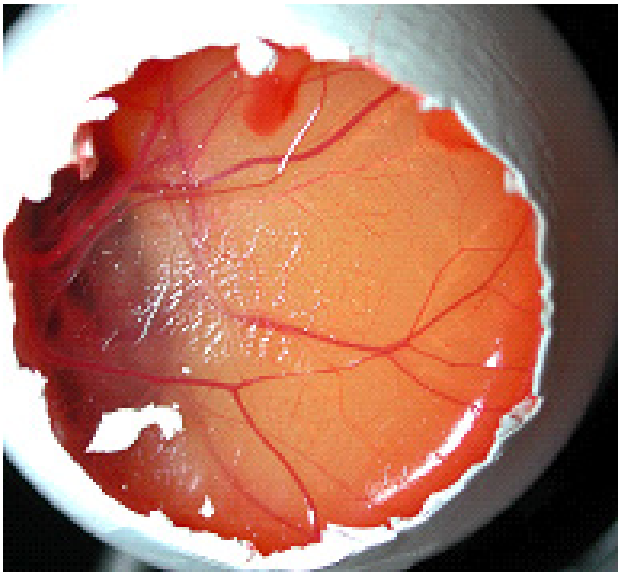

Figure 9: This picture shows a typical blood vessels network at the 13th embryo development day of the chorioallantoic membrane (CAM) of the chicken embryo. At this stage of development, the largest blood vessels have a diameter of about 300 µm, rendering possible the i.v. injection.

The chorioallantoic membrane of the chicken has been used in angiogenic research and is also a good model for the assessment of phototoxicity and vascular behaviour of drugs [99, 100]. The intravenous injection is close to the clinical situation of PDT-treated choroidal neovessels appearing in age-related macular degeneration [45] and somehow comparable to the vascular PDT of blood vessels feeding cancer. This model has several advantages. It offers an accessible developed neovascular network allowing intravenous injections [101] or topical applications [102]; it is very cheap compared to other in vivo models and it is not considered as a living animal by the veterinary and ethical committees up to the 17th embryo development day allowing spontaneous change in protocols. Furthermore, quantitative relationship between the PDT effects and the kinetics of leakage of drugs observed in the CAM model and in the clinical tests was established, rendering possible the extrapolation of observations in the CAM model to clinical situation [45]. For the compounds and conditions of treatment that appear promising in this model, assays could be performed in a mammal model such as described below and in the Ryan's cynomolgus monkey model of CNV that will be the final step of the preclinical studies for new CNV in AMD treatments [103].

2. Skinfold chamber of nude mice observed by intravital microscopy (IVM)

The dorsal skinfold chamber in nude mice was the second model used for the study. Before the experimental procedure, the nude mice were housed in groups of 2 to 3 animals, and after the implantation of the chamber, they were then caged individually. The experimental procedures have previously been approved by the local ethical committee. It is a highly standardised and controlled model that has been used previously for experiments on the vasculature [104-106]. At the time of the experiments, the animals were about 5 weeks old and had a body weight of about 24-28g. The microsurgical procedure was performed under sterile conditions and the animal was placed on an operation table warmed at 37°c. The titanium chambers and the surgical implantation procedure used in this study are based on that of Lehr et al. [106] with only a few minor modifications. The mouse was anesthetised by intraperitoneal injection of ketamine-xylazine. The dorsal skin was stretch to form a double layer skinfold that will be sandwiched between two symmetrical titanium frames (Fig. 11 A, B). A circular area of 15 mm in diameter from one area of skin was carefully completely removed (Fig. 11 C), and the remaining layers (consisting of the epidermis, subcutaneous tissue, and thin striated skin muscle) were covered with a glass cover slip incorporated into one of the frames (Fig. 11 D, E).

The animals tolerated the dorsal skinfold chambers well, and no effect on the eating and sleeping habits were observed. The experimental observations were made after a recovery period of 48 hours to eliminate the effects of anaesthesia and surgical trauma on the microvasculature, and may last up to 2 weeks.

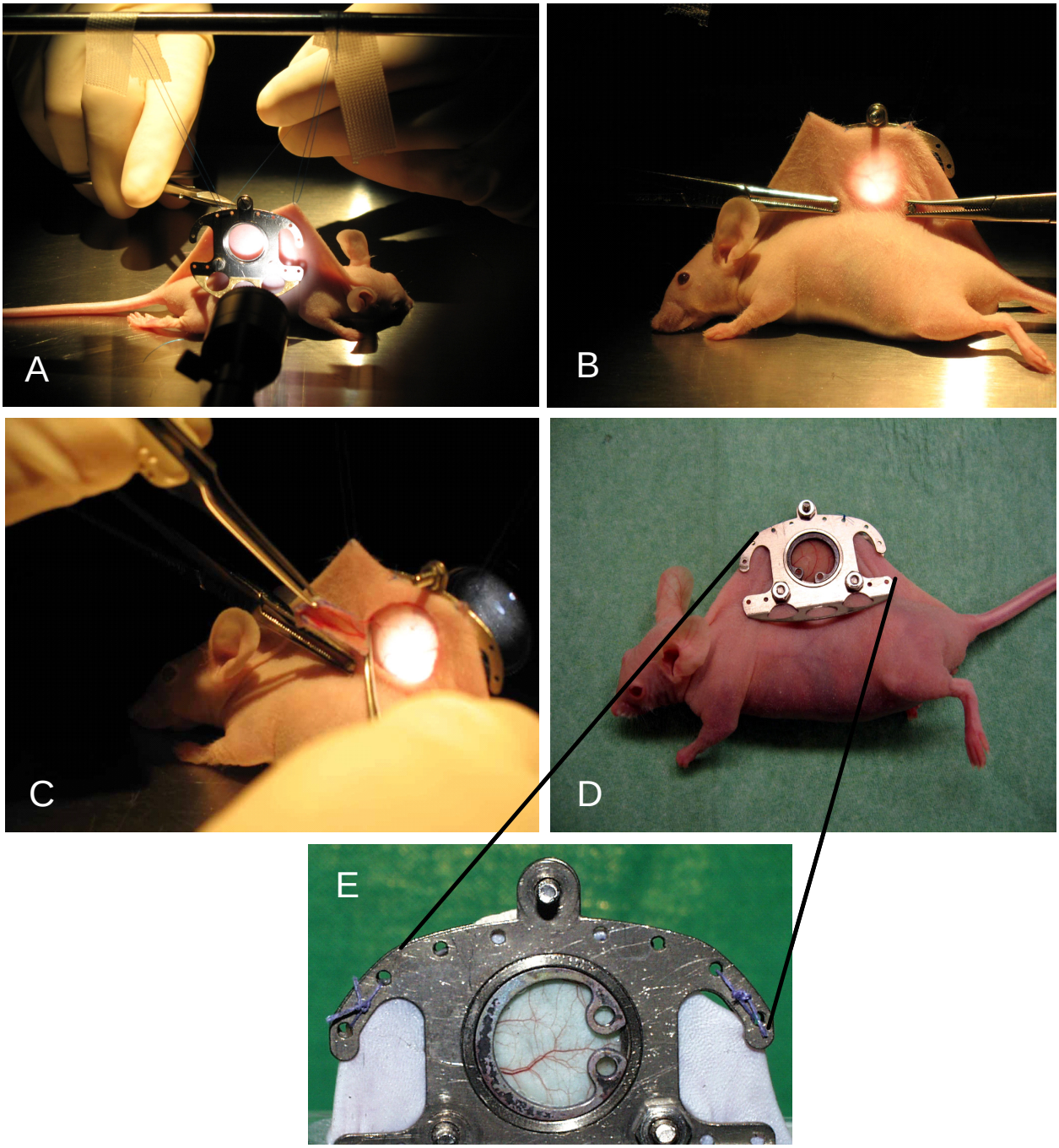

Figure 10: Microsurgical preparation of the optical chamber. (A) The dorsal skin of the nude mouse was stretch to form a double layer skinfold. (B) A titanium frame is fixed in one side. And the area of observation is chosen by transparency. (C) A circular area of 15 mm in diameter from one area of skin was carefully completely removed and (D) the remaining layers were covered with a glass cover slip incorporated into one of the frames. (E) Details of the observation chamber.

To verify the integrity of the vasculature and the good acceptance of the surgical process, a rhodamine-6-G injection was performed into the tail vein to exclude from the study acute vascular inflammation conditions. This fluorescent dye labelling the leucocytes allows to follow the kinetics of their rolling and adhesion to the vessel wall of veins, characteristic of inflammatory reactions [105, 107]. The further experiments were then performed by intravital microscopy (IVM), allowing the real-time observation of the vascular phenomenon through the glass window. For the experiments, the awake animals were immobilised in a Plexiglas tube and the chamber was attached to an epi-illumination microscope stage, which was computer controlled to allow observations of the microvessels.

References

1. Ackroyd, R., et al., *The history of photodetection and photodynamic therapy.* Photochemistry and Photobiology, 2001. **74**(5): p. 656-669.
2. Boughton, H.C. The Valley Echo. Regina: Commercial Printers Ltd., 1923/4:4(5):2. . May 1923.
3. Finsen, N., *Phototherapy*. London: Arnold, 1901.
4. Fitzpatrick, T. and M. Pathak, *Historical Aspect of Methoxsalen and other Furocoumarins* Journal of Investigative Dermatology 1959. **32**(2): p. 229-231.
5. Raab, O., *Uber die Wirkung fluoreszierender Stoffe auf Influsorien.* . Z Biol 1900. **39**: p. 524-46.
6. von Trappeiner, H. and A. Jesionek, *Therapeutische Versuche mit fluoreszierenden Stoffen.* Med Worchenschr, 1903. **47**: p. 2042-4.
7. von Trappeiner, H. and A. Jodlbauer, *Uber Wirkung der photodynamischen (fluorieszierenden) Stoffe auf Protozan und Enzyme.* Dtsche Arch Klin Med, 1904. **80**: p. 427-87.
8. von Trappeiner, H. and A. Jodlbauer, *Die Sensibilisierende Wirkung fluorieszierender Substanzer. Gesammte Untersuchungen über die photodynamische Erscheinung.* F.C.W. Vogel, Leipzig, 1907.
9. Prime, J., *Les accidentes toxiques par l'eosinate de sodium.* Parie: Jouve & Boyer, 1900.
10. Hausmann, W., *Die sensibilisierende Wirkung des Hämatoporphyrins.* Biochem Z, 1911. **30**: p. 276-316.
11. Meyer-Betz, F., *Untersuchungen über die biologische (photodynamische) Wirkung des Hämatoporphyrins und anderer Derivate des Blut- und Gallenfarbstoffs.* Dtsche Arch Klin Med, 1913. **112**: p. 476-503.
12. Policard, A., *Etude sur les aspects offerts par des tumeurs expérimentales examinées à la lumière de Wood.* C R Soc Biol, 1924. **91**: p. 1423-1424.
13. Diamond, I., S. Granelli, and A. McDonagh, *Photochemotherapy and Photodynamic Toxicity- Simple Methods for Identifying Potentially Active Agents* Biochemical Medicine, 1977. **17**(2): p. 121-127.
14. Dougherty, T., *Activated dyes as antitumor agents.* J Natl Cancer Inst 1974. **52**(4): p. 1333-1336.
15. Kelly, J., M. Snell, and M. Berenbaum, *Photodynamic Destruction of Human Bladder Carcinoma.* Br J Cancer, 1975. **31**(2): p. 237-244.
16. Kelly, J. and M. Snell, *Hematoporphyrin Derivative- Possible aid in Diagnosis and Therapy of Carcinoma of Bladder.* J Urol, 1976. **115**(2): p. 150-151.
17. Mitton, D. and R. Ackroyd, *History of photodynamic therapy in Great Britain* Photodiagnosis and Photodynamic Therapy 2005. **2** (4): p. 239-246.
18. van den Bergh, H., *Light and porphyrins in cancer therapy* Chemistry in Britain, 1986. **22**(5): p. 430-439
19. Schuitmaker, J., et al., *Photodynamic therapy: A promising new modality for the treatment of cancer.* Journal of Photochemistry and Photobiology B-Biology, 1996. **34**(1): p. 3-12.
20. van Lier, J., *Photosensitization: reaction pathways*. Photobiological techniques, ed. D. Valenzeno. 1990, New York: Plenum press 85-97.
21. Dougherty, T., et al., *Photodynamic therapy.* Journal of the National Cancer Institute, 1998. **90**(12): p. 889-905.

22. van den Bergh, H. and J.P. Ballini, *Principles of Photodynamic Therapy*. Photodynamic Therapy of Ocular Diseases, ed. E. Gragoudas, J. Miller, and L. Zografos. 2004, Philadelphia, PA, USA: Lippincott Williams & Wilkins. 11-42.
23. Fernandez, J., M. Bilgin, and L. Grossweiner, *Singlet oxygen generation by photodynamic agents.* Journal of Photochemistry and Photobiology B-Biology, 1997. **37**(1-2): p. 131-140.
24. Fingar, V.H., *Vascular effects of photodynamic therapy.* J Clin Laser Med Surg, 1996. **14**(5): p. 323-8.
25. Sharman, W.M., C.M. Allen, and J.E. van Lier, *Photodynamic therapeutics: basic principles and clinical applications.* Drug Discov Today, 1999. **4**(11): p. 507-517.
26. Chen, B., T. Roskams, and P. de Witte, *Antivascular tumor eradication by hypericin-mediated photodynamic therapy.* Photochemistry and Photobiology, 2002. **76**(5): p. 509-513.
27. Dolmans, D., et al., *Vascular accumulation of a novel photosensitizer, MV6401, causes selective thrombosis in tumor vessels after photodynamic therapy.* Cancer Research, 2002. **62**(7): p. 2151-2156.
28. Huang, Z., et al., *Studies of a vascular-acting photosensitizer, Pd-bacteriopheophorbide (Tookad), in normal canine prostate and spontaneous canine prostate cancer.* Lasers Surg Med, 2005. **36**(5): p. 390-7.
29. West, C., et al., *A comparison of the sensitivity to photodynamic treatment of endothelial and tumour cells in different proliferative states* International Journal of Radiation Biology, 1990. **58**(1): p. 145-156.
30. Boekelheide, K., et al., *Microtubule assembly inhibition by porphyrins and realted-compounds.* Photochem Photobiol, 1987. **46**(5): p. 657-661.
31. Dadosh, N. and N. Shaklai, *Effect of protoporphyrin-IX on red blood-cell membrane cytoskeleton.* Journal of muscle research and cell motility, 1988. **9**(1): p. 86-86.
32. Nelson, J., L. Liaw, and M. Berns, *Tumor destruction in photodynamic therapy.* Photochemistry and Photobiology, 1987. **46**(5): p. 829-835.
33. Sporn, L. and T. Foster, *Photofrin and light induces microtubule depolymerization in cultured human endothelial-cells.* Cancer Research, 1992. **52**(12): p. 3443-3448.
34. Henderson, B.W., et al., *Effects of photodynamic treatment of platelets or endothelial cells in vitro on platelet aggregation.* Photochem Photobiol, 1992. **56**(4): p. 513-21.
35. Fingar, V., et al., *Vascular damage after photodynamic therapy of solid tumors: A view and comparison of effect in pre-clinical and clinical models at the University of Louisville.* In Vivo, 2000. **14**(1): p. 93-100.
36. Foster, T.H., et al., *Photosensitized release of von Willebrand factor from cultured human endothelial cells.* Cancer Res, 1991. **51**(12): p. 3261-6.
37. Ben-Hur, E., et al., *Release of clotting factors from photosensitized endothelial cells: A possible trigger for blood vessel occlusion by photodynamic therapy* FEBS Letters, 1988. **236**(1): p. 105-108.
38. Schuster, A., et al., *Simultaneous arterial calcium dynamics and diameter measurements: application to myoendothelial communication.* Am J Physiol Heart Circ Physiol, 2001. **280**(3): p. H1088-96.
39. Zhou, C., *Mechanisms of tumor necrosis induced by photodynamic therapy.* Journal of photochemistry and photobiology. B, 1989. **3**(3): p. 299-318.
40. Zieve, P., H. Solomon, and J. Krevans, *The effect of hematoporphyrin and light on human platelets. I. Morphologic, functional, and biochemical changes.* Journal of Cellular Physiology 1966. **67**(2): p. 271-&.

41. Doukas, J., H. Hechtman, and D. Shepro, *Vasoactive amines and eicosanoids interactively regulate both polymorphonuclear leukocyte diapedesis and albumin permeability in vitro* Microvascular Reserach, 1989. **37**(2): p. 125-137.
42. Fingar, V., et al., *The role of microvascular damage in photodynamic therapy: The effect of treatment on vessel constriction, permeability, and leukocyte adhesion* Cancer Research, 1992. **52**(18): p. 4914-4921.
43. Reed, M.W., et al., *The microvascular effects of photodynamic therapy: evidence for a possible role of cyclooxygenase products.* Photochem Photobiol, 1989. **50**(3): p. 419-23.
44. Krammer, B., *Vascular effects of photodynamic therapy.* Anticancer Res, 2001. **21**(6B): p. 4271-7.
45. Lange, N., et al., *A new drug-screening procedure for photosensitizing agents used in photodynamic therapy for CNV.* Invest Ophthalmol Vis Sci, 2001. **42**(1): p. 38-46.
46. van den Bergh, H., *Photodynamic therapy of age-related macular degeneration: history and principles.* Seminars in Ophthalmology, 2001. **16**(4): p. 181-200.
47. Gupta, D., et al., *The natural history of geographic atrophy, the advanced dry form of age-related macular degeneration (AMD).* Journal of the American Geriatrics Society, 2003. **51**(4): p. S229-S230.
48. Sunness, J.S., et al., *The development of choroidal neovascularization in eyes with the geographic atrophy form of age-related macular degeneration.* Ophthalmology, 1999. **106**(5): p. 910-919.
49. Gehrs, K.M., et al., *Age-related macular degeneration - emerging pathogenetic and therapeutic concepts.* Annals of Medicine, 2006. **38**(7): p. 450-471.
50. Beaumont, P.E. and H.K. Kang, *Lesion morphology in age-related macular degeneration and its therapeutic significance.* Archives of Ophthalmology, 2006. **124**(6): p. 807-812.
51. Slakter, J.S. and M. Stur, *Quality of life in patients with age-related macular degeneration: Impact of the condition and benefits of treatment.* Survey of Ophthalmology, 2005. **50**(3): p. 263-273.
52. Berman, K. and H. Brodaty, *Psychosocial effects of age-related macular degeneration.* International Psychogeriatrics, 2006. **18**(3): p. 415-428.
53. Sivaprasad, S., et al., *Proportion of treatable subtypes of choroidal neovascular membranes in age-related macular degeneration,* in *International Congress Series*. 2005. p. 312-316.
54. Hunt, D.W.C. and P. Margaron, *Status of therapies in development for the treatment of age-related macular degeneration.* Idrugs, 2003. **6**(5): p. 464-469.
55. Chakravarthy, U., et al., *Evolving European guidance on the medical management of neovascular age related macular degeneration.* British Journal of Ophthalmology, 2006. **90**(9): p. 1188-1196.
56. Schmidt-Erfurth, U.M. and C. Pruente, *Management of neovascular age-related macular degeneration.* Progress in Retinal and Eye Research, 2007. **26**(4): p. 437-451.
57. TAP Study Group, *Verteporfin Therapy for Subfoveal Choroidal Neovascularization in Age-Related Macular Degeneration. Three-Year Results of an Open-Label Extension of 2 Randomized Clinical Trials - TAP Report 5.* Arch. Ophthalmol., 2002. **120**(10): p. 1307-1314.
58. TAP Study Group, *Effects of verteporfin therapy on contrast on sensitivity: Results From the Treatment of Age-Related Macular Degeneration With Photodynamic Therapy (TAP) investigation-TAP report No 4.* Retina, 2002. **22**(5): p. 536-44.
59. TAP Study Group, *Photodynamic Therapy of Subfoveal Choroidal Neovascularization in Age-Related Macular Degeneration With Verteporfin: Two-Year Results of 2*

Randomized Clinical Trials--TAP Report 2. Arch. Ophthalmol., 2001. **119**: p. 198-207.
60. TAP Study Group, *Photodynamic Therapy of subfoveal choroidal neovascularisation in age-related macular degeneration with verteporfin. One year results of 2 randomized clinical trials. TAP report 1.* Arch. Ophthalmol., 1999. **117**(10): p. 1329-45.
61. Allison, R.R., et al., *Photosensitizers in clinical PDT.* Photodiagnosis and Photodynamic Therapy, 2004. **1**(1): p. 27-42.
62. Richter, A.M., et al., *Photosensitising potency of structural analogues of benzoporphyrin derivative (BPD) in a mouse tumour model.* British Journal of Cancer, 1991. **63**(1): p. 87-93.
63. Masutani, M., et al., *Application of benzoporphyrin derivatives to photodynamic therapy.* Nihon University Journal of Medicine, 1996. **38**(1): p. 51-64.
64. McGinnis, T.J., *Significant FDA approvals in 2000.* American Family Physician, 2001. **63**(10): p. 2061-2064.
65. Miller, J.W., et al., *Photodynamic therapy with verteporfin for choroidal neovascularization caused by age-related macular degeneration: results of a single treatment in a phase 1 and 2 study.* Arch Ophthalmol, 1999. **117**(9): p. 1161-73.
66. Costa, R.A., et al., *Immediate indocyanine green angiography and optical coherence tomography evaluation after photodynamic therapy for subfoveal choroidal neovascularization.* Retina, 2003. **23**(2): p. 159-65.
67. Sun, Y., *Transpupillary thermotherapy for age-related macular degeneration.* Chinese Ophthalmic Research, 2007. **25**(4): p. 317-320.
68. Reichel, E., et al., *Transpupillary thermotherapy of occult subfoveal choroidal neovascularization in patients with age-related macular degeneration.* Ophthalmology, 1999. **106**(10): p. 1908-14.
69. Finger, P., et al., *Radiation therapy for subretinal neovascularization.* Ophtalmology, 1996. **103**(6): p. 878-889.
70. Kvanta, A., et al., *Subfoveal fibrovascular membranes in age-related macular degeneration express vascular endothelial growth factor.* Investigative Ophtalmology & Visual Science, 1996. **37**(9): p. 1929-1934.
71. Augustin, A.J. and I. Offermann, *Emerging drugs for age-related macular degeneration.* Expert Opin Emerg Drugs, 2006. **11**(4): p. 725-40.
72. Jonas, J.B., I. Kreissig, and R.F. Degenring, *Factors influencing visual acuity after intravitreal triamcinolone acetonide as treatment of exudative age related macular degeneration.* Br J Ophthalmol, 2004. **88**(12): p. 1557-62.
73. Kulkarni, A. and B. Kuppermann, *Wet age-related macular degeneration.* Advanced Drug Delivery Reviews, 2005. **57**(14): p. 1994-2009.
74. Stewart, B.W. and P. Kleihues, *World Cancer Report.* IARC Nonserial Publication, 2003.
75. Lagarde, P., *Tout savoir sur le cancer*, ed. Favre. 1999, Lausanne.
76. Bremers, A.J., E.J. Rutgers, and C.J. van de Velde, *Cancer surgery: the last 25 years.* Cancer Treat Rev, 1999. **25**(6): p. 333-53.
77. Bugat, R., et al., *Le cancer*, ed. PRIVAT. 2000, Toulouse.
78. Plunkett, T. and D. Miles, *Immunotherapy: the last 25 years.* Cancer Treatment Reviews, 1999. **25**(6): p. 355-363.
79. Russell, N.S. and H. Bartelink, *Radiotherapy: the last 25 years.* Cancer Treat Rev, 1999. **25**(6): p. 365-76.
80. Jain, R.K., *Transport of molecules in the tumor interstitium: A review.* Cancer Research, 1987. **47**(12): p. 3039-3051.

81. Jain, R.K., *Delivery of Novel Therapeutic Agents in Tumors - Physiological Barriers and Strategies.* Journal of the National Cancer Institute, 1989. **81**(8): p. 570-576.
82. Jain, R.K., *Delivery of molecular and cellular medicine to solid tumors.* Advanced Drug Delivery Reviews, 2001. **46**(1-3): p. 149-168.
83. Steyger, P.S., et al., *Intratumoural distribution as a determinant of tumour responsiveness to therapy using polymer-based macromolecular prodrugs.* Journal of Controlled Release, 1996. **39**(1): p. 35-46.
84. Reddy, L.H., *Drug delivery to tumours: Recent strategies.* Journal of Pharmacy and Pharmacology, 2005. **57**(10): p. 1231-1242.
85. Krueger, T., et al., *Antegrade versus retrograde isolated lung perfusion: Doxorubicin uptake and distribution in a sarcoma model.* Annals of Thoracic Surgery, 2006. **82**(6): p. 2024-2030.
86. Jain, R.K., *Tumor angiogenesis and accessibility: role of vascular endothelial growth factor.* Seminars in oncology, 2002. **29**(6 Suppl 16): p. 3-9.
87. Jain, R.K., *Normalization of tumor vasculature: An emerging concept in antiangiogenic therapy.* Science, 2005. **307**(5706): p. 58-62.
88. Yuan, F., *Transvascular drug delivery in solid tumors.* Seminars in Radiation Oncology, 1998. **8**(3): p. 164-175.
89. Maeda, H., et al., *Tumor vascular permeability and the EPR effect in macromolecular therapeutics: A review.* Journal of Controlled Release, 2000. **65**(1-2): p. 271-284.
90. Maeda, H., et al., *Vascular permeability enhancement in solid tumor: Various factors, mechanisms involved and its implications.* International Immunopharmacology, 2003. **3**(3): p. 319-328.
91. Huang, S.K., et al., *Liposomes and Hyperthermia in Mice - Increased Tumor Uptake and Therapeutic Efficacy of Doxorubicin in Sterically Stabilized Liposomes.* Cancer Research, 1994. **54**(8): p. 2186-2191.
92. Ponce, A.M., et al., *Hyperthermia mediated liposomal drug delivery.* International Journal of Hyperthermia, 2006. **22**(3): p. 205-213.
93. Davies, C.D.L., et al., *Radiation Improves the Distribution and Uptake of Liposomal Doxorubicin (Caelyx) in Human Osteosarcoma Xenografts.* Cancer Research, 2004. **64**(2): p. 547-553.
94. Baban, D.F. and L.W. Seymour, *Control of tumour vascular permeability.* Advanced Drug Delivery Reviews, 1998. **34**(1): p. 109-119.
95. Roberts, W.G. and T. Hasan, *Role of neovasculature and vascular permeability on the tumor retention of photodynamic agents.* Cancer Res, 1992. **52**(4): p. 924-30.
96. Randles, C. and A. Romanoff, *A study of internal environment of the developing avian egg* Poultry Science 1950. **29**(5): p. 776-776.
97. Romanoff, A., *Role of chemical embryology in the field of avian reproduction and physiology* Poultry Science 1950. **29**(5): p. 777-777.
98. Romanoff, A.L., *Biochemistry of the Avian Embryo: a Quantitative Analysis of Prenetal Development.* 1967, New York: John Wiley & Sons. 398.
99. Gottfried, V., E. Lindenbaum, and S. Kimel, *Vascular damage during PDT as monitored in the chick chiorioallantoic membrane* International Journal of Radiation Biology, 1991. **60**(1-2): p. 349-354.
100. Gottfried, V., E. Lindenbaum, and S. Kimel, *The chick chorioallantoic membrane (CAM) as an in vivo model for photodynamic therapy* Journal of Photochemistry and Photobiology B- Biology, 1992. **12**(2): p. 204-207.
101. Hornung, R., et al., *Systemic application of photosensitizers in the chick chorioallantoic membrane (CAM) model: photodynamic response of CAM vessels and*

5-aminolevulinic acid uptake kinetics by transplantable tumors. Journal of Photochemistry and Photobiology B: Biology, 1999. **49**(1): p. 41-49.
102. Hammer-Wilson, M.J., et al., *Photodynamic parameters in the chick chorioallantoic membrane (CAM) bioassay for topically applied photosensitizers.* J Photochem Photobiol B, 1999. **53**(1-3): p. 44-52.
103. Kramer, M., et al., *Liposomal benzoporphyrin derivative verteporfin photodynamic therapy - Selective treatment of choroidal neovascularization in monkeys.* Ophtalmology, 1996. **103**(3): p. 427-438.
104. Endrich, B., et al., *A new chamber technique for micro-vascular studies in unanesthetized hamsters.* Research in Experimental Medicine, 1980. **177**(2): p. 125-134.
105. Lehr, H., et al., *Leukotrienes as mediators in ischemia-reperfusion injury in a microcirculation model in the hamster* Journal of Clinical Investigation, 1991. **87**(6): p. 2036-2041.
106. Lehr, H., et al., *Intravital fluorescence microscopy for the study of leukocyte interaction with platelets and endothelial cells.* Oxidants and Antioxydants, PT B, 1999. **300**: p. 462-481.
107. Schafer, S., et al., *Paradoxical attenuation of leukocyte rolling in response to ischemia-reperfusion and extracorporeal blood circulation in inflamed tissue.* American Journal of Physiology-Heart and Circulatory Physiology 2005. **289**(1): p. H330-H335.

Chapitre 2

Combination Therapy Using Aspirin-enhanced photodynamic selective drug delivery

Published in Vascular Pharmacology

Available online at www.sciencedirect.com
ScienceDirect
Vascular Pharmacology 46 (2007) 171–180
Vascular Pharmacology
www.elsevier.com/locate/vph

Combination therapy using aspirin-enhanced photodynamic selective drug delivery

E. Debefve, B. Pegaz, J.-P. Ballini, Y.N. Konan, H. van den Bergh *

Ecole Polytechnique Fédérale de Lausanne (EPFL) Laboratory of Photomedicine, CH-1015 Lausanne, Switzerland

Received 13 March 2006; received in revised form 23 June 2006; accepted 19 September 2006

Abstract

In photodynamic therapy (PDT), excitation of a drug by light leads to a cascade of biochemical processes that can cause closure of blood vessels. It has been observed clinically that significant short-term leakage from the irradiated vasculature can occur prior to vessel closure and blood flow stasis. In this paper we demonstrate in a chicken embryo model that this leakage can be significantly enhanced by the presence of the cyclo-oxygenase inhibitor, aspirin. We also observe that following this aspirin-enhanced leakage, blood vessels close as effectively as after PDT in the absence of aspirin. Consequently we propose that this PDT-induced aspirin-enhanced leakage can be used to locally deliver a drug for combination therapy. This is then demonstrated in the chicken embryo using Visudyne® as a PDT agent in combination with aspirin and fluorescein isothiocyanate dextran 10 kDa as leakage indicator. The latter represents a hypothetical drug to be delivered in various kinds of combination therapy. Two examples of this procedure would be the photodynamic treatment of choroidal neovasculature associated with exudative age-related macular degeneracy (AMD) where local delivery of an anti-angiogenic or an anti-inflammatory drug has been shown to be effective, or PDT of cancer where local dosing of a chemotherapeutic drug may well increase the treatment efficacy.

Keywords: Photodynamic therapy (PDT); Chorioallantoic membrane (CAM); Leakage; Drug delivery; Age-related macular degeneration (AMD); Cancer

1. Introduction

Vascular hyperproliferation characterises several diseases, including cancer and exudative age-related macular degeneration (AMD). Strategies aimed at diminishing the vascular networks associated with these diseases and inhibiting the growth of new vessels are among the promising new treatment approaches. One therapeutic approach that is based in part on the closure of blood vessels and that has been proven clinically to be effective against several of the above-mentioned pathologies is photodynamic therapy (PDT) (Miller et al., 1999; van den Bergh, 2001). PDT is based on a systemically or topically applied photosensitizing agent (or its precursor), which upon activation with agent-specific light produces singlet oxygen (van den Bergh, 2001; Sharman et al., 1999) and/or other reactive intermediates. Interaction of the latter with the endothelium can lead to significant vascular damage, thrombus formation, and finally blood flow stasis. This is often a significant and sometimes even the predominant mechanism of tissue damage in PDT *in vivo*. PDT damage to vascular endothelial cells has been documented (Fingar, 1996; Fingar et al., 1999; Krammer, 2001; Michels and Schmidt-Erfurth, 2003). In one scenario, endothelial cell damage is proposed to cause the rearrangement of the cytoskeletal structure (Sporn and Foster, 1992) leading to the shrinkage of endothelial cells and the opening of inter-endothelial cell junctions (Fingar, 1996) (Fig. 1A,B). This in turn results in exposure of the vascular basement membrane, which can in principle temporarily, increase vascular permeability and leakage (Fingar et al., 1997; Yamamoto et al., 1999) and also induces platelet binding and aggregation at the site of damage (Fig. 1C). The activated platelets release vasoactive mediators such as serotonin and

* Corresponding author. Ecole Polytechnique Fédérale de Lausanne, EPFL-ENAC-ISTE-LPAS, Station 6, CH-1015 Lausanne, Switzerland. Tel.: + 41 21 693 36 23; fax: + 41 21 693 36 26.
E-mail address: hubert.vandenbergh@epfl.ch (H. van den Bergh).

1537-1891/$ - see front matter © 2006 Elsevier Inc. All rights reserved.
doi:10.1016/j.vph.2006.09.006

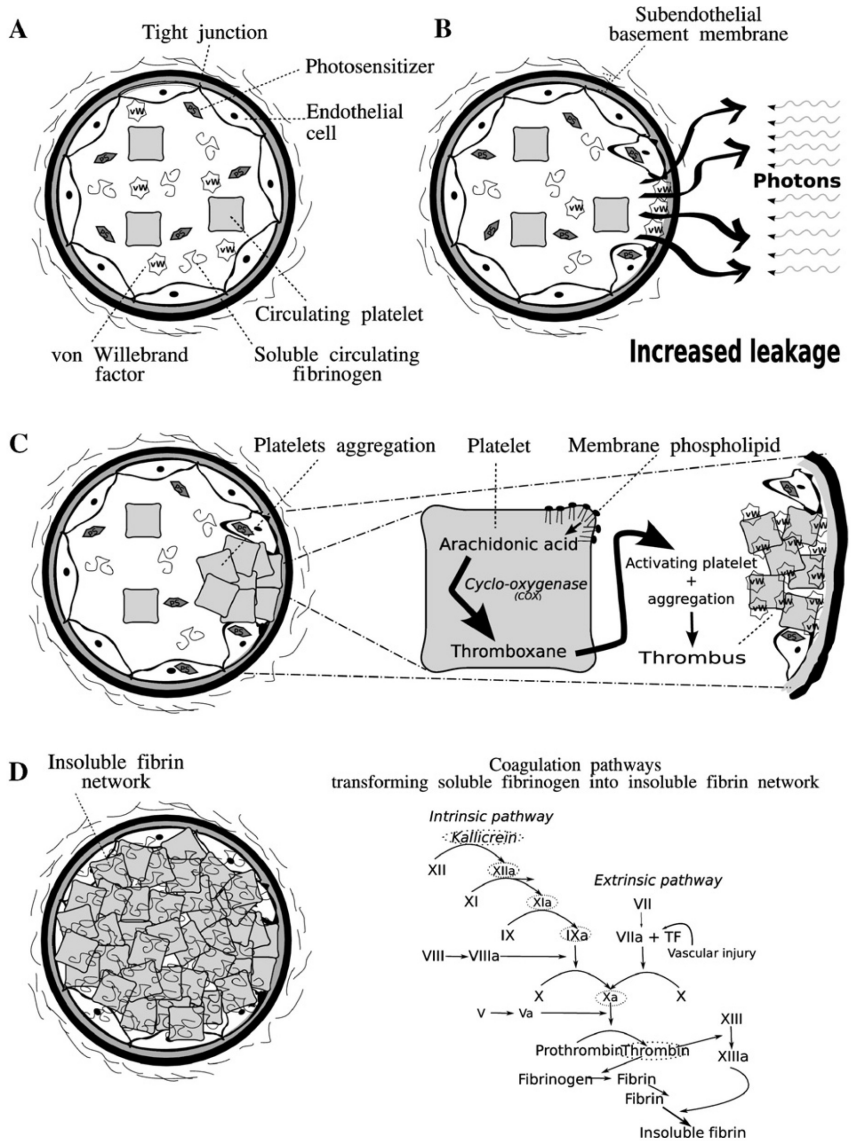

Fig. 1. Simplified Schema of the PDT-induced hemostasis pathway. PS = photosensitizer; vW = von Willebrand factor. A. A blood vessel prior to PDT. Endothelial cells lining the vessel wall are flat and linked to each other by tight junctions. B. The blood vessel treated by PDT. PDT induces oxydative stress to the endothelial cells causing modifications among others to the cytoskeleton. This damage induces a change of cell shape and opening of tight junctions. The retraction of the endothelial cells exposes parts of the subendothelial connective tissue inducing release of clotting factors such as von Willebrand factor (vWF) and might also induce an increased vessel wall permeability. C. Formation of the initial plug. vWF and other clotting factors lead to platelet activation. PDT damage to the membrane lipids also causes the release of arachidonic acid that is transformed by cyclooxygenase into thromboxane that activates and aggregates platelets. 1.D. Finally the thrombus is stabilized with fibrin by coagulation.

thromboxane that can trigger a cascade of events, including amplification of platelet activation (Yamamoto et al., 1999), coagulation and vasoconstriction (Krammer, 2001) (Fig. 1D). The final result is vascular collapse and blood flow stasis leading to the temporary or permanent occlusion of the irradiated neovascularization (Fingar, 1996; Fingar et al., 1999; Krammer, 2001). By this process, occlusion of pathological neovessels can be achieved. Visudyne® has been approved for the closure of choroidal neovessels associated with AMD by PDT (TAP Study Group, 1999; TAP Study Group, 2001; TAP Study Group, 2002a; TAP Study Group, 2002b; TAP Study Group, 2002c). However one possible drawback is the lack of selectivity for the choroidal neovessels versus normal choriocapillaries. Furthermore in a majority of cases, recurrence of the leaking choroidal neovessels following treatment is observed by indocyanine green (ICG) and/or fluorescein angiography. It has thus been reported that weeks/months after PDT, the re-opening and/or re-growth of neovessels is observed. Thus the patients are retreated on the average 2–3 times/year for at least 2 years (Miller et al., 1999;

van den Bergh, 2001; Costa et al., 2003). This renewed observation of leaky choroidal neovessels may be attributed to local hypoxia possibly combined with the release of angiogenic factors and/or inflammation following PDT. Thus one possible way to reduce the recurrence of choroidal neovessels, and consequently the number of re-treatments, is to locally add an anti-angiogenic or an anti-inflammatory agent (AACSG, accepted for publication; Krzystolik et al., 2002) during or shortly after PDT. Thus one may diminish the inflammatory and angiogenic responses to PDT and inhibit the regrowth of the neovasculature (Miller et al., 1999). If an anti-angiogenic agent or a corticosteroid is co-injected with Visudyne®, the observed PDT-induced leakage (Michels and Schmidt-Erfurth, 2003; Costa et al., 2003; Fingar et al., 1992; Schmidt-Erfurth et al., 2005) that takes place before the formation of the blood clot may then cause a significant amount of the anti-inflammatory or anti-angiogenic drug to be selectively released at the right place and at the right time, i.e. at the location where PDT is inducing the inflammatory and/or neoangiogenic response. The subsequent reduction in inflammatory and angiogenic responses should then contribute to inhibiting and delaying the regrowth and reperfusion of choroidal neovessels.

The goal of the present study was to develop a strategy aimed at maximising the local vascular permeability and leakage during and immediately after PDT with Visudyne® (Visudyne®–PDT) in order to deliver a drug that will diminish the inflammatory and/or angiogenic response and thus inhibit the recurrence of the disease. Because it has been reported (Fingar, 1996) that following the light application in PDT, a physiological cascade of responses including platelet aggregation occurs at the treated site, an increase of the time-interval between PDT-induced endothelial cell deformation and platelet aggregation should lead to extended leakage and hence, in the case of one of the proposed combination therapies, enhanced anti-angiogenic drug leakage at the site of damage. It is proposed here that this increase in PDT-induced local drug delivery can be achieved by delaying the blood clot formation. Thus, the presence of Liquemin®, which is a heparin derivative that acts as anti-coagulating agent and which inhibits the stabilisation of the thrombus with fibrin, and/or the presence of an anti-aggregating agent such as acetylsalicylic acid, aspirin, a cyclooxygenase inhibitor, should increase the desired, temporary Visudyne®–PDT-induced leakage. Here we report on enhanced leakage that has been investigated in a first assay using a fluorescent probe (Fluorescein isothiocyanate–dextran 10 kDa (FITC–dextran 10 kDa)) (Mori et al., 1997) in the vasculature of the chorioallantoic membrane (CAM) of the chicken embryo that we used as an *in vivo* model.

2. Materials and methods

2.1. Materials

Visudyne® (verteporfin, BPD-MA associated with liposomes) was obtained from Novartis (Hettlingen, Switzerland) and its reconstitution was performed shortly before i.v. injection as recommended by Novartis. Liquemin® was provided by Roche Pharma (Reinach, Switzerland) and aspirin by Bayer (Zürich, Switzerland). Sulforhodamine 101 (R101) was obtained from Fluka Biochemika (Buchs, Switzerland). Fluorescein isothiocyanate dextran 10 kDa (FITC–dextran 10 kDa) was obtained from Sigma-Aldrich (Buchs, Switzerland). Phosphate-buffered saline (PBS) was provided by Life Technologies (Invitrogen Corporation, UK), NaCl 0.9% by B. Braun (Emmenbrücke, Switzerland) and glucose 5% solution by Bichsel (Interlaken, Switzerland). Fertilized chicken eggs were provided by Animalco (Staufen, Switzerland).

2.2. Methods

2.2.1. CAM preparation

For fluorescence pharmacokinetic and PDT studies, fertilized chicken eggs were disinfected and transferred into a hatching incubator set at 37 °C and 60% humidity equipped with an automatic rotator (SARL SAVIMAT, Chauffry, France) that was activated during the first 2 days. On the third day of embryo development (EDD3), an approximately 3 mm diameter hole was bored into the eggshell at the narrow apex and then covered with a cling foil. Egg incubation was then continued in a static position. On EDD13, the holes were extended to a diameter of about 3 cm and the embryos were placed under an epi-fluorescence microscope (Nikon Eclipse E600 FN, Japan) equipped with a Nikon objective CFI achromat (magnification 4X, N.A.=0.10, Working Distance=30 mm) and with an F-view II 12 bit monochrome Peltier-cooled digital CCD camera driven with analySIS® docu software from Soft Imaging System (Münster, Germany). For the estimation of all drug doses, the mean embryo weight at EDD 13 was considered to be 10 (Romanoff, 1967).

2.2.2. Vascular occlusion assessment and leakage study during PDT with Visudyne®

2.2.2.1. Vascular occlusion assessment. On EDD 13, the eggs were placed under the microscope and a small Teflon ring (internal ∅ 5 mm) was placed on the CAM and used as a marker, in order to easily find again the treated area on the following day. Prior to dye injection, an autofluorescence image of the CAM surface was recorded. Subsequently, an intravenous (i.v.) injection (Hornung et al., 1999) of the reconstituted

Table 1
The occlusion scale based on the size of blood vessels observed to be closed by PDT in the CAM model

Occlusion scale	Observable criteria
0	No occlusion.
1	Partial occlusion of capillaries (∅<10 μm).
2	Complete closure of capillaries and partial closure of blood vessels (∅<30 μm) as well as size reduction of bigger blood vessels.
3	Closure of vessels (∅<30 μm) and partial closure of bigger vessels.
4	Total closure of vessels (∅<70 μm) and partial closure of bigger vessels.
5	Total occlusion of all vessels in the irradiated area.

photosensitizer Visudyne® (2 μg/embryo, corresponding to 0.2 mg/kg body weight (b.w.)) was performed *in situ* under the microscope and its circulation was observed by Visudyne®-specific fluorescence microscopy (λ_{exc}=420±20 nm; λ_{em}≥610 nm)(Chroma Technology Corps, Rockingham, USA). About 1 min after the i.v. injection, the photosensitizer fluorescence indicated that the Visudyne® was apparently homogeneously distributed in the blood vessel and PDT was performed using light from a filtered Hg-arc lamp at 420±20 nm at a fluence rate of 167 mW/cm^2. A light dose of 20 J/cm^2 was applied to the CAM surface determined by an excitation diaphragm. In order to compare the time-dependent occlusion of blood vessels and the blood flow stasis induced by PDT, an observation of the vascular occlusion was undertaken immediately after illumination and again 18 h later by means of fluorescence angiography. The latter was performed by an i.v. injection of 20 μl of a 0.9% saline solution containing 5 mg of sulforhodamine 101 (R101)/ml. Between these measurements the eggs were re-covered with cling foil and returned to the incubator for 18 h. Fluorescence angiographies pre- and post-PDT were compared and photothrombic efficacy was visually assessed for each CAM according to the vessel closure efficacy using the scoring procedure described in Table 1 (Gottfried et al., 1995; Hammer-Wilson et al., 1999; Lange et al., 2001). For each light dose, at least 5 embryos were used and the resulting photothrombic efficacies were averaged.

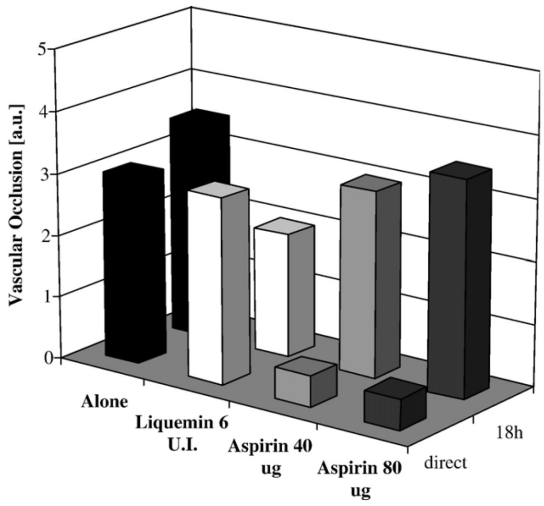

Fig. 2. Comparison of the vascular occlusion obtained in the CAM model directly and 18 h after PDT with Visudyne® (2 μg/embryo intravenously injected 1 min prior to irradiation) and a light dose of 20 J/cm^2 (λ_{ex}=420±20 nm). Four cases are shown: PDT alone; PDT when Visudyne® was co-injected with Liquemin® (6 U.I./embryo), and PDT with 2 doses of co-injected aspirin (40 μg and 80 μg/embryo). For all drug dose estimates, the mean embryo weight at EDD 13 was considered to be 10 g.

2.2.2.2. Fluorescence pharmacokinetic studies for measuring vessel leakage. The fluorescence pharmacokinetic profile of FITC–dextran 10 kDa was determined as follows. Typically, 1 min after injecting the Visudyne®, a volume of 20 μl containing FITC–dextran 10 kDa (25 mg/ml PBS) was intravenously (i.v.) injected under the microscope just before applying the light for the PDT. Fluorescence images of the CAM surface were recorded as a function of time at regular intervals over a 15 min period, using excitation light from a Hg-arc lamp filtered for excitation at 470±20 nm that mostly permits to avoid exciting Visudyne® and long pass emission filter (λ>520 nm) for observation of the FITC–dextran fluorescence.

Using ImageJ (''Image Processing with ImageJ'', ImageJ, U. S. National Institutes of Health, Bethesda, USA), at least 5 regions of interest (ROI) are chosen just outside the blood vessels and the mean fluorescence value was calculated for the ROI situated in the treated and in the non-treated areas. Thus the time-dependent evolution of the mean FITC–dextran fluorescence intensity outside the blood vessels was measured for both PDT-treated and non-treated areas. The linear correlation of this time dependence has been extracted and the ratio of these linear correlation coefficients was calculated. This ratio then should not be too sensitive to the inhomogeneity of illumination of the images. This ratio is then used to quantify the local PDT-induced increase of leakage of the FITC–dextran 10 kDa solution in PDT-treated versus non-treated areas. Again, at least 5 embryos were injected for each experimental condition and at least 5 ROI were defined for each embryo to obtain a mean value of the PDT-induced leakage.

2.2.3. The influence of Liquemin® and aspirin on PDT-induced vascular occlusion and leakage

2.2.3.1. The influence of Liquemin® and aspirin on PDT-induced vascular occlusion. To evaluate the influence of these anti-coagulating and anti-aggregating agents on PDT-induced vascular closure, a number of experimental conditions were defined. First, Liquemin®, the anti-coagulating agent (Novacek et al., 1997), was i.v. administered (6 I.U./20 μl PBS, corresponding to 600 I.U./kg b.w.) in a co-injection with Visudyne® (2 μg) 1 min prior to the start of the irradiation, in order to try to at least temporarily inhibit the coagulation at the site of damage. Second, aspirin (Stern et al., 1992; Taber et al., 1993), a well known cyclo-oxygenase inhibitor which significantly reduces platelet aggregation, was i.v.

Fig. 3. PDT on CAM blood vessels using intravenously applied Visudyne® (2 μg/embryo). (A) Visudyne® fluorescence angiography 10 s before irradiation (λ_{ex}=420±20 nm; λ_{em}>610 nm, exposure time 1 s). (B) Visudyne® fluorescence angiography (λ_{ex}=420±20 nm; λ_{em}>610 nm, exposure time 1 s) during irradiation. The encircled diameter of the irradiated area is 2 mm; irradiation conditions: 20 J/cm^2, 60 s after (co-)injection of the drug(s) (2 μg Visudyne®/embryo). The bar in (1B) representing 400 μm is the same for all images. (C) Sulforhodamine 101 (R101) fluorescence angiography (λ_{ex}=500–550 nm; λ_{em}>610 nm, exposure time 1 s) showing the vascular occlusion induced in the circular irradiated area directly or 18 h after PDT. (1C) Direct vascular occlusion when Visudyne® was injected alone. (2C) Vascular occlusion observed 18 h after treatment when Visudyne® was injected alone (3C) Direct vascular occlusion when Visudyne® was co-injected with Liquemin® (6 U.I./embryo) (4C) Vascular occlusion observed 18 h after treatment when Visudyne® was co-injected with Liquemin® (6 U.I./embryo) (5C) Direct vascular occlusion when Visudyne® was co-injected with aspirin (40 μg/ embryo) (6C) Vascular occlusion observed 18 h after treatment when Visudyne® was co-injected with aspirin (40 μg/embryo) (7C) Direct vascular occlusion when Visudyne® was co-injected with aspirin (80 μg/embryo) (8C) Vascular occlusion observed 18 h after treatment when Visudyne® was co-injected with aspirin (80 μg/embryo).

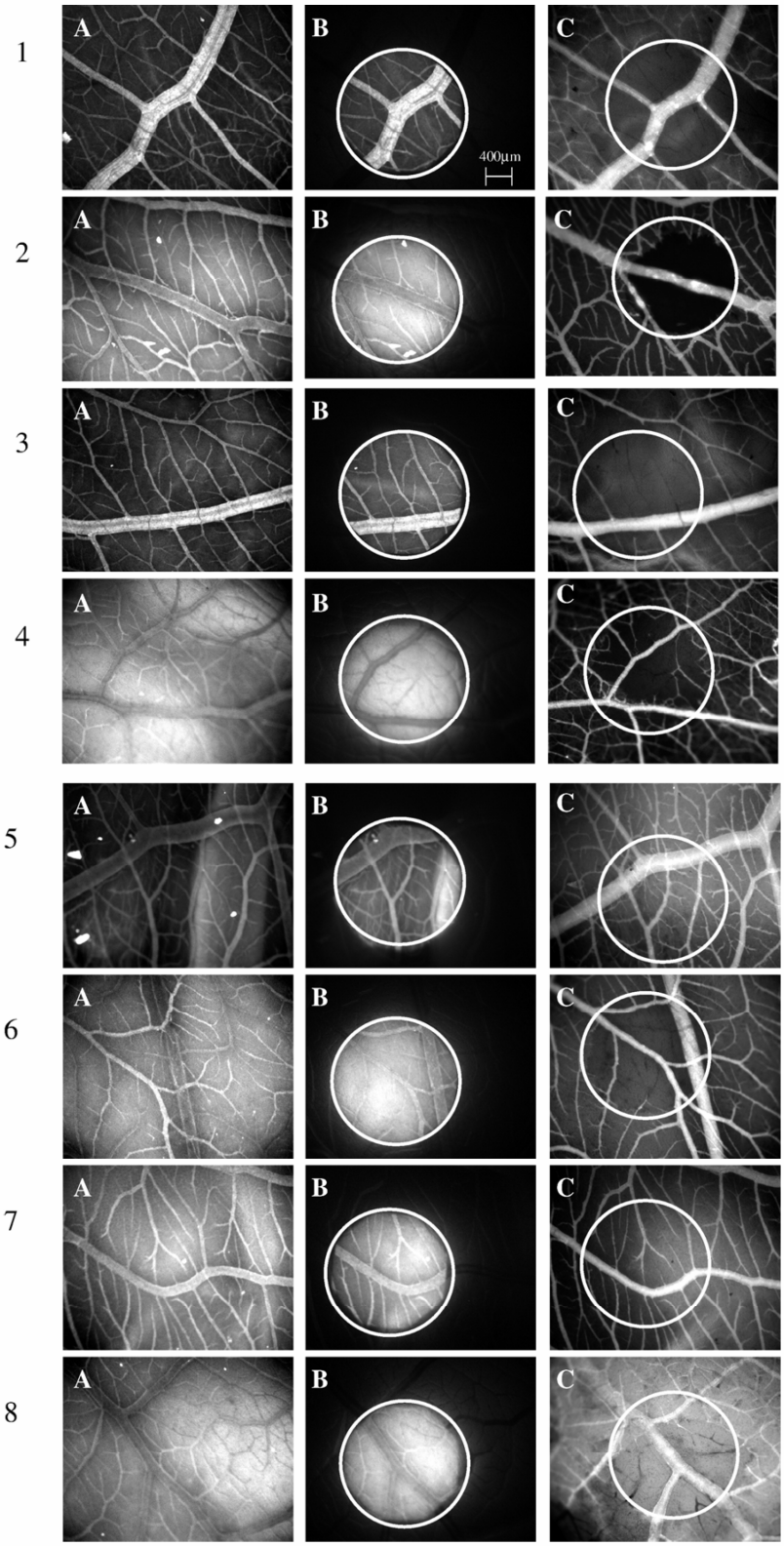
1
2
3
4
5
6
7
8
A
B
C
400µm

administered in a co-injection with Visudyne® also 1 min prior to irradiation, in order to temporarily delay the formation of the thrombus at the site of photo-damage. Two aspirin drug doses were applied: 40 μg/10 μl PBS and 80 μg/10 μl PBS, corresponding respectively to 4 mg and 8 mg/kg b.w. The vessel closure assessment was similar to the method described under 2.2.2.1. The vascular closure caused by PDT was measured at times less than 1 min after PDT (irradiation duration ≅ 2 min) and also 18 h after treatment. The vessel closures in the "combined" therapies (i.e. PDT + aspirin or PDT + Liquemin®) were compared with the closure obtained with PDT only (as described under 2.2.2.1), with the same drug and light doses.

2.2.3.2. The influence of Liquemin® and aspirin on PDT-induced dye leakage. To evaluate the influence of the anti-coagulating and the anti-aggregating agents on PDT-induced dye leakage, Liquemin® and aspirin were respectively i.v. administered into the CAM model 1 min prior to irradiation. The time-dependent evolution of the mean fluorescence intensity outside the blood vessels was measured for both treated and non-treated areas as indicated under 2.2.2.2. The ratio of the linear correlation coefficient of these values was calculated, in order to quantify the local PDT-induced increase of leakage of the FITC–dextran 10 kDa, during Visudyne®-PDT). These measurements were performed first for PDT alone, subsequently for PDT with Liquemin® (6 I.U./embryo) and finally for PDT with aspirin (2 drug doses: 40 μg and 80 μg/embryo corresponding to about 250 and 500 mg/patient). Again, at least 5 embryos were injected for each condition.

3. Results

3.1. PDT-induced vascular occlusion

In a previous study on the CAM model, the vascular occlusion observed 24 h after PDT with Visudyne® with the same drug dose and with an irradiation using a fluence of 25 J/cm^2, also at 420 ± 20 nm, was found to be at score 3 according to the same occlusion efficacy scale as used here. (Table 1)(Lange et al., 2001). The vascular occlusion observed in the present study 18 h after treatment with a radiation fluence of 20 J/cm^2 was scored between 3 and 4, showing only a very minor difference with this previous work (Lange et al., 2001) (Figs. 2 and 3.2). In the present work, we also assessed the vascular occlusion obtained directly, i.e. less than 1 min after PDT, with the same drug and light doses on the CAM model was also assessed. This vascular occlusion score was between 2 and 3 (Figs. 2 and 3.1).

To evaluate the influence of an anti-coagulating agent on PDT with Visudyne®, a co-injection of Liquemin® (6 U.I./20 μl) and Visudyne® was performed 1 min prior to PDT irradiation. The resulting vascular occlusion obtained directly after PDT scored between 2 and 3 (Figs. 2 and 3.3) and the occlusion obtained 18 h after treatment scored 2 (Figs. 2 and 3.4).

To evaluate the influence of an anti-aggregating agent on PDT with Visudyne®, a co-injection of aspirin (40 μg/20 μl) and Visudyne® was performed 1 min prior to irradiation, resulting in a very low direct occlusion score, between 0 and 1 (Figs. 2 and 3.5). Eighteen hours after treatment the occlusion score was 2 (Figs. 2 and 3.6).

A higher dose of aspirin (80 μg/20 μl) was then i.v. co-administered with Visudyne® to assess its influence on vascular occlusion. In this case a direct vascular occlusion score of 0 to 1 was observed at short delays (Figs. 2 and 3.7). It reached 3 to 4 eighteen hours after treatment (Figs. 2 and 3.8).

3.2. PDT-induced vascular leakage

To evaluate the influence of PDT with Visudyne® on the blood vessel permeability, a volume of 20 μl containing FITC–dextran 10 kDa (25 mg/ml PBS) (this concentration was always kept the same throughout this work otherwise specified) was i.v.

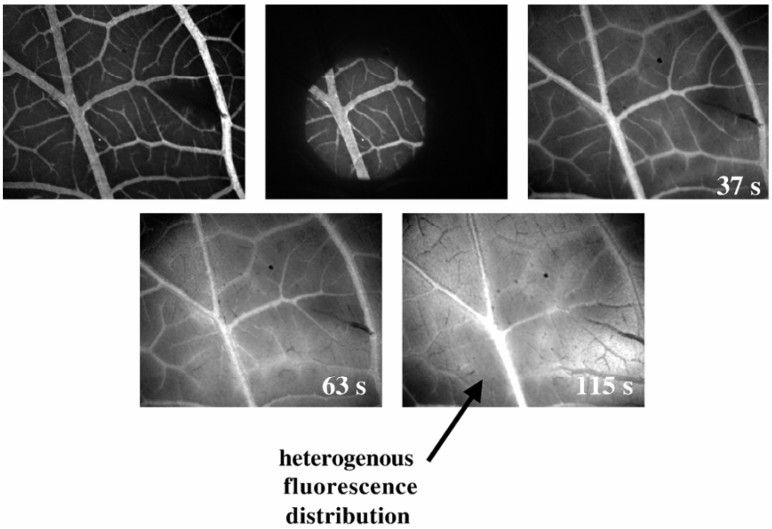

Fig. 4. These pictures show the heterogenous distribution of FITC–dextran 10 kDa after intravenous injection of the dye during PDT.

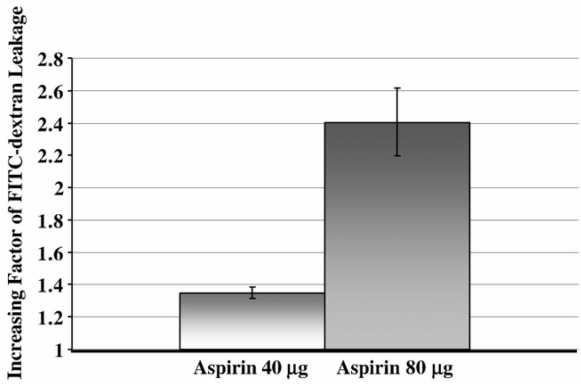

Fig. 5. Measurements of the leakage of FITC–dextran 10 kDa obtained during PDT with Visudyne® (2 µg/embryo) and 2 doses of aspirin (40 and 80 µg/embryo) intravenously co-injected 1 min before irradiation (λ_{ex}=420±20 nm; λ_{em}>610 nm) with a light dose of 20 J/cm^2. FITC–dextran 10 kDa leakage in non-treated area corresponding to 1. FITC–dextran 10 kDa was locally increased with PDT combined with aspirin 40 and 80 µg/embryo, 1.35 fold (±0.03) and 2.4 fold (±0.21) respectively.

injected under the microscope just before PDT was initiated. It was observed that as the PDT-induced vascular effects evolved, the FITC–dextran 10 kDa appeared to stick to the treated site, presenting a hyper-fluorescence in the treated area (Fig. 4). Under these conditions, the influence of PDT on the leakage profile of the fluorescent dye could not be quantified.

3.3. Influence of Liquemin® on PDT-induced leakage

To evaluate the influence of the anti-coagulating agent, Liquemin®, on PDT-induced vascular leakage (2.2.3.2), a volume of 20 µl containing FITC–dextran 10 kDa was i.v. injected under the microscope at the beginning of the PDT. As in Section 3.2 above, the dye fluorescence was observed not to be homogenously distributed in the blood stream, and thus the leakage profile could not be quantified.

3.4. The influence of aspirin on PDT-induced leakage

To evaluate the influence of an anti-aggregating agent on PDT-induced vascular leakage (2.2.3.2), aspirin was i.v. administered in a co-injection with Visudyne® also 1 min prior to irradiation and a volume of 20 µl containing FITC–dextran 10 kDa was i.v. injected just before PDT was initiated. Under these conditions, the dye was observed to be rapidly homogenously distributed in the blood stream shortly after injection. Thus, the influence of PDT on the fluorescence pharmacokinetics of FITC–dextran 10 kDa during PDT combined with aspirin (40 µg/embryo) could be assessed. The leakage of the fluorescent dye was increased locally by the combination therapy by a factor of 1.35±0.03 (Fig. 5).

To improve on this first observation of a PDT-induced leakage sustained by aspirin, the same experiment was performed with a higher dose of aspirin (80 µg/embryo). This resulted in a locally induced increase in leakage of a factor of 2.4±0.21 (Fig. 5). A typical fluorescent profile of this increased leakage is shown in Fig. 6.

4. Discussion

It has been reported that the perturbation of endothelial cell membranes by PDT results in the loss of tight junctions responsible for the sealing properties between adjacent cells, and consequently leaving enlarged gaps between cells that should increase the vascular permeability to macromolecules following the PDT (Fingar, 1996; Krammer, 2001). We observed that PDT did not have a marked effect on the vascular permeability observed under the experimental conditions used in the first part of this study (2.2.2.1; Fig. 4). This may in part be because leucocytes are not found in any great number in the circulating blood of the chick embryo until the very last days of incubation. A few young and immature white blood cells are found only prior to and shortly after hatching (Romanoff, 1967). In an adult mature model, these white blood cells would be activated in response to vascular injury and

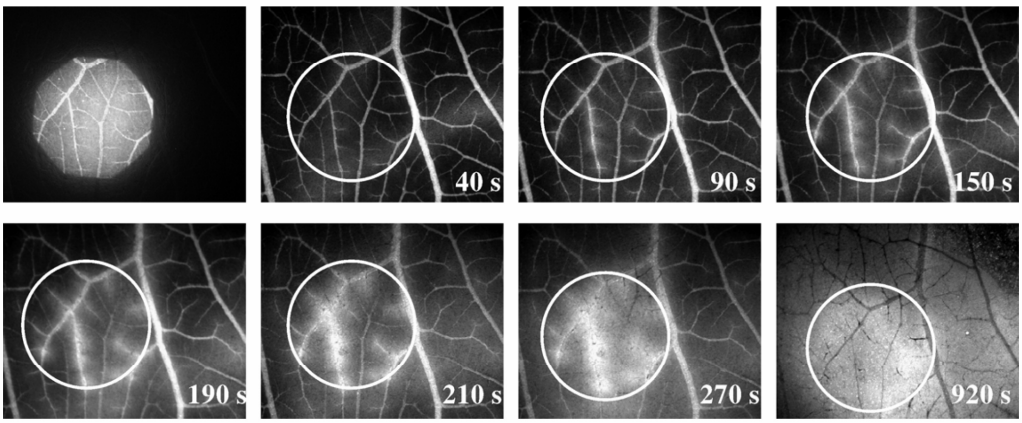

Fig. 6. Typical fluorescence pharmacokinetics obtained with FITC–dextran 10 kDa (25 mg/ml PBS) (λ_{ex}=470±20 nm) during PDT with Visudyne® (2 µg/embryo) co-injected with aspirin (80 µg/embryo) from the beginning of the irradiation (λ_{ex}=420±20 nm; λ_{em}>610 nm) with a light dose of 20 J/cm^2. The first picture shows the fluorescence of Visudyne® (2 µg/embryo) intravenously co-injected with aspirin (80 µg/embryo). Irradiation was performed 1 min after injection (λ_{ex}=420±20 nm; 20 J/cm^2). Typical fluorescence pharmacokinetic of FITC–dextran 10 kDa during this PDT showed that PDT with Visudyne® associated with aspirin significantly increases the locally FITC–dextran 10 kDa leakage.

would be likely to contribute to the increase of vascular permeability. The absence of PDT-induced leakage can in principle also be attributed to rapid platelet aggregation at the irradiated site.

Shortly after the beginning of PDT, the shrinkage of endothelial cells inducing the appearance of gaps induces rapid clogging of the blood vessel. This causes blood flow stasis and prevents the dye from leaking between the endothelial cells. Hence, to significantly enhance the PDT-induced vascular permeability, the formation of the blood clot has to be delayed. For this purpose, PDT in our case was combined with 2 drugs acting on different steps of the hemostasis. Firstly, Liquemin® was i.v. co-injected with Visudyne®, 1 min prior to irradiation. Liquemin® is a heparin derivative that, when combined with its co-factor antithrombin III, acts as anti-coagulating agent by neutralizing several coagulating activated factors (kallicrein, XIIa, XIa, IXa, Xa factors and thrombine) (Morant and Ruppaner, 2002). By means of this anti-coagulating agent, the transformation of the soluble fibrinogen into insoluble fibrin is inhibited, leading to an unstable plug, which is already partially dissolved 18 h after the PDT-treatment. This leads to decreased vascular occlusion during the 18 h following PDT. Nevertheless, Liquemin® does not influence the platelet aggregation and the formation of the early thrombus, and hence did not visibly delay the obstruction by a thrombus of the potential leakage path. Thus the fluorescent dye, FITC dextran 10 kDa, that was used to perform pharmacokinetic assays, did not show any local PDT-induced vascular leakage in this case. In fact, as shown with PDT using Visudyne® without combination therapy, the homogenous distribution of the fluorescent dye is perturbed and the FITC–dextran appears to be trapped at the PDT site as soon as the platelets begin to aggregate there, i.e. only a few seconds after the beginning of exposure with light. We thus conclude that we should try to inhibit the formation of the thrombus one step earlier, i.e. we must try to inhibit platelet aggregation instead of inhibiting coagulation. Consequently we assumed that the delay of the blood clot formation that leads to an efficient enhancement of the local vascular permeability might be achieved by the injection, prior to PDT, of a cyclo-oxygenase inhibitor such as aspirin. In fact, aspirin significantly prolongs the time required to initiate platelet aggregation (Rosenblum and El-Sabban, 1977).

Indeed, during the photodynamic treatment in the presence of aspirin (40 μg/embryo corresponding to about 250 mg/human), a rapid increase of the fluorescent dye leakage, 1.35 times greater than the corresponding case with no aspirin, could be measured exclusively in the treated area. The same PDT treatment in combination with a higher dose of aspirin (80 μg/embryo corresponding to about 500 mg/human), induced a 2.4 fold increase in leakage. We conclude that a substantial increase in vascular permeability was obtained by this approach, resulting in the enhanced leakage of FITC–dextran from blood vessels. This may well be useful for combination therapies as described below.

In a previous study, Taber et al. (1993) evaluated the effects of aspirin on microvasculature after PDT in a cremaster muscle model and in a tumour interstitial pressure model in Sprague–Dawley rats. The photosensitizer used was Photofrin®. A very high dose of aspirin (100 mg/kg) was intraperitoneally administered prior to light treatment and the changes in vascular permeability to macromolecules were measured by monitoring the leakage of an FITC-albumin solution. Under these conditions, no enhancement of the vascular leakage was observed. This may in part be due to the high molecular weight of the albumin (66 kDa) used by these investigators, as compared to the FITC–dextran 10 kDa used for this study, or else due to the difference in animal model used (Romanoff, 1967). In our study, FITC was coupled with a smaller molecular weight molecule, the 10 kDa dextran. The size of the FITC-coupled dextran was chosen in our case from among 5 sizes (10, 20, 40, 70 and 250 kDa) by measuring their fluorescence pharmacokinetics in standard conditions (without PDT) in our CAM model (data not shown). One of the reasons for the choice of the 10 kDa dextran for the present study was the observation of a slight leakage without PDT. This was obtained with FITC 20 and 10 kDa. The latter was chosen for this study. The comparison between the PDT-induced leakage of different dextran sizes in the presence of various doses of aspirin is currently under investigation.

Another significant difference between this study and that of Taber et al. is the administration pathway and the dose of aspirin. In fact, aspirin has different therapeutic effects depending on the drug dose and administration pathway. In addition to its influence on platelet cyclo-oxygenase, aspirin inhibits the activity of platelet adenylate cyclase found in the platelet membrane. The effect is probably caused by an unspecific acetylation of platelet membrane proteins, something that has already been suggested following the observation of platelet shape changes during aspirin therapy. Thus, high doses of aspirin suppress not only prostaglandin plasma levels but also make the platelets less sensitive to the dis- and anti-aggregatory effects of this prostaglandin. Since platelet adenylate cyclase activity during low-dose aspirin treatment is not changed, but the anti-aggregating effect is well preserved, aspirin should be taken in relatively small doses if used as anti-platelet drug (Janka, 1981).

In the present study, the extent of vascular occlusion induced by PDT with Visudyne® combined with aspirin was assessed immediately after, as well as 18 h after the light treatment and compared with the vascular occlusion induced by PDT with Visudyne® alone. As shown in Figs. 2 and 3.5, blood vessels treated by PDT with Visudyne® combined with aspirin showed little occlusion directly after treatment. Despite this, fluorescence angiography performed 18 h post-irradiation exhibited a substantial vascular closure suggesting that under these experimental conditions, blood flow stasis is due to time-delayed effects appearing during the 18 h post-irradiation. This may be explained by the fact that by inhibiting blood clotting, aspirin delayed the activation of a cascade of chemical and physiological responses that normally lead to vascular collapse and blood flow stasis. This was previously observed by Reed et al. in a study evaluating the inhibition of the microcirculation response to “early” PDT by prostanoid antagonists (Reed et al., 1991). Directly after administration of the salicylic acid derivative aspirin, circulating platelets are irreversibly inhibited by acetylation. Acetylsalicylic acid inhibits both cyclo-

oxgenase I and II, that can lead to a dramatic decrease of thromboxane A_2 synthesis, and that in turn leads to an inactivation of platelet aggregation. Because platelets are degenerated cells without any nucleus, inhibition induced by aspirin is irreversible (Morant and Ruppaner, 2002). Nevertheless, with low drug doses i.v. administered in bolus, almost 30% of the acetylsalicylic acid injected is transformed into salicylic acid in the liver on first passage. This metabolite, unlike the aspirin, has a reversible activity on COX-I. Thus, after clearance of the drug, the platelets inhibited by this metabolite can recover their aggregating properties and thus old platelets, irreversibly inhibited by acetylsalicylic acid, are replaced by new functional ones. This may explain why the extent of occlusion of the irradiated vascularization induced by the aspirin and PDT combination therapy was marginally less important than that obtained with Visudyne®–PDT (Figs. 4,5).

We hence deduce that a combination therapy could take advantage of the transiently enhanced vascular permeability with PDT associated with aspirin, in order to selectively locally release chemotherapeutic or other agents. Indeed, it should be possible to inject the Visudyne® together with aspirin and a smaller amount of steroid, or an alternative substance such as a VEGF receptor inhibitor, so that the PDT-induced leakage that takes place before the formation of the thrombus, will cause the steroid to be selectively released at the place and time where it is needed, i.e. at the location where PDT is inducing the inflammatory and angiogenic responses. The reduction in inflammatory and angiogenic responses should then lead to a delayed regrowth and/or reperfusion of neovessels that can in turn improve the therapeutic outcome (i.e. reduce the number of treatments) of PDT of choroidal neovessels associated with AMD.

This concept of enhanced PDT-induced local drug release and combination therapy could also be tested in the treatment of cancer or other diseases like rheumatoid arthritis. The injection of a reduced amount of a chemotherapeutic drug (or larger amounts of such drugs with a short body half-life) could be effective due to enhanced local delivery rendered possible by combining Visudyne-PDT with aspirin. When applying the PDT, the resulting enhanced vascular leakage would release the chemotherapeutic drug selectively at the site of the cancer, and this will be followed by PDT-induced closure of most of the smaller blood vessels. The synergy of the local chemotherapy with local closure of the blood vessels that supply the tumour could then lead to new and more effective treatment possibilities for various neoplasms. A similar suggestion, but without the use of the aspirin-enhancing effect, has been made by Snyder et al. (2003) who showed some leakage of a chemotherapeutic agent after "low dose" PDT in another animal model using a different photosensitizer. Our goal in the present paper is clearly different from theirs in that we deposit a second drug (i.e. which might be a chemotherapeutic or another drug like an angiostatin) as a co-therapy, using the aspirin-enhanced leakage induced by PDT, while at the same time preserving the photothrombic efficacy of PDT for closing blood vessels. This delayed closure of vessels has been observed to occur without loss of its efficacy as compared to the case where aspirin is not used. It should probably be noted that for the PDT of larger tumours, interstitial radiation applied with an optic fibre can be used so that methods proposed here are not limited to small superficial neoplasms. Indeed many pathologies involving significant neovascularisation may make good candidates for the new combination of treatments with PDT that is suggested above.

5. Conclusion

In this study, we establish that the permeability of the CAM vessels is strongly influenced by the photodynamic treatment when combined with aspirin. Delay in the clotting of blood by a cyclo-oxygenase inhibitor appears to be a pivotal process in enhancing vascular permeability. After a delay of approximately 18 h, vessels in the irradiated region were still observed to be closed efficiently following PDT with aspirin. The vessel closure under these conditions is essentially as effective as the closure at shorter times with no aspirin present. We are currently investigating how to take advantage of this effect in order to develop a novel combination therapy approach, i.e. such transiently enhanced vascular permeability in PDT could be used to selectively release an anti-angiogenic or anti-inflammatory factor to prevent recurrence of the neovasculature in the case of AMD or to release chemotherapeutic agents in the case of PDT of a malignant tumour.

References

D'Amico, D.J., et al., 2003. Anecortave Acetate as Monotherapy for the Treatment of Subfoveal Lesions in Patients with Exudative Age-related Macular Degeneration (AMD): Interim (Month 6) Analysis of Clinical Safety and Efficacy. Retina 23 (1), 14–23.

Costa, R.A., et al., 2003. Immediate indocyanine green angiography and optical coherence tomography evaluation after photodynamic therapy for subfoveal choroidal neovascularization. Retina 23 (2), 159–165.

Fingar, V.H., 1996. Vascular effects of photodynamic therapy. J. Clin. Laser Med. Surg. 14 (5), 323–328.

Fingar, V., et al., 1992. The role of microvascular damage in photodynamic therapy — the effect of treatment on vessel constriction, permeability and leucocyte adhesion. Cancer Res. 52 (18), 4914–4921.

Fingar, V.H., Wieman, T.J., Haydon, P.S., 1997. The effects of thrombocytopenia on vessel stasis and macromolecular leakage after photodynamic therapy using photofrin. Photochem. Photobiol. 66 (4), 513–517.

Fingar, V.H., et al., 1999. Analysis of acute vascular damage after photodynamic therapy using benzoporphyrin derivative (BPD). Br. J. Cancer 79 (11–12), 1702–1708.

Gottfried, V., et al., 1995. In vivo damage to chorioallantoic membrane blood vessels by porphycene-induced photodynamic therapy. J. Photochem. Photobiol., B Biol. 30 (2–3), 115–121.

Hammer-Wilson, M.J., et al., 1999. Photodynamic parameters in the chick chorioallantoic membrane (CAM) bioassay for topically applied photosensitizers. J. Photochem. Photobiol., B Biol. 53 (1–3), 44–52.

Hornung, R., et al., 1999. Systemic application of photosensitizers in the chick chorioallantoic membrane (CAM) model: photodynamic response of CAM vessels and 5-aminolevulinic acid uptake kinetics by transplantable tumors. J. Photochem. Photobiol., B Biol. 49 (1), 41–49.

Janka, H.U., 1981. Inhibition of platelet adenylate–cyclase by aspirin — a further argument for a low-dose regimen in anti-platelet drug-therapy. IRCS Med. Sci., Biochem. 9 (11), 1019-1019.

Krammer, B., 2001. Vascular effects of photodynamic therapy. Anticancer Res. 21 (6B), 4271–4277.

Krzystolik, M.G., et al., 2002. Prevention of experimental choroidal neovascularization with intravitreal anti-vascular endothelial growth factor antibody fragment. Arch. Ophthalmol. 120 (3), 338–346.

Lange, N., et al., 2001. A new drug-screening procedure for photosensitizing agents used in photodynamic therapy for CNV. Investig. Ophthalmol. Vis. Sci. 42 (1), 38–46.

Michels, S., Schmidt-Erfurth, U., 2003. Sequence of early vascular events after photodynamic therapy. Investig. Ophthalmol. Vis. Sci. 44 (5), 2147–2154.

Miller, J.W., et al., 1999. Photodynamic therapy with verteporfin for choroidal neovascularization caused by age-related macular degeneration: results of a single treatment in a phase 1 and 2 study. Arch. Ophthalmol. 117 (9), 1161–1173.

Morant, J., Ruppaner, H., 2002. Compendium Suisse des Médicaments. Documed SA, Basel, Switzerland.

Mori, K., et al., 1997. Angiography by scanning laser ophthalmoscope with fluorescein compounds of different physicochemical properties. Nippon Ganka Gakkai Zasshi 101 (4), 318–326.

Novacek, G., et al., 1997. Enhanced blood coagulation and enhanced fibrinolysis during hemodialysis with prostacyclin. Thromb. Res. 88 (3), 283–290.

Reed, M.W., Schuschke, D.A., Miller, F.N., 1991. Prostanoid antagonists inhibit the response of the microcirculation to ''early'' photodynamic therapy. Radiat. Res. 127 (3), 292–296.

Romanoff, A.L., 1967. Biochemistry of the Avian Embryo: a Quantitative Analysis of Prenetal Development. John Wiley and Sons, New York, p. 398.

Rosenblum, W., El-Sabban, F., 1977. Platelet-aggregation in cerebral microcirculation—effect of aspirin and other agents. Circ. Res. 40 (3), 320–328.

Schmidt-Erfurth, U., et al., 2005. Time course and morphology of vascular effects associated with photodynamic therapy. Ophtalmology 112 (12), 2061–2069.

Sharman, W.M., Allen, C.M., van Lier, J.E., 1999. Photodynamic therapeutics: basic principles and clinical applications. Drug Discov. Today 4 (11), 507–517.

Snyder, J.W., et al., 2003. Photodynamic therapy: a means to enhanced drug delivery to tumors. Cancer Res. 63 (23), 8126–8131.

Sporn, L.A., Foster, T.H., 1992. Photofrin and light induces microtubule depolymerization in cultured human endothelial cells. Cancer Res. 52 (12), 3443–3448.

Stern, S.J., et al., 1992. Effect of aspirin on photodynamic therapy utilizing chloroaluminum sulfonated phthalocyanine (CASP). Lasers Surg. Med. 12 (5), 494–499.

Taber, S.W., Wieman, T.J., Fingar, V.H., 1993. The effects of aspirin on microvasculature after photodynamic therapy. Photochem. Photobiol. 57 (5), 856–861.

TAP Study Group, 1999. Photodynamic therapy of subfoveal choroidal neovascularisation in age-related macular degeneration with verteporfin. One year results of 2 randomized clinical trials. TAP report 1. Arch. Ophthalmol. 117 (10), 1329–1345.

TAP Study Group, 2001. Photodynamic therapy of subfoveal choroidal neovascularization in age-related macular degeneration with verteporfin: two-year results of 2 randomized clinical trials—TAP report 2. Arch. Ophthalmol. 119, 198–207.

TAP Study Group, 2002a. Verteporfin therapy for subfoveal choroidal neovascularization in age-related macular degeneration. three-year results of an open-label extension of 2 randomized clinical trials — TAP report 5. Arch. Ophthalmol. 120 (10), 1307–1314.

TAP Study Group, 2002b. Verteporfin therapy of subfoveal choroidal neovascularization in patients with age-related macular degeneration: additional information regarding baseline lesion composition's impact on vision outcomes—TAP report No. 3. Arch. Ophthalmol. 120 (11), 1443–1454.

TAP Study Group, 2002c. Effects of verteporfin therapy on contrast on sensitivity: results from the treatment of age-related macular degeneration with photodynamic therapy (TAP) investigation—TAP report No 4. Retina 22 (5), 536–544.

van den Bergh, H., 2001. Photodynamic therapy of age-related macular degeneration: history and principles. Seminars in Ophthalmology 16 (4), 181–200.

Yamamoto, Y., et al., 1999. Fibrin plugging as a cause of microcirculatory occlusion during photodynamic therapy. Lasers Med. Sci. 14 (2), 129–135.

Chapitre 3

Controlled FITC-dextran Leakage Induced by Combination of photodynamic Therapy and Different doses of Aspirin: Arterial and venous responses in the CAM model

Submitted to Vascular Pharmacology

Controlled FITC-dextran Leakage Induced by Combination of Photodynamic Therapy and Different Doses of Aspirin: Arterial and Venous Responses in the CAM model

Debefve E., Pegaz B., Ballini J-P and van den Bergh H.

Ecole Polytechnique Fédérale de Lausanne (EPFL), Laboratory of Photomedicine, CH-1015 Lausanne, Switzerland.

§Abstract

In exudative age-related macular degeneration (AMD) the goal of photodynamic therapy (PDT) is to occlude the proliferative neovessels. The main drawback of PDT in AMD is the reappearance of the pathological neovasculature a few weeks after their occlusion. This could be avoided by adding an anti-angiogenic and/or an anti-inflammatory drug at the treated site, using an efficient local drug delivery. In a former study performed in the chorioallantoic membrane (CAM) model, we demonstrated that PDT locally increases the leakage of macromolecules before occluding the treated vessels when aspirin is used to delay the blood clot formation. This PDT-induced local vascular leakage could then be used to perform a local photodynamic drug delivery. In this framework, to better understand and to optimize the combination therapy pathway, the aim of the present study is to assess this controlled leakage with FITC-dextran, using different aspirin doses (from 4 to 64 mg/ kg b.w.) and to compare the PDT effects on arteries and veins in the CAM model. We observed that arteries and veins present different kinetics of photo-occlusion pathways during photodynamic therapy, but no statistical difference in the PDT-induced vascular permeability.

§ **Corresponding author:** Prof. H. van den Bergh
Ecole Polytechnique Fédérale de Lausanne
Faculté des Sciences de base
Laboratory of Photomedicine
EPFL Station 6 CH-1015 Lausanne, Switzerland.
Tel: + 41 21 693 36 23
Fax:+ 41 21 693 36 26
E-mail : hubert.vandenbergh@epfl.ch

Keywords: Photodynamic therapy; Aspirin; Arteries; Veins; Visudyne®; Vascular leakage; Fluorescein isothiocianate dextran (FITC-dextran); CAM; Photodynamic drug delivery; Photo-occlusion.

Introduction

In exudative age-related macular degeneration (AMD), the goal of photodynamic therapy (PDT) is to close the leaking choroidal neovascularisation (CNV) [1]. This photodynamic closure of the CNV should be selective, i.e. with the least possible damage (closure) of the retinal capillaries, of the normal choroidal capillaries and of the deeper lying larger choroidal and feeder vessels. Closure of the small physiological retinal vessels for instance can lead to immediate blindness at this point. As PDT damage also tends to enhance cytokines like vascular endothelial growth factor (VEGF) [2-5], as well as inflammation [6, 7] and hypoxia [8, 9], suggestions have been made to try to combine the PDT treatment modality with the local application of an anti-VEGF compound and/or an anti-inflammatory substance. The combination therapy between PDT and an anti-VEGF agent appears to be attractive in that PDT closes the CNV effectively, and the added VEGF blockers should help both to maintain the PDT effect and slow down, or even invert, the progression of the disease [10-13].

In the clinical trials for the PDT of CNV associated with AMD, some enhanced leakage of the irradiated vasculature was observed [14-16]. This may be due to the light-induced microtubule depolymerisation in the endothelial cells, which were previously exposed to the photosensitiser [17-20]. This damage to the microtubules and the cytoskeleton can lead to shrinkage and deformation of the endothelial cells, and rupture of inter-endothelial cell junctions [2, 8, 21-24]. The latter in turn may result in enhanced leakage. It has previously been suggested that this enhanced leakage can be used to locally dose a drug that is useful in combination therapy [25, 26]. For instance in the case of PDT of CNV related to AMD, one could locally enhance delivery of an anti-VEGF agent [11, 27], whereas in PDT of cancer one could locally enhance delivery of an anti-tumor substance. We have

furthermore suggested that such enhanced local drug delivery can be further improved upon by adding a cyclo-oxygenase inhibitor to the process [25]. Thus we have shown that the addition of aspirin can delay the cascade of coagulation induced by damage to the endothelium which finally leads to vessel occlusion and blood flow stasis [21, 22, 28-32]. This aspirin-induced delay in the blood coagulation process, and the subsequent enhanced leakage of a macromolecular substance from the damaged tissue, was demonstrated in the chorioallantoic membrane (CAM) of the chicken embryo [25]. Although as yet it is not clear which parameters could be modified to induce the same enhanced leakage, in the case of exudative AMD in humans, we report here on 1) a study of the influence of aspirin dose on the enhanced leakage of a macromolecule (FITC-10 kDa) and 2) a comparison between the PDT-induced vascular occlusion during the treatment in the two kinds of blood vessels, artery and vein. As they are physiologically different and as the concentration of oxygen differs in these two types of vessels, the PDT was performed to observe the different pathways of vessel occlusion, vasoconstriction and thrombus formation following treatment. The leakage phenomenon was then observed separately on arteries and veins to appreciate the potential difference of leakage attributed to the different thrombogenicity of these two kinds of vessels.

Materials and methods

Materials

Visudyne® (verteporfin, BPD-MA) [33] was obtained from Novartis (Hettlingen, Switzerland) and Aspegic Inject®, an injectable formulation of aspirin [33], by Sanofi-Synthélabo (Meyrin, Switzerland). This formulation of aspirin was used for the whole study. Sulforhodamine 101 (R101) was provided by Fluka Biochemika (Buchs, Switzerland). Fluorescein isothiocyanate dextrans (FITC-dextran 10 kDa and 150 kDa) were obtained from Sigma-Aldrich (Buchs, Switzerland). Phosphate buffer saline (PBS) was provided by Life Technologies (Invitrogen Corporation, UK), NaCl 0.9% by B. Braun (Emmenbrücke, Switzerland) and glucose 5% solution by Bichsel (Interlaken, Switzerland). Fertilised chicken eggs were provided by Animalco (Staufen, Switzerland).

Methods

CAM model

For fluorescence pharmacokinetic and PDT studies, fertilised chicken eggs were disinfected and transferred into a hatching incubator set at 37°C and 60 % humidity equipped with an automatic rotator (SARL SAVIMAT, Chauffry, France) that was activated during the 2 first days. On the third day of embryo development (EDD3), an approximately 3 mm diameter hole was bored into the eggshell at the narrow apex and then covered with a cling foil. Egg incubation was then continued in a static position. On EDD13, the holes were extended to a diameter of about 3 cm and the embryos were placed under an epi-fluorescence microscope (Nikon Eclipse E600 FN, Japan) equipped with a Nikon objective CFI achromat (magnification 4X, N.A.=0.10, Working Distance=30 mm; or Plan Fluor magnification 10X, N.A. =0.30, W.D.= 16 mm) and with a Peltier cooled Electron Multiplier CCD Digital Camera C9100-12 (EM-CCD) (Hamamatsu, Japan) driven with High Performance Image Control System (HiPic 32) software. This allowed us to record images with a higher dynamic range, up to 16 bits grey levels, with a high controlled sensitivity. For the estimation of all drug doses, the mean embryo weight at EDD 13 was considered to be 10g [34].

Photodynamic therapy followed by fluorescence pharmacokinetic studies for dosing vessel leakage

Photodynamic therapy

On EDD 13, the eggs were placed under the microscope and a small Teflon ring (internal ∅ 5 mm) was placed on the CAM in order to easily visualise the treated area on the following day. Prior to dye injection, an autofluorescence image of the CAM surface was recorded. Subsequently, an intravenous (i.v.) co-injection [35] of the photosensitiser Visudyne® (2μg/embryo, corresponding to 0.2 mg/ kg body weight (b.w.)) and Aspegic Inject® (4 different doses for arteries and 3 different doses for veins between 40 and 640 μg/embryo, respectively corresponding to 4 to 64 mg/ kg b.w.) was performed *in situ* under the microscope and the circulation was observed by Visudyne®-specific fluorescence microscopy (λ_{exc}= 420 ± 20 nm; λ_{em}≥ 610 nm). One minute after the i.v. injection, the photosensitiser is well homogeneously distributed in the blood vessel and

PDT was performed using light from a filtered Hg-arc lamp at 420 ± 20 nm with a magnification 10x objective at a fluence rate of 150 mW/cm^2. A light dose of 20 J/cm^2 was applied to a circular CAM surface with a diameter of 680 μm defined with a controlled excitation diaphragm, comprising a vessel (either artery or vein) with a diameter between 150 and 200 μm. In order to verify the efficacy of the blood flow stasis and vascular occlusion induced by PDT, observations of the vascular occlusion was undertaken during the irradiation and 18 hours after illumination by means of fluorescence angiographies. The latter was performed by an i.v. injection of 20 μl of a solution containing 25 mg of FITC-dextran/ml. Between the treatment and this measurement, the eggs were re-covered with cling foil and returned to the incubator. Fluorescence angiographies pre- and post- PDT were compared and photothrombic efficiency was assessed according to the vessel closure efficacy using an arbitrary score [36-38]. For each condition, at least 5 embryos were used and the resulting photothrombic efficiencies were averaged.

Fluorescence pharmacokinetic studies for measuring vessel leakage

The fluorescence pharmacokinetic profile of FITC-dextran 10 kDa was determined as follows. Typically, a volume of 20 L containing FITC-dextran (25 mg/ml PBS) was intravenously (i.v.) injected under the microscope directly after the PDT. At regular time intervals, fluorescence images of the CAM surface were recorded as a function of time over a 8 minute period, using excitation light from a Hg-arc lamp filtered for excitation at 470 ± 20 nm and long pass emission filter (λ > 520 nm), with a magnification 4x objective.

The time-dependent evolution of the FITC-dextran fluorescence at the treated site was quantified and compared to the surrounding non-treated areas.

As the excitation by the Hg-arc lamp is not entirely homogenous (decreasing from the centre to the surrounding of the irradiated field) and to allow comparison of the results (that can change in time principally due to the change in power of the Hg-lamp), the fluorescence reference for excitation flat field correction was carried out with a disk of Rubis 8-SP3 (diameter 1cm, thickness 1mm) from Hans Stettler SA (Lyss, Switzerland). The reference fluorescence value of the rubis was taken every day under same conditions. The pictures of the FITC-dextran fluorescence evolution were divided (pixel by pixel) by this daily fluorescence image to rectify the fluorescence values that would be obtained with a perfectly homogenous and stable light (flat field or shading correction).

All images treatments are being done with the open source software ImageJ 1.37 from Research Services Branch at the NIH (Bethesda, USA), and using self developed and downloadable plugging [39, 40].

After a registration of the different images of the stack, that makes them superimposed, a region of interest (ROI) could be defined as a circle comprising the irradiated area. By using ImageJ software, the mean fluorescence value of the non-irradiated areas <fluo(ref)> was subtracted from the mean fluorescence value within the ROI <fluo(ROI)>. Afterwards this value was multiplied by the surface of the ROI, S(ROI). As the non-irradiated area (ref) is chosen to have the same vascular density than the irradiated area (ROI), this final value corresponds to the accumulation of the fluorescent dye (FITC-dextran 10 kDa) outside the vasculature in the treated site. It reflects the local PDT-induced integrated leakage of the dye.

$$IntFluo(ROI) = [\langle fluo(ROI)\rangle - \langle fluo(ref)\rangle] * S(ROI)$$

Again, at least 5 embryos were injected for each experimental condition.

Results

PDT-induced vascular occlusion

In a previous study on the CAM model, the vascular occlusion observed 18 hours after PDT with Visudyne® with an irradiation using a fluence of 20 J/cm^2 was found to be at score 3 to 4 according to the established occlusion scale [25, 38]. To evaluate the influence of different doses of an anti-aggregating agent on PDT with Visudyne®, co-injections of Aspegic Inject® (4 to 64 mg /kg b.w.) and Visudyne® were performed 1 minute prior to irradiation, resulting in a very low direct occlusion score, between 0 and 1 independent of the aspirin drug dose used. Eighteen hours after treatment, the occlusion score was 3 to 4 (Figure 1), as well as observed after PDT treatment with Visudyne® without aspirin.

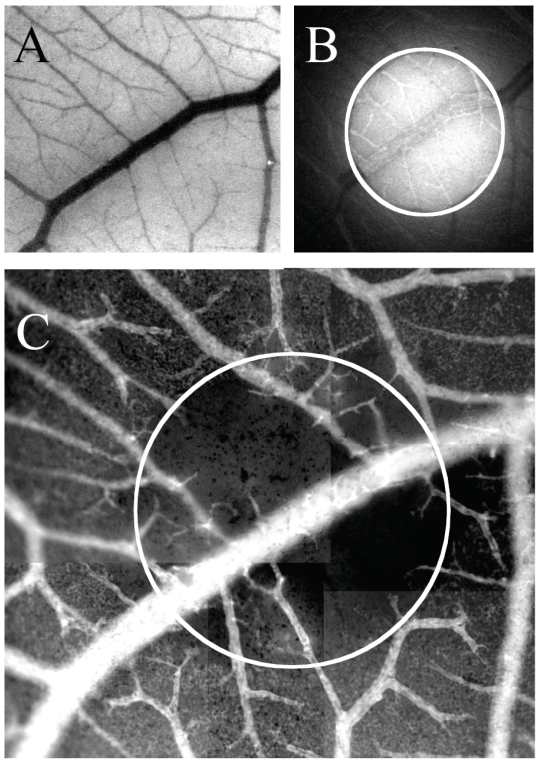

Figure 1: **PDT with Visudyne®**, on CAM blood vessels using intravenously applied Visudyne® (200 µg/kg b.w.). **(A)** Autofluorescence of the CAM before injection (λ_{ex} = 420 ± 20 nm; exposure time 1 second); image obtained with magnification 4x objective **(B)** Visudyne® fluorescence angiography (λ_{ex} = 420 ± 20 nm; λ_{em} >610 nm, exposure time 1 second) during irradiation. The encircled diameter of the irradiated area is 2 mm; irradiation conditions: 20 J/cm^2, 60 seconds after co-injection of 200 µg Visudyne® and 64 mg aspirin/kg embryo b.w.); image obtained with magnification 4 objective **(C)** FITC 150 kDa fluorescence angiography (λ_{ex} = 500-550nm; λ_{em} >610 nm, exposure time 1 second) showing the **vascular occlusion** induced in the circular irradiated area 18 h after PDT); composition of images obtained with magnification 10x objective to see the details of capillaries.

Figure 2 shows 2 sequences of Visudyne® angiography pictures taken during PDT. The first sequence focuses on the typical behaviour of an artery treated by PDT, showing a drastic vasoconstriction during irradiation. The second sequence focus on a vein typically reacting during PDT by an evident platelets aggregation together with a vasoconstriction. In the sequence of pictures taken under identical conditions but when PDT was performed with Aspegic Inject®, the vasoconstriction was similar to the one presented in Figure 2 but there was no thrombus formation during the time of observation (data not shown). No vascular modification was observed when Aspirin was administered without PDT.

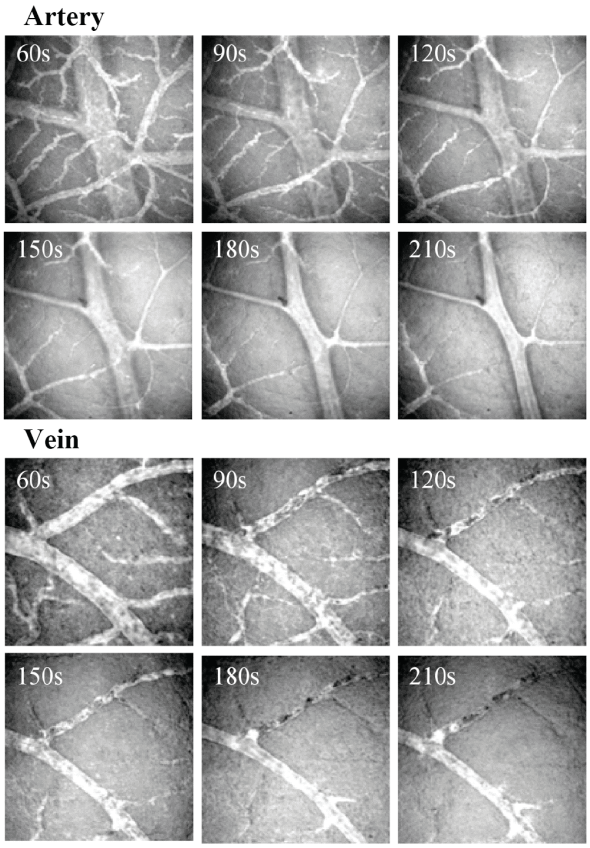

Figure 2: This figure shows 2 sequences of **Visudyne® angiography** pictures taken **during Visudyne®-PDT**. The drug-light interval was 60 seconds and the first picture was taken at the very beginning of irradiation. The first sequence shows a field comprising an artery and the second sequence focus on a vein with the same order of diameter (150-20 µm). The whole field was irradiated with 420 ± 20 nm during 210 seconds to observe the PDT-induced occlusion differences in the two kinds of blood vessels. In arteries, one can observe the dramatic decrease of the vessel diameter during the time of observation, when the vein also presented a platelets adhesion and aggregation (see the black spots appearing already after 30 seconds of irradiation (at time 90s) in the upper right branch of the blood vessel and then the thrombus progression leading to almost the total occlusion of the vein after 210 seconds. This phenomenon was not observed in arteries during the observation time.

Local vascular leakage induced in veins or arteries treated by PDT with different doses of aspirin

In a previous work, we established that the permeability of the CAM vessels is strongly influenced by the photodynamic treatment when

combined with aspirin. Delay in the clotting of blood by a cyclo-oxygenase inhibitor appears to be a pivotal process in temporarily enhancing vascular permeability. As illustrated in this previous work, the PDT-induced vascular leakage without aspirin was not observed in the CAM model, due to a too fast vaso-occlusion of the treated area [25]. To evaluate the influence of the drug dose of aspirin on PDT-induced vascular leakage, 4 different doses of the drug (4, 24, 48 and 64 mg/ kg b.w.) were i.v. administered in a co-injection with Visudyne® 1 minute prior to irradiation and a volume of 20 µl containing FITC-dextran 10 kDa was i.v. injected as soon as the PDT was ended. Under these conditions, the dye was observed to be rapidly homogenously distributed in the blood stream after injection. Thus, the influence of PDT on the fluorescence pharmacokinetics of FITC-dextran 10 kDa after PDT combined with aspirin could be assessed.

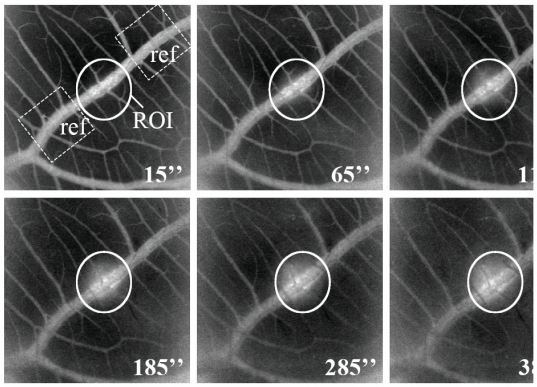

Figure 3: Typical **fluorescence pharmacokinetics** obtained with **FITC-dextran 10 kDa** (25 mg/ml PBS) (λ_{ex} = 470 ± 20 nm) when injected directly after **PDT with Visudyne®** (2 µg/embryo) **co-injected with aspirin** (320 µg/ embryo) (λ_{ex} = 420 ± 20 nm; λ_{em} >610 nm) with a light dose of 20 J/cm^2. PDT was performed 1 minute after injection (λ_{ex} = 420 ± 20 nm; 20 J/cm^2). Typical fluorescence pharmacokinetic of FITC-dextran 10 kDa directly after this PDT showed that PDT with Visudyne® associated with aspirin significantly increases the locally FITC-dextran 10 kDa leakage. These pictures were obtained after shadding correction. In the first picture, the references areas (ref) and the region of interest comprising the treated area (ROI) used for the quantification of the leakage are shown.

The leakage of the fluorescent dye was increased locally by the PDT. This phenomenon was monitored by mean of the FITC-dextran observation directly after injection, at the end of PDT. The sequence of pictures taken at regular time intervals with a CCD camera showed a continuous increase in the leakage (figure 3) until reaching a plateau about 150 seconds after injection, for each drug dose, except for the highest dose tested (64 mg/ kg b.w.) where the leakage kept increasing until the end of the observation (500 seconds). Except for this profile of kinetic, no significant difference was observable with the 4 drug doses of aspirin.

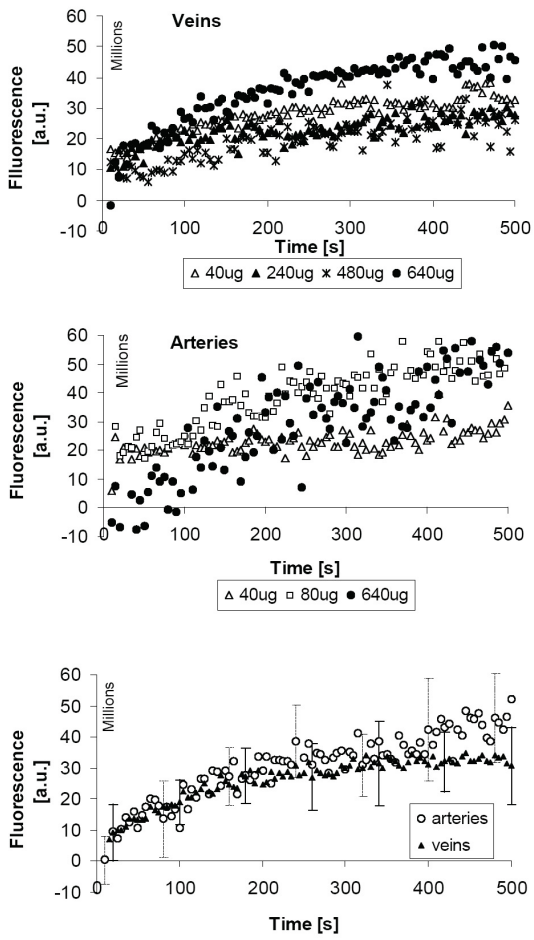

Figure 4: Evolution of the **FITC-dextran 10 kDa integrated fluorescence** obtained locally in the treated area, directly after **PDT with Visudyne®** (2 µg/embryo) **and aspirin** (with different doses) intravenously co-injected 1 minute before irradiation (λ_{ex} = 420 ± 20 nm; λ_{em} >610 nm) with a light dose of 20 J/cm^2. **(A)** Comparison of the leakage obtained after treatment by PDT with 4 doses of aspirin in an area comprising a vein with a diameter comprised between 150 and 200 µm. **(B)** Comparison of the leakage obtained after treatment by PDT with 3 doses of aspirin in an area comprising an artery with a diameter comprised between 150 and 200 µm. **(C)** Comparison of the mean values of leakage obtained after treatment by PDT on arteries and veins.

The fluorescent profile of the increased leakage with different doses of aspirin after treatment by PDT on a vein is shown in Figure 4.A. This graph represents the mean integrated fluorescence values in the treated area obtained with at least 5 embryos per condition.

The same experiments were conduced with PDT treatment on an artery. To evaluate the influence of the drug dose of aspirin on PDT-induced vascular leakage, 3 different doses of the drug (4, 8 and 64 mg/ kg b.w.) were i.v. administered in a co-injection with Visudyne® also 1 minute prior to irradiation and a volume of 20 µl containing FITC-dextran 10 kDa was i.v. injected as soon as the PDT was ended. The leakage of the fluorescent dye was also locally increased by the combination therapy, but the increase in leakage was not as regular as observed when the treated area comprised a vein with the highest dose of aspirin. The lower dose (4mg/ kg b.w.) induced a leakage rapidly reaching a plateau already 100 seconds after injection, when with the dose of 8 mg/kg b.w., the leakage kept increasing during the observation time. The fluorescent profiles of the increased leakage with different doses of aspirin after treatment by PDT centred in an artery is shown in Figure 4.B. This graph represents the mean integrated fluorescence values in the treated area obtained with at least 5 embryos per condition.

The Figure 4.C. shows the comparison between the mean kinetic profiles observed in the two kinds of blood vessels, which according to the standard deviations of the values, demonstrates a very slight difference in leakage. In this model, under our experimental conditions, arteries were a little bit more permeable to the drug after treatment by PDT than veins.

There was no leakage induced when aspirin was administered without PDT (data not shown).

Discussion

In a former study, we reported that the permeability of the CAM vessels is strongly influenced by photodynamic treatment when combined with aspirin [25]. Delay in the clotting of blood by a cyclo-oxygenase inhibitor appears to be a pivotal process in enhancing vascular permeability, at least in this CAM vasculature model. After a delay of approximately 18 h, vessels in the irradiated region were still observed to be closed efficiently following PDT with aspirin. The vessel closure under these conditions is essentially as effective as the closure at shorter times with no aspirin present. We are currently investigating how to take advantage of this effect in order to develop a novel combination therapy approach, i.e. such transiently enhanced vascular permeability in PDT could be used to release chemotherapeutic agents in the case of PDT of a malignant tumor or to selectively release an anti-angiogenic or anti-inflammatory factor to prevent recurrence of the neovasculature in the case of AMD.

This present study consists in evaluating Aspegic Inject®, the injectable formulation of acetylsalicylic acid, at different doses co-administered with Visudyne® to obtain PDT-induced leakage after irradiation, nevertheless keeping an optimal PDT-induced vascular occlusion. The direct observation of the treated area by mean of a FITC 150 kDa injection showed a regular unperturbated vascularisation, as observed with low doses of aspirin. As shown in Figure 1, the efficacy of occlusion by PDT was not affected by even high doses of aspirin in this model. Eighteen hours after treatment, the observation of the perfusion in the treated area revealed the same effect as observed without aspirin showing no perturbation of the vascular efficacy of PDT by aspirin doses up to 68 mg/kg b.w.

We could then follow the evolution of the FITC leakage directly after the end of the PDT. The treatment was performed by co-injecting Visudyne® and aspirin one minute before irradiation of as circular area (680 µm diameter) with a magnification 10x objective. The fluorescent dye was then injected 10 seconds after the end of the irradiation and the quantification of the local integrated leakage was measured by taking fluorescence images with a magnification 4x objective at regular time intervals during 8 minutes. This change of objective between the PDT and the leakage study allowed having a larger field of observation comprising the treated and also surrounding non-irradiated blood vessels that can be used as references. To assess the difference of behaviors between veins and arteries treated by PDT, the area to be irradiated was carefully chosen to have in its center either a vein or an artery with the same range of diameter. No drastic difference in FITC leakage was observed with the different doses of aspirin in each kind of blood vessel but the fluorescence leakage profiles observed in the veins are more regular and reproducible with small standard deviations than the ones observed under similar conditions in arteries. Normally a bigger difference between veins and arteries could be expected because the venous thrombus is usually less rich in platelets than the arterial thrombus {Wu, 2005 #42}. It was also observed that the PDT effect on arteries is first of all characterized by a vasoconstriction [41]

already during irradiation, sometimes followed by the formation of a thrombus when the effect of PDT on veins shows a rapid platelets aggregation with slight vasoconstriction. Normally, in the systemic circulation, the venous thrombus is principally made of fibrin and red blood cells {Wu, 2005 #42}. This difference in thrombus composition and kinetic of formation could make them react differently to the aspirin. As this aspirin acts on the platelets [33], one can think that its activity would be more important in arteries where the thrombus is slower to be formed but contains more platelets. Nevertheless, as the veins contain more von Willebrand Factor receptors, they are potentially more thrombocytogenic [42]. Aspirin activity could then be almost as important in both arteries and veins, as observed in this study.

According to Major et al. [41], vascular damages induced by PDT occur earlier in arteries than in veins in a rat model. If this fast reaction is attributed to the higher availability of oxygen in arteries leading to a better PDT efficacy, this could be different in the CAM model. As the chorioallantoic membrane vasculature is comparable to the pulmonary circulation [34], arteries, by definition going from the heart to the periphery, contain less oxygen than veins bringing back blood to the heart after oxygenation trough the shell. The oxygen level is then lower in arteries than in veins, like in the pulmonary circulation of the human being and maybe influences the efficacy of PDT. The efficacy of PDT would then be higher and maybe faster in veins than in arteries of the CAM model.

The doses of aspirin used in this study were chosen to be between 4 mg/kg b.w. corresponding to the bolus prophylactic dose of 300 mg/ human-being (80kg) and 64mg/kg b.w. almost corresponding to the maximum recommended dose of 5g/human-being [33]. With these drug doses, aspirin does not have only an effect on platelets aggregation but also could diminish a potential inflammation. This experiment should be performed in a well developed mammal model, containing a higher level of leukocytes potentially reactive to PDT effects and susceptible to take part in the PDT-induced leakage, principally in veins, containing more endothelial leukocytes receptors (selectins) than arteries [43]. The difference of leakage between veins and arteries could then be higher than the one observed in the embryonic model, CAM, used for the present study.

Conclusion

This work focused on the optimization of the photodynamic delivery enhanced by delaying the photo-occlusion in the chorioallantoic membrane model. In this study, we observed that arteries and veins present different kinetic of photo-occlusion pathways during photodynamic therapy. The primary event occurring in arteries is the vasoconstriction when veins react first by platelets adhesion followed by vasoconstriction. Visudyne®-PDT combined with aspirin at different doses, aimed at optimizing the delay of the blood clot formation to try to enhance and control the PDT-induced local vascular leakage already observed in our previous study. The vascular permeability was locally enhanced by PDT directly after treatment, independently of the drug dose of aspirin tested (from 4 to 64 mg/ kg b.w.). All these conditions allowed reaching the occlusion of the treated vessels, one day after treatment, also independently of the aspirin dose used. In this model, there were no statistical significant difference between photodynamic leakage observed in arteries and veins. This observed leakage could be optimized in a further study by temporary inhibiting not only the platelets aggregation but also the vasoconstriction induced by PDT. Delaying these two phenomena could then be a possibility to optimize the photodynamic drug delivery. This study enter in the context of the development of a novel combination therapy approach, taking advantage of a transiently enhanced vascular permeability during or shortly after PDT to selectively release a chemotherapeutic agent in a local cancer before occluding the vessels feeding the tumour.

References

1. TAP Study Group, *Photodynamic Therapy of Subfoveal Choroidal Neovascularization in Age-Related Macular Degeneration With Verteporfin: Two-Year Results of 2 Randomized Clinical Trials--TAP Report 2.* Arch. Ophthalmol., 2001. **119**: p. 198-207.
2. Michels, S. and U. Schmidt-Erfurth, *Sequence of early vascular events after photodynamic therapy.* Investigative Ophtalmology & Visual Science, 2003. **44**(5): p. 2147-2154.
3. Tatar, O., et al., *Expression of VEGF and PEDF in choroidal neovascular membranes following verteporfin photodynamic therapy.* American Journal of Ophtalmology, 2006. **142**(1): p. 95-104.
4. Solban, N., et al., *Mechanistic investigation and implications of photodynamic therapy induction of vascular endothelial growth factor in prostate cancer.* Cancer Research, 2006. **66**(11): p. 5633-5640.
5. Zhang, X., et al., *Low-dose photodynamic therapy increases endothelial cell proliferation and VEGF expression in nude mice brain.* Lasers in Medical Science, 2005. **20**(2): p. 74-79.

6. Gollnick, S., et al., *Role of cytokines in photodynamic therapy-induced local and systemic inflammation.* British Journal of Cancer, 2003. **88**(11): p. 1772-1779.
7. Nowis, D., et al., *The influence of photodynamic therapy on the immune response.* Photodiagnosis and Photodynamic Therapy, 2005. **2**(4): p. 283-298.
8. Fingar, V.H., *Vascular effects of photodynamic therapy.* J Clin Laser Med Surg, 1996. **14**(5): p. 323-8.
9. Sitnik, T., J. Hampton, and B. Henderson, *Reduction of tumour oxygenation during and after photodynamic therapy in vivo: effects of fluence rate.* British Journal of Cancer 1998. **77**(9): p. 1386-1394.
10. Chakravarthy, U., et al., *Evolving European guidance on the medical management of neovascular age related macular degeneration.* British Journal of Ophthalmology, 2006. **90**(9): p. 1188-1196.
11. Eter, N., T. Krohne, and F. Holz, *New pharmacologic approaches to therapy for age-related macular degeneration.* Biodrugs, 2006. **20**(3): p. 167-179.
12. Hunt, D.W.C. and P. Margaron, *Status of therapies in development for the treatment of age-related macular degeneration.* Idrugs, 2003. **6**(5): p. 464-469.
13. Krzystolik, M.G., et al., *Prevention of experimental choroidal neovascularization with intravitreal anti-vascular endothelial growth factor antibody fragment.* Archives of Ophthalmology, 2002. **120**(3): p. 338-346.
14. Costa, R.A., et al., *Immediate indocyanine green angiography and optical coherence tomography evaluation after photodynamic therapy for subfoveal choroidal neovascularization.* Retina, 2003. **23**(2): p. 159-65.
15. Miller, J.W., et al., *Photodynamic therapy with verteporfin for choroidal neovascularization caused by age-related macular degeneration: results of a single treatment in a phase 1 and 2 study.* Arch Ophthalmol, 1999. **117**(9): p. 1161-73.
16. van den Bergh, H., *Photodynamic therapy of age-related macular degeneration: history and principles.* Seminars in Ophthalmology, 2001. **16**(4): p. 181-200.
17. Boekelheide, K., et al., *Microtubule assembly inhibition by porphyrins and realted-compounds.* Photochem Photobiol, 1987. **46**(5): p. 657-661.
18. Dadosh, N. and N. Shaklai, *Effect of protoporphyrin-IX on red blood-cell membrane cytoskeleton.* Journal of muscle research and cell motility, 1988. **9**(1): p. 86-86.
19. Nelson, J., L. Liaw, and M. Berns, *Tumor destruction in photodynamic therapy.* Photochemistry and Photobiology, 1987. **46**(5): p. 829-835.
20. Sporn, L. and T. Foster, *Photofrin and light induces microtubule depolymerization in cultured human endothelial-cells.* Cancer Research, 1992. **52**(12): p. 3443-3448.
21. Fingar, V., et al., *The Role of Microvascular Damage in Photodynamic Therapy - The Effect of Treatment on Vessel Constriction, permeability and Leucocyte adhesion.* . Cancer Research, 1992. **52**(18): p. 4914-4921.
22. Fingar, V.H., et al., *Analysis of acute vascular damage after photodynamic therapy using benzoporphyrin derivative (BPD).* Br J Cancer, 1999. **79**(11-12): p. 1702-8.
23. Krammer, B., *Vascular effects of photodynamic therapy.* Anticancer Res, 2001. **21**(6B): p. 4271-7.
24. van den Bergh, H. and J.P. Ballini, *Principles of Photodynamic Therapy.* Photodynamic Therapy of Ocular Diseases, ed. E. Gragoudas, J. Miller, and L. Zografos. 2004, Philadelphia, PA, USA: Lippincott Williams & Wilkins. 11-42.
25. Debefve, E., et al., *Combination therapy using aspirin-enhanced photodynamic selective drug delivery.* Vascular Pharmacology, 2007. **46**(3): p. 171-180.
26. Snyder, J.W., et al., *Photodynamic therapy: a means to enhanced drug delivery to tumors.* Cancer Res, 2003. **63**(23): p. 8126-31.
27. Schmidt-Erfurth, U., et al., *Antiangiogenesis in neovascular macular degeneration: New therapeutical strategies* Spektrum der Augenheilkunde, 2005. **19**(16): p. 317-325.
28. Fingar, V.H., T.J. Wieman, and P.S. Haydon, *The effects of thrombocytopenia on vessel stasis and macromolecular leakage after photodynamic therapy using photofrin.* Photochem Photobiol, 1997. **66**(4): p. 513-7.
29. Janka, H.U., *Inhibition of Platelet Adenylate-Cyclase by Aspirin - a Further Argument for a Low-Dose Regimen in Anti-Platelet Drug-Therapy.* Ircs Medical Science-Biochemistry, 1981. **9**(11): p. 1019-1019.
30. Reed, M.W., D.A. Schuschke, and F.N. Miller, *Prostanoid antagonists inhibit the response of the microcirculation to "early" photodynamic therapy.* Radiat Res, 1991. **127**(3): p. 292-6.
31. Stern, S.J., et al., *Effect of aspirin on photodynamic therapy utilizing chloroaluminum sulfonated phthalocyanine (CASP).* Lasers Surg Med, 1992. **12**(5): p. 494-9.
32. Taber, S.W., T.J. Wieman, and V.H. Fingar, *The effects of aspirin on microvasculature after photodynamic therapy.* Photochem Photobiol, 1993. **57**(5): p. 856-61.
33. Morant, J. and H. Ruppaner, *Compendium Suisse des Médicaments. Basel, Switzerland.* 2002.
34. Romanoff, A.L., *Biochemistry of the Avian Embryo: a Quantitative Analysis of Prenetal Development.* 1967, New York: John Wiley & Sons. 398.
35. Hornung, R., et al., *Systemic application of photosensitizers in the chick chorioallantoic membrane (CAM) model: photodynamic response of CAM vessels and 5-aminolevulinic acid uptake kinetics by transplantable tumors.* Journal of Photochemistry and Photobiology B: Biology, 1999. **49**(1): p. 41-49.
36. Gottfried, V., et al., *In vivo damage to chorioallantoic membrane blood vessels by porphycene-induced photodynamic therapy.* J Photochem Photobiol B, 1995. **30**(2-3): p. 115-21.
37. Hammer-Wilson, M.J., et al., *Photodynamic parameters in the chick chorioallantoic membrane (CAM) bioassay for topically applied photosensitizers.* J Photochem Photobiol B, 1999. **53**(1-3): p. 44-52.
38. Lange, N., et al., *A new drug-screening procedure for photosensitizing agents used in photodynamic therapy for CNV.* Invest Ophthalmol Vis Sci, 2001. **42**(1): p. 38-46.
39. Rasband, W.S., *ImageJ.* 1997-2006, National Institutes of Health (NIH): Bethesda, USA.
40. Abramoff, M.D., P.J. Magelhaes, and S.J. Ram, *Image processing with ImageJ.* Biophotonics International, 2004. **11**(7): p. 36-42.
41. Major, A., et al., *Microvascular photodynamic effects determined in vivo using optical Doppler tomography.* IEEE Journal of Selected Topics in Quantum Electronics, 1999. **5**(4): p. 1168-1175.
42. Cho, J. and K. Ouriel, *Differential thrombogenicity of artery and vein: The role of von Willebrand factor.* Annals of Vascular Surgery, 1995. **9**(1): p. 60-70.
43. Kubes, P., *Introduction: The complexities of leukocyte recruitment.* Seminars in Immunology, 2002. **14**(2): p. 65-72.

Chapitre 4

Experimental Visudyne®-mediated Photodynamic Therapy Affords Selective Drug Delivery: An Intravital Microscopy Study in Nude mice

To be submitted to Microcirculation

Experimental Visudyne®-mediated Photodynamic Therapy Affords Selective Drug Delivery:

An Intravital Microscopy Study in Nude Mice

Debefve E.[1], Krueger T.[2], Cheng C.[2], Schäfer S.C.[3], Yan H.[2], Ballini J.-P.[1], van den Bergh H.[1], Lehr H.-A.[3], Ris H.-B.[2]

[1] Ecole Polytechnique Fédérale de Lausanne (EPFL) Laboratory of Photomedicine, 1015 Lausanne, Switzerland

[2] Centre Hospitalier Universitaire Vaudois (CHUV), 1005 Lausanne, Switzerland

[3] Institut de pathologie, Quartier UNIL-CHUV, 1015 Lausanne, Switzerland

To be submitted to Microcirculation

Keywords: drug delivery, photodynamic therapy, verteporfine, fluorescein isothiocyanate dextran (FITC-dextran), animal model, dorsal skinfold chamber, intravital microscopy (IVM), vasculature, endothelial cells.

Abstract

Objective: Photodynamic therapy (PDT) has been investigated as treatment for solid tumours, age-related macular degeneration (AMD) and other diseases. PDT acts by direct phototoxicity and by an indirect vascular-mediated effect by interruption of vessel integrity. We hypothesized that the PDT related interruption of vessel integrity may be used for an increased trans-vascular passage of drugs.

Methods: Nude mice underwent implantation of a dorsal skinfold chamber for in-vivo analysis of microvascular leakage and inflammatory response by intravital microscopy. PDT was performed 10 minutes after intravenous administration of Visudyne®. Control animals had no PDT (n=4). Vascular permeability was determined during a 60min period of observation of cumulative integrated fluorescence after intravenous injection of Fluorescein isothiocyanate dextran (FITC-dextran 2000kDa). FITC-dextran was injected immediately (group A, n=11), or 120min after PDT (group B, n=14). Acute inflammatory response was assessed by in-vivo staining of leukocytes by rhodamin 6-G and consecutive repeated determination of intravascular leukocyte rolling. All dorsal skin fold chambers underwent histological analysis (HE staining).

Results: PDT induces a time dependent acute inflammatory tissue response as shown by increased leukocyte rolling after treatment. Continuous FITC-dextran leakage to the interstitial space was observed in all animals after PDT. No leakage was observed in control animals.

Conclusion: Visudyne®-mediated PDT results in an acute inflammatory tissue response and leads to a time-dependent transient increase of local vascular permeability with an enhanced uptake of FITC-dextran in the interstitial space. This concept has the potential to improve uptake of cytostatic drugs in chemoresistant tumours or anti-angiogenic drugs in AMD.

1. Introduction

Many diseases such as age-related macular degeneration (AMD) and malignant tumours are associated with a proliferation of pathological neovessels. One treatment modality for these diseases is photodynamic therapy (PDT), which is based on the interruption of the vessel integrity thus causing vascular collapse of the pathological neovessels [1, 2]. The aim of the present work is to explore the possibility of improving the PDT treatment of these diseases by combining it with another therapy, for instance chemotherapy or anti-VEGF therapy. In the case of cancer therapy, the “starvation” of tumor cells induced by the PDT-induced occlusion of blood vessels feeding the tumor might be combined with a chemotherapeutic effect on the tumor. In the case of AMD, the recurrence of the disease weeks/months after PDT observed by the re-opening and/or re-growth of neovessels [1-3] could possibly be avoided by adding an anti-angiogenic and/or anti-inflammatory drug during either before or shortly after PDT. A problem in the administration of chemotherapeutic drugs which potentially improve the treatment of cancer or AMD in combination therapy is to find a way to improve the drug delivery to reach the therapeutic dose locally. Efficacy of any drug treatment depends on the ability of the therapeutic agent to reach the target cell. Delivery of therapeutics to the target after systemic intravenous injection is influenced by the blood supply to the region of interest, the drug transport through the vessel wall, and the drug transport through the interstitial space to the target cell [4]. In the case of the treatment of AMD by a combination of PDT and anti-VEGF therapy the problem lies in the monthly repeated intravitreal injections required for the anti-VEGF therapy. Experimental approaches to improve delivery of chemotherapy or anti-VEGF drugs are of major interest.

It has been reported that following the light application in PDT, a physiological cascade of responses in one hand leads to vascular occlusion but could also temporarily induce a vascular permeability enhancement depending on the applied conditions [5, 6]. Within the framework

of the present study performed in the skinfold chamber in the nude mice observed by intravital microscopy (IVM), we propose to assess the influence of PDT on the vascular permeability. In a recent study performed in the chorioallantoic membrane of a chicken embryo, Visudyne®-PDT combined with aspirin administration, was shown to strongly enhance the local leakage [7]. The mammal model used here allows assessing the PDT-induced leakage in physiological mature blood vessels and thus to obtain preliminary results on normal vascularisation. The goal of this project is thus to study the capacity of PDT to specifically make the treated blood vessels more permeable in order to improve local drug delivery. The results obtained in the present model comprising normal blood vessels will be extended in the near future to neovasculature.

Materials and methods

Animal model: preparation of the observation chamber

The Swiss nude mice were provided by Charles River Laboratories (L'Arbresle, France). The dorsal skinfold chamber preparation in nude mice was used for intravital microscopy. The experimental preparation used in this study is similar to that described by Lehr et al. [8, 9]. Briefly, nude mice weighing 24-28 g were fed with standard rodent diet with free access to tap water. They were anesthetised by an intraperitoneal injection of ketamin (100mg/kg) (Ketalar®, Pfizer, Zürich, Switzerland) and xylazine (10mg/kg) (Rompun®, Bayer, Zürich, Switzerland). Buprénorphine (0.5g/kg) (Temgesic®, Essex Chemie, Lucerne, Switzerland) was administered at the end of the surgical preparation to relieve pain. The animals were equipped with the dorsal skinfold chamber for intravital microscopy as described elsewhere [9]. Between the implantation of the observation chamber and the microscopic observation, a recovery period of 3-4 days was allowed to eliminate the effect of anesthesia and surgical trauma. Trans-illumination microscopy and an Achroplan objective 4x (described below) were used to select an area comprising a crossing between a vein and an artery with about the same size (35-60 µm in diameter). A volume of 100 µl of rhodamine-6-G (0.05%) (Sigma-Aldrich, Buchs, Switzerland) was intravenously administered 10 minutes before the observation with a microscope described below using a Carl Zeiss “cube filter set 15” (Exc. BP 546/12, BS FT580, Em. LP590) to visualize leukocyte-endothelium interaction, i.e. leukocyte rolling and adhering to the vessel wall. This is done with the objective to exclude from the study mice with acute vascular signs of inflammation in their skinfold chambers [10]. The experiments were conducted in accordance with the national and institutional guides for the care and use of animals (cantonal veterinary authorization n°1915).

Quantification of the inflammation

The dorsal skinfold chamber in mice observed by intravital fluorescence microscopy was at first used to study venular rolling leukocytes before PDT treatments to exclude from the study animals with acute vascular signs of inflammation [10-12]. An ideal chamber with a physiological microcirculation should present less than 30 rolling leukocytes/mm vessel circumference in 30s. Chambers presenting 30-100 rolling leukocytes/mm are considered as borderline, and inflamed chambers were the ones having higher numbers of rolling leukocytes at baseline (>100 leukocytes/mm) [10].

Although in most acutely prepared tissues, there are always "spontaneous" rolling leukocytes at baseline conditions, baseline leukocyte rolling is virtually absent in carefully executed chronically instrumented tissues and is even considered a marker of acute inflammation 3 days after surgical preparation. Each mouse was thus tested for its inflammation in this way and only the ones presenting “ideal” physiological microcirculation were used for the further assessments. This quantification of acute inflammation was also used in this study to observe the inflammatory response of leukocytes at different times (directly, 30 minutes, 1h and 2 h) following PDT.

Photodynamic therapy followed by fluorescence pharmacokinetic studies for measuring vessel leakage

Photodynamic therapy

For these treatments, the mouse, presenting no inflammation, as controlled by the observation of rolling leukocytes, is placed in a plexiglas tube which is positioned under the epi-fluorescence microscope. The Plexiglas tube holder allows easy exchange of the mice already placed in a tube. The chamber on the back of the mouse is fixed horizontally and its position under the microscope allows trans-illumination from the bottom side or epi-illumination for

fluorescence observation. Subsequently, an intravenous (i.v.) injection of 50 µl of the photosensitiser Visudyne® (with increasing doses between 200µg and 800 µg/kg body weight (b.w.)) was performed into the tail vein. Visudyne® (verteporfin, BPD-MA) was obtained from Novartis (Hettlingen, Switzerland) [13]. For dilutions, Phosphate Buffer Saline (PBS) was provided by Life Technologies (Invitrogen Corporation, UK), NaCl 0.9% by B. Braun (Emmenbrücke, Switzerland) and glucose 5% solution by Bichsel (Interlaken, Switzerland). The circulation of the drug was observed in the blood stream of the skinfold chamber by Visudyne®-specific fluorescence microscopy (λ_{exc}= 420 ± 20 nm; λ_{em}≥ 610 nm). The microscope used for intravital observation, is a Carl Zeiss Axiotech Vario 100, allowing observations made at different elevations above the sample. Achroplan Carl Zeiss objectives Plan Neofluar 2.5x/ 0.0075 and 4x/ 0.10 are used for a large field of view (3x3 mm for the 4x), Achroplan objectives 10x/0.25 and 20x/0.50 with water immersion are used for PDT excitation and close observation of the vessels and capillaries (field of view 600x600 µm). Excitation is performed via a filtered 100W HBO103 light source, powered through a variable FluoArc device, allowing to lower the light power during data recording, thus preventing any undesired PDT excitation. A Uniblitz shutter VS25 with its controller WMM-D1 (Vincent Associates, Rochester, NY, USA) is also added to be able to cut off the HBO lamp. Images and video sequences are recorded with an on chip amplified Hamamatsu electron multiplier consisting of a back illuminated thinned Peltier cooled CCD camera (EM-CCD C9100-12), (400 to 1000 nm) giving us an up to 2000x amplified signal gain. This allows to lower the excitation light and permits to work under conditions of illumination similar to those applied in treating CNV associated with AMD. Images and sequences are recorded through the Hamamatsu camera controller with the Hamamatsu HiPic version 7.0 software, giving 512x512 pixels and 16 bits grey level images. A STAC (Seitama, Japan) Multiscan Rate Converter MSC-12A-HPK between the EM-CCD and the controller provide us the digital and

video signals in parallel. The video signal, on which we superimpose the date and time with a FOR-A VTG-33 Video Timer S-VHS is recorded on a JVC (Japan) SR-S388E video recorder. A Sony (Japan) UP-895CE B/W printer is used to print video images.

Shortly after injection (≅ 1 min), the photosensitiser luminescence is homogeneously distributed in the blood vessels and the PDT was performed ten minutes after the i.v. injection using light from a filtered Hg-arc lamp at 420 ± 20 nm using the Carl Zeiss "cube filter set 05" (Exc. BP 395-440, DM FT 460, Em. LP470), with the 20x water immersion objective at a fluence rate of 300 mW/cm^2. A light dose (comprised between 50 and 200 J/cm^2) was applied to a circular surface with a diameter of 400 μm previously chosen comprising a crossing between a vein and an artery, both with the similar diameters (35-60 μm). Adding a Chroma filter LP610 before the EM-CCD detector, we can record Visudyne® fluorescence angiographies. In order to verify the efficacy of the blood flow stasis and vascular occlusion induced by PDT, and to define the conditions necessary to obtain damages (i.e. closure) comparable to that observed in clinical trials [14], observation of the vascular occlusion was undertaken up to 13 days after PDT by means of fluorescence angiography. The latter were performed by i.v. injections into the tail vein of 100 μl of a solution containing Fluorescein isothiocyanate dextran (FITC-dextran 2000 kDa) 25 mg/ml PBS. FITC-dextran was obtained from Sigma-Aldrich (Buchs, Switzerland). In between the treatment and these measurements the mouse was returned to its individual cage and was fed with standard rodent diet with free access to tap water. Fluorescence angiographies recorded on S-VHS video tape pre- and post-PDT allowed to compare the number of functional blood vessels and to deduce the photothrombic efficiency at each set of PDT conditions. For each set of conditions, at least 5 mice were used.

Fluorescence pharmacokinetic studies for measuring vessel leakage

The fluorescence pharmacokinetic leakage profile of FITC-dextran 2000kDa was determined as follows. Typically, a volume of 100 µl containing FITC-dextran (25 mg/ml PBS) was intravenously (i.v.) injected in the tail vein under the microscope in a co-injection with Visudyne®, 10 minutes before irradiation, or separately two hours after the PDT. At regular time intervals, fluorescence images of the optical chamber were recorded as a function of time over a 4000 to 6000 second period, using excitation light from a Hg-arc lamp filtered for excitation at 470 ± 20 nm using a Carl Zeiss "cube filter set 09" (Exc. BP 450-490, DM FT510, Em. LP515), with the magnification 2.5x objective, allowing the observation of a field 1.875 mm large. The time-dependent evolution of the FITC-dextran fluorescence at the treated site was quantified and compared to the surrounding non-treated areas.

As the excitation by the Hg-arc lamp is not entirely homogenous (slightly decreasing from the centre to the surrounding of the irradiated field) and to allow comparison of the results (that can change over time principally due to the change in power of the Hg-lamp), a disc of rubis $8Sp_3$ (diameter 12mm, thickness 1mm) (Hans Stettler, Lyss, Switzerland) is used as reference to allow us to estimate the homogeneity of the irradiation and the relative value of illumination as it varies from day to day. A fluorescence specific band pass filter was added between the "cube filter" and the EM-CCD detector. Chroma filter D693.5/5 and OD2 were used for the recording of the reference fluorescence from the rubis. The pictures of the FITC-dextran fluorescence evolution were divided (pixel by pixel) by this daily "standardising" fluorescence image in order to make an intensity correction that will rectify the fluorescence values to yield fluorescence intensities quite close to those that we would have obtained with a perfectly homogenous and stable excitation light.

After performing a registration of the different images of the stack, they become super imposable, and a region of interest (ROI) could be defined as a circle comprising the irradiated area. All computation on images are performed with the public domain ImageJ version 1.37 software (Rasband, W.S., ImageJ, US National Institute of Health, Bethesda, Maryland, USA, http://rsb.info.nih.gov/ij/1997-2006) [15]. The mean fluorescence value of the non-irradiated areas <fluo(ref)> was subtracted from the mean fluorescence value of the ROI <fluo(ROI)>. Afterwards this value was multiplied by the surface of the ROI, S(ROI). As the non-treated area (ref) is chosen to have the same vascular density as the irradiated area (ROI), this final value corresponds to the accumulation of the fluorescent dye fluorescence (FITC-dextran 2000 kDa) outside the vasculature in the treated site. Taking into account the very small corrections for tissue optics in this model, this reflects the local PDT-induced integrated leakage of the dye.

$$\text{IntFluo(ROI)} = [\langle\text{fluo(ROI)}\rangle - \langle\text{fluo(ref)}\rangle] * \text{S(ROI)}$$

Histological analyses of the tissue in the optical chambers

In order to assess the tissular histo-pathology within the optical chamber used in this study, a number of groups of animals were sacrificed by cervical dislocation for histological examination. These groups included mice that had not undergone PDT ($n = 5$), and mice sacrificed 30 minutes ($n = 5$), or 150 minutes ($n = 8$) after PDT. Tissue was fixed for 48 hours in 5% buffered formalin solution. The skin within the observation chamber was sliced in 1mm thick sections, orientated perpendicular to the main vessel axis and embedded in paraffin. Four µm thick sections were processed using a standard hematoxylin & eosin staining protocol. The histological samples were entirely examined by a professional pathologist in a

blinded fashion. The degree of oedema in the connective tissue as well as the amount of inflammatory cells attached to the vessel wall and those already migrated into the surrounding connective tissue was scored using a four-level system and expressed semi-quantitatively. Six randomly selected areas of each tissue block were digitalized using a high resolution colour camera (Nikon digital camera DXM 1200, Japan) mounted on a Photo head microscope (Nikon Eclipse E 800 Photo head V-TP, Japan). 200-fold magnification high resolution pictures were computed using commercial available image software (Adobe Photoshop 7.0). The thickness of the superficial tissue and muscular layer lying over the treated vessels were measured and expressed in μm.

Results

PDT occlusion efficacy on physiological mature blood vessels

In order to verify the efficacy of the blood flow stasis and vascular occlusion induced by PDT in the skinfold chamber model, and to define the conditions necessary to obtain vessel closure comparable to the ones observed in the chorioallantoic membrane model (CAM) [16] and in clinical trials [14], an observation of the vascular occlusion induced by PDT was undertaken up to 13 days after treatment by means of FITC-dextran fluorescence angiography. In preliminary experiments, the tests under clinical conditions (drug-light interval (DLI) of 10 minutes; Visudyne® 200µg BPD-MA/kg; 50 J/cm^2) [14] showed almost no occlusion of the treated vessels (data not shown). Hence the mice were treated by Visudyne®-PDT under adapted conditions, by increasing drug and light doses (drug between 200µg and 800 µg/kg body weight; light between 50 and 200 J/cm^2) until reaching a blood vessel occlusion comparable to that seen in the CAM and in clinical tests. Before the beginning of irradiation, all the blood vessels are well perfused by the photosensitiser at all drug doses. Three hours after the end of a treatment using a drug dose of 800 µg/kg and an irradiation of 200 J/cm^2, the perfusion of the large vessels is not significantly perturbed but most of the capillaries are closed, as observed in the clinic.

This occlusion was present up to 6 days after treatment but thirteen days after treatment, a reperfusion of the treated larger vessels is observed and even some of the capillaries are reperfused (data not shown). These conditions (DLI: 10 minutes; 800µg BPD-MA/kg; 200 J/cm^2) which lead to semi-permanent PDT effects in term of vascular occlusion were kept for the entire study unless otherwise notified.

Leukocyte rolling before and after PDT

The labeling of leukocytes by rhodamine-6-G allows a clear visualization of their behavior inside the venous bloodstream [10, 12]. The rolling ("slow") leukocytes are counted as indicated above to quantify the vascular acute inflammatory status in the chamber. The influence of PDT on leukocyte adhesion was assessed at different times during and after PDT, under the applied PDT conditions. As each mouse was tested for its inflammation and as only the ones presenting ideal (i.e. non-inflamed) physiological microcirculation were used for the assessments, all the mice used for this study presented less than 30 rolling leukocytes/mm vessel circumference in 30s, corresponding to "ideal" optical chambers which are defined as being essentially without acute inflammation [10]. The quantification of the inflammation before PDT was actually 26 ± 3 leukocytes /30s and per mm. As shown in figure 1, this quantification of acute inflammation was also performed in this study to observe the response of leukocytes after PDT at different times (directly, 30 min, 1h, 2h after PDT). Directly after the end of PDT, the rolling leukocytes were counted again, showing that no change in reaction of these cells had occurred yet (33 ± 2 leukocytes /30s and per mm). The same observation repeated 30 minutes later still did not show any significant increase in the number of rolling leukocytes (27 ± 4 leukocytes /30s and per mm). However, 1h after PDT, 106 ± 4 leukocytes /30s and per mm were counted characterizing an optical chamber with a sign of a slight acute inflammation in the vasculature. The inflammatory response induced by PDT was more obvious 2 hours after treatment when 213 ± 8 leukocytes /30s and per mm were counted.

Micropharmacokinetics

Assessment with different sizes of FITC

Fluorescein isothiocyanate (FITC) linked with different sizes of dextran (10, 70, 150 and 2000 kDa) were first assessed by observing the fluorescence pharmacokinetics of their leakage in standard conditions (without PDT) in our skinfold chamber model (data not shown). From these observations of leakage, the biggest FITC-dextran available in the market was chosen (2000 kDa) as fluorescent leakage indicator for this study. This fluorescent dye presented almost no leakage without PDT allowing a "clean" the observation of the PDT-induced leakage and keeping a positive fluorescent contrast between intra- and extra-vascular compartments for over 2 hours in the non-treated area.

Fluorescein isothiocyanate dextran (FITC-dextran) 2000 kDa leakage directly after PDT

To assess the effect of PDT on a dye leakage directly after treatment, a solution of FITC-dextran 2000kDa was intravenously (i.v.) administered in a co-injection with Visudyne®, 10 minutes before irradiation. PDT was then performed as described above and fluorescence images of the FITC distribution inside the optical chamber were recorded as a function of time over a 4000 seconds period. Typical sequences of pictures obtained under these conditions are presented in figure 2 (A,B), showing an obvious increased leakage from the treated area, which furthermore increases with time. The time-dependent evolution of the FITC-dextran fluorescence at the treated site was quantified and compared to the surrounding non-treated areas.

The quantification of the accumulation of the fluorescent dye (FITC-dextran 2000 kDa) at the treated site reflects the local PDT-induced leakage directly after treatment. It is shown in the graph of figure 3.A. where the time 0 corresponds to the bolus co-injection of Visudyne® and FITC-dextran. As the FITC-dextran was co-injected with Visudyne®, 10 minutes before

irradiation, the first pictures taken immediately after finishing the therapeutic irradiation would reflect the early leakage potentially occurring during PDT. Figures 2 and 3.A,B show that no significant local leakage was induced during PDT under our conditions in this mammal model.

FITC-dextran 2000 kDa leakage 2 hours after PDT

To assess the effect of PDT on dye leakage 2 hours after treatment, PDT was performed as described above. In this case, 2 hours after the end of irradiation, FITC-dextran 2000kDa was intravenously (i.v.) injected. The fluorescence images of the FITC distribution inside the optical chamber were recorded as a function of time over a 6000 second period. Typical sequences of pictures obtained under these conditions are presented in figure 2 (B,C), showing an obvious increased leakage at the treated area and its direct surroundings, which increased with time. The time-dependent evolution of the FITC-dextran fluorescence at the treated site was quantified and compared to the surrounding non-treated areas.

The quantification of the accumulation of the fluorescent dye (FITC-dextran 2000 kDa) around the treated site reflecting the local induced leakage 2 hours after PDT is represented in the second part of the graph of figure 3.A. where the time 0 again corresponds to the bolus injection of Visudyne® for PDT.

In both conditions assessed in this study, a clear PDT-induced local leakage was observed in every mice, but the leakage quantification (directly and 2 hours after PDT) at the two times of observation presented a wide distribution within each treatment group. To clarify these possibly bimodal distributions, histological analyses were conducted.

Histological analyses of the optical chambers

In mice with low extravascular leakage after PDT treatment no significant sign of preexisting edema was detectable by standard histological examination. The striated muscle tissue remained in its regular histological limits and the connective tissue remained compact. No inflammatory infiltration was observed in these compartments. Sporadic inflammatory cells were observed attaching to the inner vessel wall of post-capillary venules in the groups with low vascular leakage without significant difference between the three groups (no PDT, 30 min and 150 min after PDT, respectively; figure 4, A).

Mice with high extravascular leakage showed increased inflammatory cell infiltration in the subcutanous tissue as well as increased adhesion of inflammatory cells to the inner vessel wall of post-capillary venules. The subcutanous connective tissue showed marked edema, which also could be observed within the striated muscle tissue (figure 4, B).

Measurements of total muscle layer thickness showed no significant difference between the two groups (figure 5, grey columns, 60.64µm ± 12.80µm and 64.34µm ± 13.18µm). Likewise, the distance between the inner surface covered by the cover glass and the treated vessels showed no significant differences between the two groups (figure 5, white columns, 155.88µm ± 28.18µm and 133.42µm ± 19.00µm, respectively).

Discussion

Photodynamic Therapy (PDT) has been found useful for managing a number of clinical disorders involving hyper-vascularisation. It is an approved treatment for solid tumors [17, 18] and age-related macular degeneration [14, 16]. The general mode of treatment involves injection of the photosensitising drug, followed by their photoactivation *in situ* [19, 20]. These drugs are chosen or designed to tend to localize, with some degreed selectivity, in abnormal tissues or in newly formed blood vessels. Light activation then produces short-lived cytotoxic oxidative species, which can induce localized tissue damage [21]. Benzoporphyrin derivative (BPD-MA or Verteporfin) is a fairly hydrophobic chlorin-like photosensitiser that has been shown to be highly effective *in vivo*. Visudyne®, a commercialized form of BPD-MA formulated in liposomes which provide an injectable hydrophobic vehicle for intravenous drug delivery [13]. With this formulation, after intravenous injection of Visudyne®, and breakup of the liposomes the drug is transferred somewhat preferentially to low density lipoproteins (LDL). These are large molecules that can transport fatty material in blood and which can form a chemical complex with the drug to vehicle it in the bloodstream. The drug thus accumulates in the pathologically growing blood vessels that express more LDL receptors [22-24]. Because new blood vessel cells have a faster growth rate, it makes their endothelial cells thus take up more of the verteporfin than endothelial cells of normal vessels. In the present study, the model used was the skinfold chamber of nude mice. This model presents a mature vascular network that probably expresses less LDL receptors than the corresponding neovessels. We observed in this study, that the vascular occlusion induced by PDT under the clinical conditions of drug-light interval (DLI), drug and light doses (DLI= 10 minutes; 200µg Visudyne®/kg b.w.; 50 J/cm^2) were much less effective than in the neovasculature of the chorioallantoic membrane of the chicken embryo [16] or in the clinical

CNV associated with AMD [14]. This decreased sensitivity to PDT may be to some extent attributed to the maturity of the blood vessels in the skinfold chamber, which furthermore express less LDL receptor than neovessels. Even in this kind of mature blood vessels, less reactive to PDT, dramatic increase in leakage could be obtained in our study, by changing the drug and light dose of treatment. In order to induce occlusion by PDT as efficiently as observed in the neovascular networks, more drastic PDT conditions were applied in order to reach a sufficient blood flow stasis. This could be achieved for instance with 4 fold higher drug and light doses (800µg Visudyne®/kg b.w.; 200 J/cm^2), while retaining the clinical DLI of 10 minutes. All the experiments of this study were thus performed using these PDT conditions. An induction of neovascularisation in our model, by deposing an angiogenic factor [25] or grafting angiogenic tumor cells [26], will probably increase the sensitivity of the endothelial cells to the Visudyne®-PDT, probably inducing an even more important local leakage. This is currently under investigation.

It is well known that following PDT, damage to the microvasculature, in particular to endothelial cells [5, 6, 27, 28] and the vascular basement membrane, is induced and leads to the establishment of thrombogenic sites within the vessel lumen. This initiates a physiological cascade of responses including platelet aggregation [28, 29], the release of vasoactive molecules, vessel constriction [30] and leukocyte adhesion. Endothelial cells (ECs) are regarded as the blood-tissue interface that rapidly responds to any change in biological conditions induced by a trauma such as PDT that can affect the interaction between ECs and circulating blood cells. The early defense response of the ECs to any trauma is associated with a very fast (within a few seconds or minutes) response to histamine- or thrombin-like agonists [31]. These factors together with leucotriene (LTB4) [32] activate the polymorphonuclear leukocyte and the up-regulation of their receptors implicated in the inflammatory response following PDT. PDT also induces the expression of adhesion molecules such as P-selectins,

integrins (such as Mac-1) [32] and intercellular adhesion molecules (ICAM-1) [33-35], all known to be involved in leukocyte migration, rolling, adhesion and invasion of the perivascular tissue. The migration of leukocytes is followed by so called rolling along the inner wall of blood vessel. The leukocytes then become activated and adhere to the endothelium and finally transmigrate to the inflammatory site [36]. The reversible adhesion (rolling) of the leukocytes along the PDT-treated vascular endothelium microcirculation was observed in the present study up to 2 hours after treatment. This rolling is mediated by interaction with specific ligands of P-selectin which are present on platelets shortly after activation, and L-selectin expressed by the leukocytes themselves [37] as well as E-selectin which is present on activated ECs principally expressed within veins. It was observed in the skinfold chamber of nude mice that PDT induced the rolling of leukocytes leading to a low grade but well defined case of inflammation [10] one hour after treatment and developing a clear and significant case of inflammation 2 hours after treatment. This behavior of the leukocytes towards the endothelium will also influence the local vascular permeability. Actually, the development of a PDT-induced acute inflammation is in relation to the importance of the PDT-induced leakage. Indeed, the FITC leakage 2 hours after PDT, when an acute inflammation was measured, was significantly more important than directly after PDT. This could be partially explained by the activity of the leukocytes rolling along the vessel wall that contribute to the phenomenon of PDT-induced leakage, thus increasing the quantity of fluorescent dye leaking from the treated site 2 hours after PDT.

A major involvement of vascular endothelial growth factor (VEGF), also referred to as vascular permeability factor, is unlikely. VEGF, a regulator vascular permeability [38], is barely detectable in untreated tissue, and minimally expressed at 4 hours after PDT under low fluence rate conditions, as observed by Snyder et al. [39]. The fact that vascular permeability

is increased even after very short time after PDT, insufficient time for up-regulation of VEGF, speaks against VEGF-mediated mechanisms.

The kinetics of PDT-induced FITC leakage represented in figure 3.A. obviously suggest a bimodal distributions (for both times of observation) translating different vascular or tissue reactions, even if the absence of vascular acute inflammation before PDT was controlled by mean of counting the leukocytes rolling along the vessel walls for every mice and despite of the identical conditions of treatments and observations. In order to verify the hypothesis that a bimodal distribution of leakage profiles does exist, histological observations were then performed. One of the hypotheses was that there could be a difference between the 2 groups of mice in term of tissue thickness of the optical chambers. The excitation light used for PDT first crosses a muscle layer containing some capillaries before passing through a subcutaneous layer full of fat cells perfused by bigger blood vessels. One could imagine that if a thicker layer of tissue has to be crossed, some photons could be absorbed before reaching the big vessels of interest, thus diminishing the efficacy of PDT. However, using the same model, lower drug and light doses were applied to perform a PDT under clinical conditions. In these conditions, no significant leakage was observed showing that a less efficient PDT-induced occlusion could dramatically decrease the induced leakage. The measurement of the different layers and the mean tissue thickness of the chambers did not explain the difference of PDT-induced leakage between the 2 groups of mice (figure 5).

Nevertheless, these histology observations revealed other clear differences of tissue within the same group of treatment. Between the microsurgical implantation of the observation chamber and the microscopic observation, a recovery period of 3 days was allowed to eliminate the effect of anesthesia and surgical trauma on the microvasculature. Although in most acutely prepared tissues, there is always a surgically-induced acute inflammation but at the time of experiment, 3 days later, this vascular acute inflammation should be absent [10]. Each mouse

was then tested for its vascular inflammation and only the ones presenting ideal physiological microcirculation were selected for the study. This assessment controlling the absence of rolling leukocytes initiating their departure from the vascularisation exclude a vascular acute inflammation but does not exclude extra-vascular differences between the 2 groups of mice. The blinded histological analysis of the optical chambers revealed some differences that can translate an inter-individual variation in the level of inflammatory response following the surgical preparation. The observation of the histology in parallel with pharmacokinetic leakage curves reveals that when the tissue was characterised by an oedema in the muscle layer together with a clear infiltration of granulocytes outside the blood vessels, invading all the subcutaneous tissues of the optical chamber, then the PDT-induced leakage of FITC-dextran was significantly higher, in both times of observation.

We can then explain the bimodal distribution by the fact that despite of the exclusion of acute vascular inflammation for all the mice at the beginning of the experiment, some of them presented some stigmatism of a former surgically induced inflammatory response.

This modification in tissue structure, linked with chronicle inflammation can potentiate the PDT-induced leakage. These histological observations prove the hypothesis that a bimodal distribution of leakage profiles does exist, allowing then to present the mean values of PDT-induced leakage like in figure 3.B. This figure shows that the mean values of the quantification of FITC leakage to the interstitial space of the fluorescent drug already reaches a high value one hour after injection. More precisely, after 40 minutes of observation, the leakage occurring directly after treatment was found to be $6.0*10^6$ ($\pm$ $2.5*10^6$) arbitrary units (a.u.) in the group of mice without any histological sign of chronicle inflammation (curve a in Figure 3.B.) when the other group of mice receiving the same conditions of treatment but presenting stigmatisms of chronicle inflammation were found to reach $24*10^6$ ($\pm$ $10*10^6$) a.u. (curve b in Figure 3.B.). For the group of mice where the leakage was assessed 2 hours after

PDT, after 40 minutes of observation, the fluorescence values were $47*10^6$ ($\pm$ $13*10^6$) and $120*10^6$ ($\pm$ $26*10^6$) a.u. respectively for healthy (curve c in Figure 3.B.) and chronically inflamed chambers (curve d in Figure 3.B.). The comparison between these values allows us to conclude that even if the local leakage obtained directly after PDT with a physiological chamber is already significant, as illustrated in figure 2.A., the leakage observed under same conditions in chronically inflamed chamber leads to 4 fold more important local accumulation of the dye. An even more impressive difference is observed in the leakage obtained after developing an acute inflammation 2 hours after PDT, when the leakage in physiological vessels was found to be 8 fold and 20 fold higher than previously observed without any kind of inflammation immediately after PDT. As both age-related macular degeneration and cancer are characterized by inflammatory tissue, one could expect a more efficient photodynamic drug delivery in these kinds of tissue than in physiological non-inflamed surrounding structures.

Moreover, the leakage observed directly after PDT was strictly localised in the close surroundings of the treated area. This could be correlated to the fact that the PDT effect in term of vascular occlusion is strictly localised at the site of irradiation. In the opposite, the evaluation of the acute inflammation status of the chambers, defined by quantitative assessment of the rolling leukocytes was found to be homogenous in the whole chamber, meaning that the PDT-induced inflammation is not strictly localised at the site of irradiation. Reason why the leakage obtained 2 hours after treatment was found to spread around the treated area, as illustrated in figure 2.C,D. No variation of the leakage was observed in the non-treated surrounding areas despite of the inflammation occurring after PDT and of course no leakage was observed in control animals.

Conclusion

The goal of this project was to study the capacity of PDT to specifically make the treated blood vessels more permeable in order to improve local drug delivery. The model used was the dorsal skinfold chamber in nude mice allowing intravital microscopy observations. The local inflammation and the transvascular leakage of a macromolecule (2000 kDa FITC dextran) were quantify at different times after Visudyne®-mediated PDT. This treatment results in interruption of endothelial integrity. We measured an increase in leukocytes rolling, translating the development of an acute inflammatory vascular response over 2 hours following PDT. Furthermore, a time-dependent transient increase of local vascular permeability was observed. This leakage was clearly influenced by the chronic tissue inflammatory status of the subcutaneous structures. This observation is of major interest as many clinical situations present PDT-treatable diseases associated with inflammatory tissue status. This concept has the potential to improve the drug delivery of cytostatic drugs in chemoresistant tumours or anti-angiogenic drugs in AMD.

References

1. Miller, J.W., et al., *Photodynamic therapy with verteporfin for choroidal neovascularization caused by age-related macular degeneration: results of a single treatment in a phase 1 and 2 study.* Arch Ophthalmol, 1999. **117**(9): p. 1161-73.
2. van den Bergh, H., *Photodynamic therapy of age-related macular degeneration: history and principles.* Seminars in Ophthalmology, 2001. **16**(4): p. 181-200.
3. Costa, R.A., et al., *Immediate indocyanine green angiography and optical coherence tomography evaluation after photodynamic therapy for subfoveal choroidal neovascularization.* Retina, 2003. **23**(2): p. 159-65.
4. Jain, R.K., *Delivery of Novel Therapeutic Agents in Tumors - Physiological Barriers and Strategies.* Journal of the National Cancer Institute, 1989. **81**(8): p. 570-576.
5. Fingar, V.H., *Vascular effects of photodynamic therapy.* J Clin Laser Med Surg, 1996. **14**(5): p. 323-8.
6. Krammer, B., *Vascular effects of photodynamic therapy.* Anticancer Res, 2001. **21**(6B): p. 4271-7.
7. Debefve, E., et al., *Combination therapy using aspirin-enhanced photodynamic selective drug delivery.* Vascular Pharmacology, 2007. **46**(3): p. 171-180.
8. Endrich, B., et al., *Technical Report - a New Chamber Technique for Micro-Vascular Studies in Unanesthetized Hamsters.* Research in Experimental Medicine, 1980. **177**(2): p. 125-134.

9. Lehr, H.A., et al., *Dorsal Skinfold Chamber Technique for Intravital Microscopy in Nude-Mice.* American Journal of Pathology, 1993. **143**(4): p. 1055-1062.
10. Schafer, S.C., et al., *Paradoxical attenuation of leukocyte rolling in response to ischemia-reperfusion and extracorporeal blood circulation in inflamed tissue.* American Journal of Physiology-Heart and Circulatory Physiology, 2005. **289**(1): p. H330-H335.
11. Lehr, H.A., et al., *Leukotrienes as Mediators in Ischemia-Reperfusion Injury in a Microcirculation Model in the Hamster.* Journal of Clinical Investigation, 1991. **87**(6): p. 2036-2041.
12. Lehr, H.A., et al., *Intravital fluorescence microscopy for the study of leukocyte interaction with platelets and endothelial cells.* Oxidants and Antioxidants, Pt B, 1999. **300**: p. 462-481.
13. Morant, J. and H. Ruppaner, *Compendium Suisse des Médicaments. Basel, Switzerland.* 2002.
14. TAP Study Group, *Photodynamic Therapy of Subfoveal Choroidal Neovascularization in Age-Related Macular Degeneration With Verteporfin: Two-Year Results of 2 Randomized Clinical Trials--TAP Report 2.* Arch. Ophthalmol., 2001. **119**: p. 198-207.
15. Abramoff, M.D., P.J. Magelhaes, and S.J. Ram, *Image processing with ImageJ.* Biophotonics International, 2004. **11**(7): p. 36-42.
16. Lange, N., et al., *A new drug-screening procedure for photosensitizing agents used in photodynamic therapy for CNV.* Invest Ophthalmol Vis Sci, 2001. **42**(1): p. 38-46.
17. Schuitmaker, J., et al., *Photodynamic therapy: A promising new modality for the treatment of cancer.* Journal of Photochemistry and Photobiology B-Biology, 1996. **34**(1): p. 3-12.
18. van den Bergh, H., *Light and porphyrins in cancer therapy* Chemistry in Britain, 1986. **22**(5): p. 430-439
19. Dougherty, T., et al., *Photodynamic therapy.* Journal of the National Cancer Institute, 1998. **90**(12): p. 889-905.
20. van Lier, J., *Photosensitization: reaction pathways*. Photobiological techniques, ed. D. Valenzeno. 1990, New York: Plenum press 85-97.
21. van den Bergh, H. and J.P. Ballini, *Principles of Photodynamic Therapy*. Photodynamic Therapy of Ocular Diseases, ed. E. Gragoudas, J. Miller, and L. Zografos. 2004, Philadelphia, PA, USA: Lippincott Williams & Wilkins. 11-42.
22. Jori, G. and E. Reddi, *The role of lipoproteins in the delivery of tumour-targeting photosensitizers.* International Journal of Biochemistry, 1993. **25**(10): p. 1369-1375.
23. Hamblin, M.R. and E.L. Newman, *Photosensitizer targeting in photodynamic therapy. II. Conjugates of haematoporphyrin with serum lipoproteins.* Journal of Photochemistry and Photobiology B: Biology, 1994. **26**(2): p. 147-157.
24. Allison, B.A., P.H. Pritchard, and J.G. Levy, *Evidence for low-density lipoprotein receptor-mediated uptake of benzoporphyrin derivative.* British Journal of Cancer, 1994. **69**(5): p. 833-839.
25. Dellian, M., et al., *Quantitation and physiological characterization of angiogenic vessels in mice: Effect of basic fibroblast growth factor, vascular endothelial growth factor/vascular permeability factor, and host microenvironment.* American Journal of Pathology, 1996. **149**(1): p. 59-71.
26. Leunig, M., et al., *Angiogenesis, microvascular architecture, microhemodynamics, and interstitial fluid pressure during early growth of human adenocarcinoma LS174T in SCID mice.* Cancer Research, 1992. **52**(23): p. 6553-6560.

27. Fingar, V., et al., *Vascular damage after photodynamic therapy of solid tumors: A view and comparison of effect in pre-clinical and clinical models at the University of Louisville.* In Vivo, 2000. **14**(1): p. 93-100.
28. Henderson, B.W., et al., *Effects of photodynamic treatment of platelets or endothelial cells in vitro on platelet aggregation.* Photochem Photobiol, 1992. **56**(4): p. 513-21.
29. Sporn, L. and T. Foster, *Photofrin and light induces microtubule depolymerization in cultured human endothelial-cells.* Cancer Research, 1992. **52**(12): p. 3443-3448.
30. Schuster, A., et al., *Simultaneous arterial calcium dynamics and diameter measurements: application to myoendothelial communication.* Am J Physiol Heart Circ Physiol, 2001. **280**(3): p. H1088-96.
31. Freidlin, I.S., *Immunophysiology of endothelial cells.* Human Physiology, 2006. **32**(3): p. 357-367.
32. Kobayashi, W., et al., *Photodynamic therapy upregulates expression of Mac-1 and generation of leukotriene B4 by human polymorphonuclear leukocytes.* Oral Oncology, 2004. **40**(5): p. 506-510.
33. Dellian, M., et al., *Effects of photodynamic therapy on leucocyte-endothelium interaction: Differences between normal and tumour tissue.* British Journal of Cancer, 1995. **72**(5): p. 1125-1130.
34. Gollnick, S., et al., *Role of cytokines in photodynamic therapy-induced local and systemic inflammation.* British Journal of Cancer, 2003. **88**(11): p. 1772-1779.
35. Yeh, D.C., et al., *Expression of leukocyte adhesion molecules in human subfoveal choroidal neovascular membranes treated with and without photodynamic therapy.* Investigative Ophthalmology and Visual Science, 2004. **45**(7): p. 2368-2373.
36. Kubes, P., *Introduction: The complexities of leukocyte recruitment.* Seminars in Immunology, 2002. **14**(2): p. 65-72.
37. Venturi, G.M., et al., *Leukocyte migration is regulated by L-selectin endoproteolytic release.* Immunity, 2003. **19**(5): p. 713-724.
38. Yuan, F., *Transvascular drug delivery in solid tumors.* Seminars in Radiation Oncology, 1998. **8**(3): p. 164-175.
39. Snyder, J.W., et al., *Photodynamic therapy: a means to enhanced drug delivery to tumors.* Cancer Res, 2003. **63**(23): p. 8126-31.

^

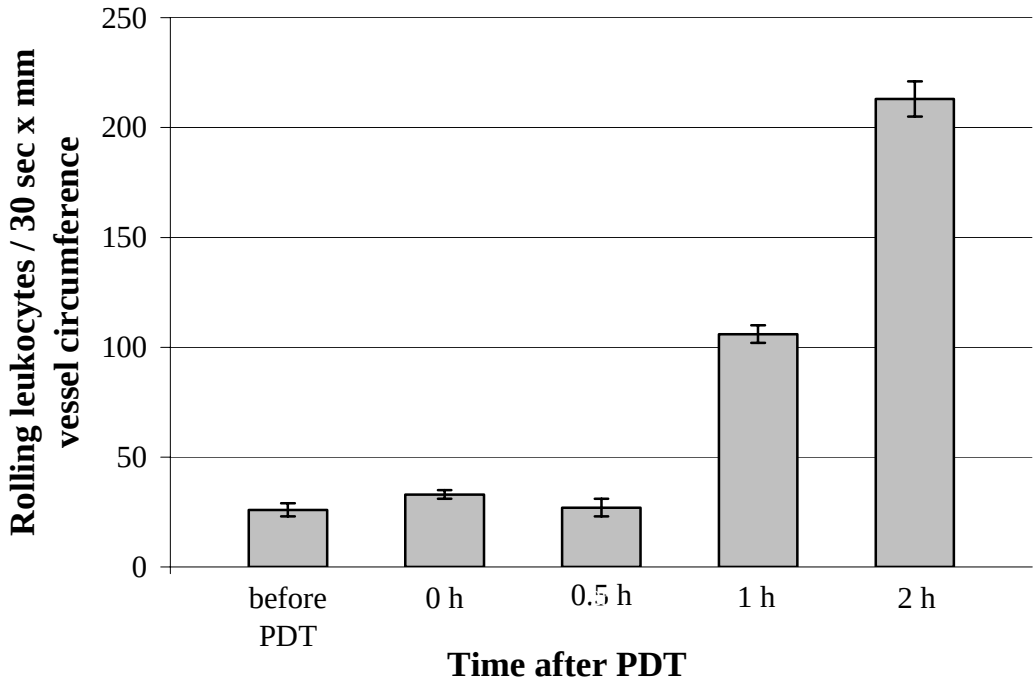

Figure 1: Quantification of the vascular acute inflammatory status of the chamber at different times after PDT (DLI of 10 minutes, 800 µg BPD-MA/kg and 200 J/cm^2). All the mice used for this study presented less than 30 rolling leukocytes/mm vessel circumference in 30s, corresponding to ideal optical chambers without any acute inflammation. The quantification of the inflammation before PDT was actually 26 ± 3 leukocytes /30s and per mm. Directly after the end of the PDT, the rolling leukocytes were counted again, showing that no change in reaction of these cells has occurred yet (33 ± 2 leukocytes /30s and per mm). The same observation repeated 30 minutes later still did not show any increase in the number of rolling leukocytes (27 ± 4 leukocytes /30s and per mm). 1h after PDT, 106 ± 4 leukocytes /30s and per mm were counted characterizing tissue in the optical chamber with a sign of a slight acute inflammation. This inflammatory response was more obvious 2 hours after treatment when 213 ± 8 leukocytes /30s and per mm were counted.

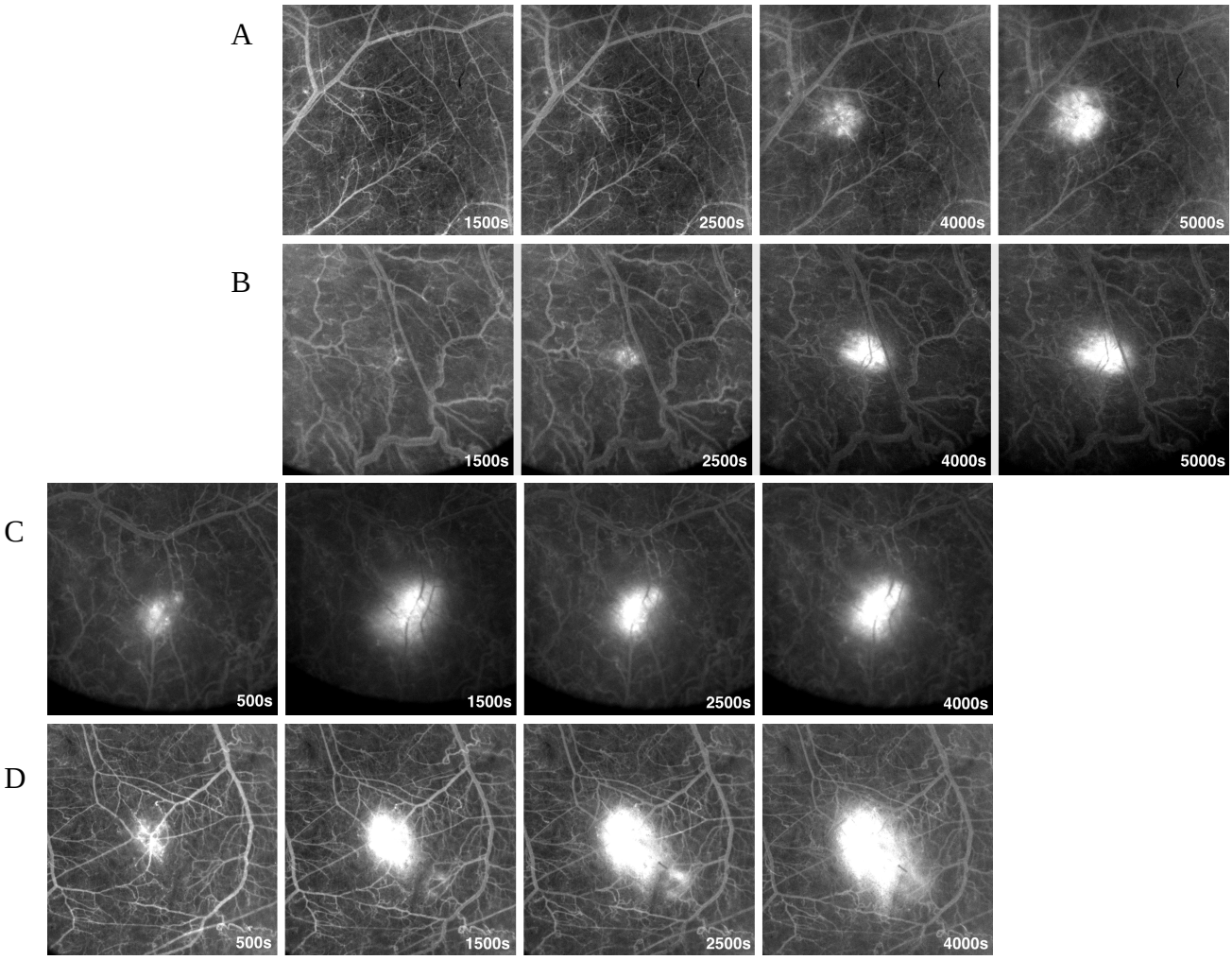

Figure 2: To assess the effect of PDT on a dye leakage directly after treatment (A, B) and 2 hours after PDT (C, D), a solution of FITC-dextran 2000kDa was intravenously (i.v.) administered 10 minutes before irradiation and 2 hours after PDT respectively. PDT was then performed and fluorescence images of the FITC distribution inside the optical chamber were recorded as a function of time over a 5000 and 4000 seconds period respectively. Typical sequences of pictures obtained under these conditions showed an obvious increased local leakage from the treated area, increasing with time. This phenomenon was more and more important from the sequence A to D.

Captions related to the discussion: After histological analysis and leukocytes behavior observations, we can conclude that the sequence A presented no sign of any kind of inflammation; sequence B corresponds to a sequence obtained with mice presenting chronicle tissue inflammation; C is a typical sequence found in mice presenting acute vascular inflammation and finally D represents the case where both acute and chronicle inflammations were observed.

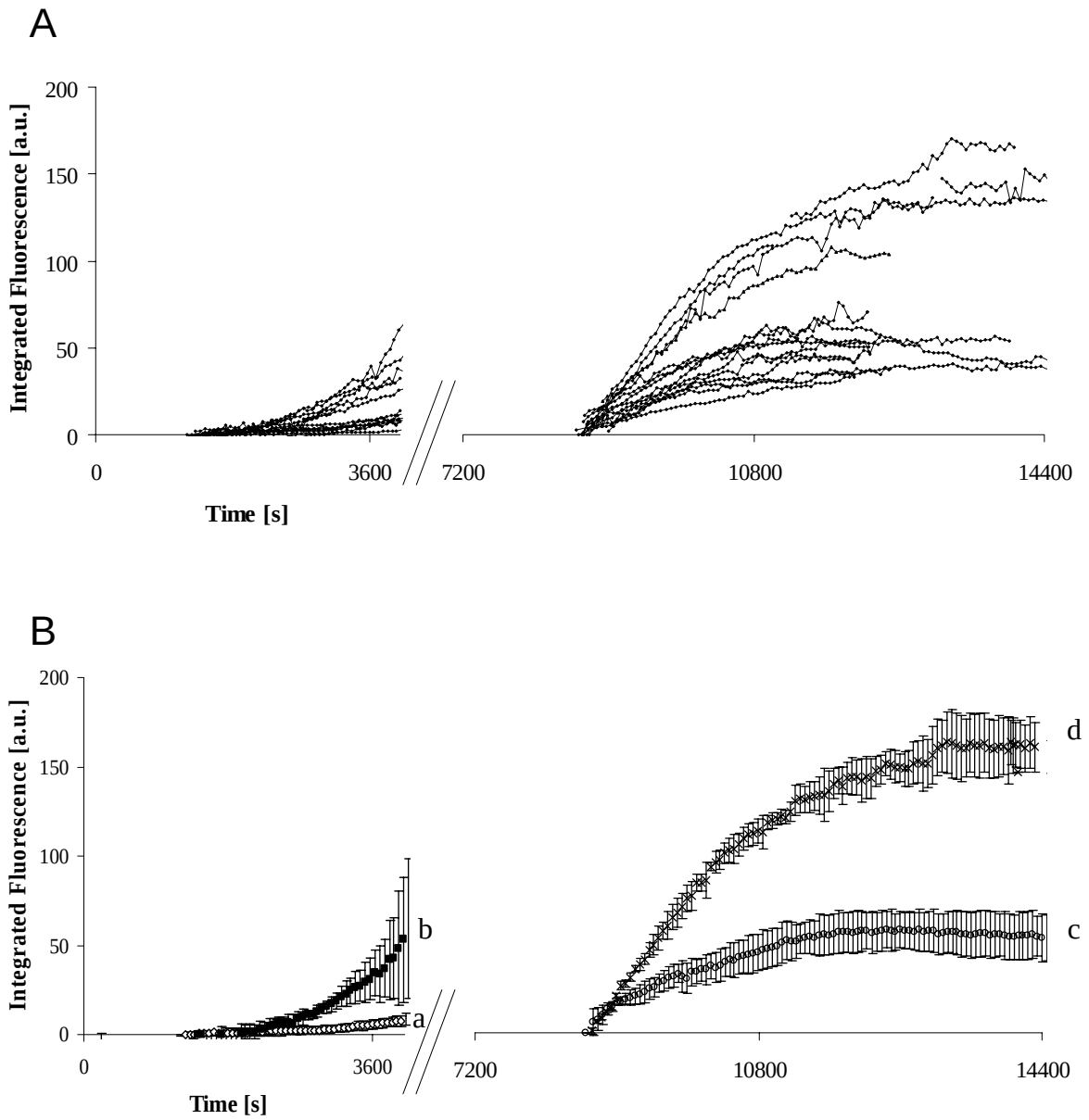

Figure 3: Quantification of the accumulation of the fluorescent dye (FITC-dextran 2000 kDa) around the treated site reflecting the local PDT-induced leakage directly after treatment is represented in the first part of the graph, where time 0 corresponds to the injection of Visudyne®. The same observation of the induced leakage 2 hours after PDT is represented in the second part of the graph. **(A)** All mice values are reported in the graph. A clear PDT-induced local leakage was observed in every mice, but the leakage quantification (directly and 2 hours after PDT) at the two times of observation presented a large distribution within the same group of treatment. **(B)** The mean values of the different groups of mice allow some comparisons. After 40 minutes of observation, the leakage occurring directly after treatment was found to be $6.0*10^6$ ($\pm$ $2.5*10^6$) arbitrary units (a.u.) in the group of mice without any histological sign of chronicle inflammation when the other group of mice receiving the same conditions of treatment but presenting stigmatisms of chronicle inflammation were found to reach $24*10^6$ ($\pm$ $10*10^6$) a.u. For the group of mice where the leakage was assessed 2 hours after PDT, after 40 minutes of observation, the fluorescence values were $47*10^6$ ($\pm$ $13*10^6$) and $120*10^6$ ($\pm$ $26*10^6$) a.u. respectively for healthy and chronically inflamed chambers.

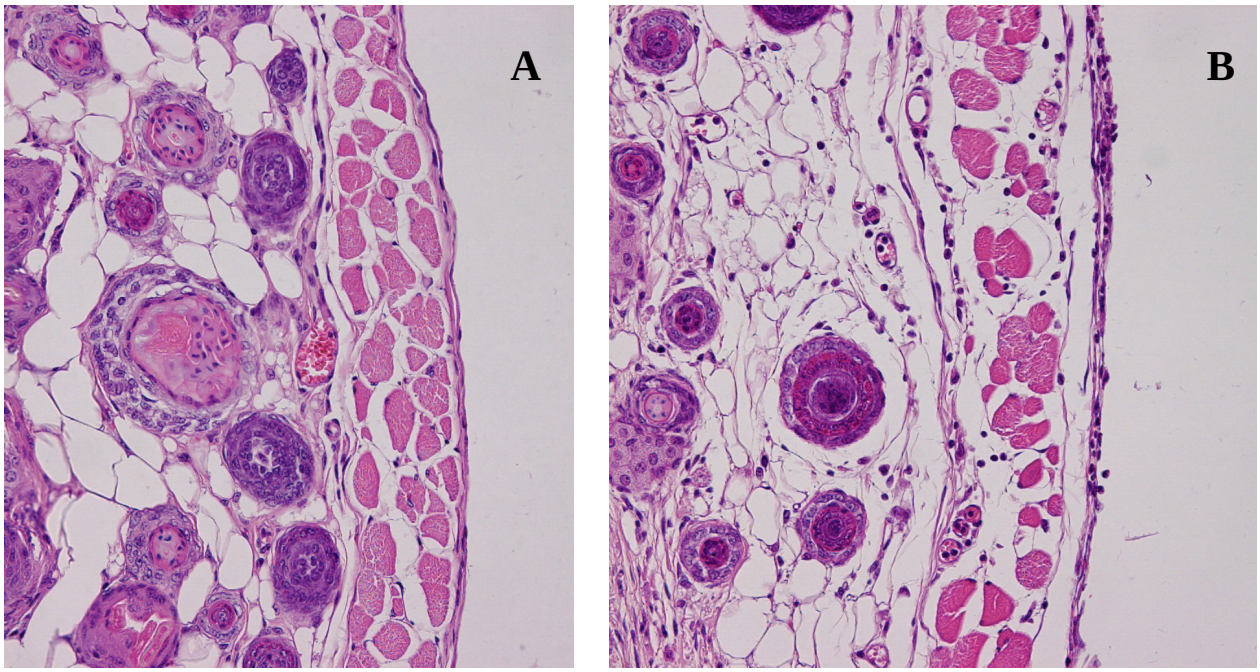

Figure 4: (A) In mice with low extravascular leakage after PDT treatment no significant sign of preexisting edema was detectable by standard histological examination. The striated muscle tissue remained in its regular histological limits and the connective tissue remained compact. No inflammatory infiltration was observed in these compartments. Sporadic inflammatory cells were observed attaching to the inner vessel wall of post-capillary venules in the groups with low vascular leakage without significant difference between the three groups (no PDT, 30 min and 150 min after PDT, respectively).
(B) Mice with high extravascular leakage showed increased inflammatory cell infiltration in the subcutanous tissue as well as increased adhesion of inflammatory cells to the inner vessel wall of post-capillary venules. The subcutanous connective tissue showed marked edema, which also could be observed within the striated muscle tissue.

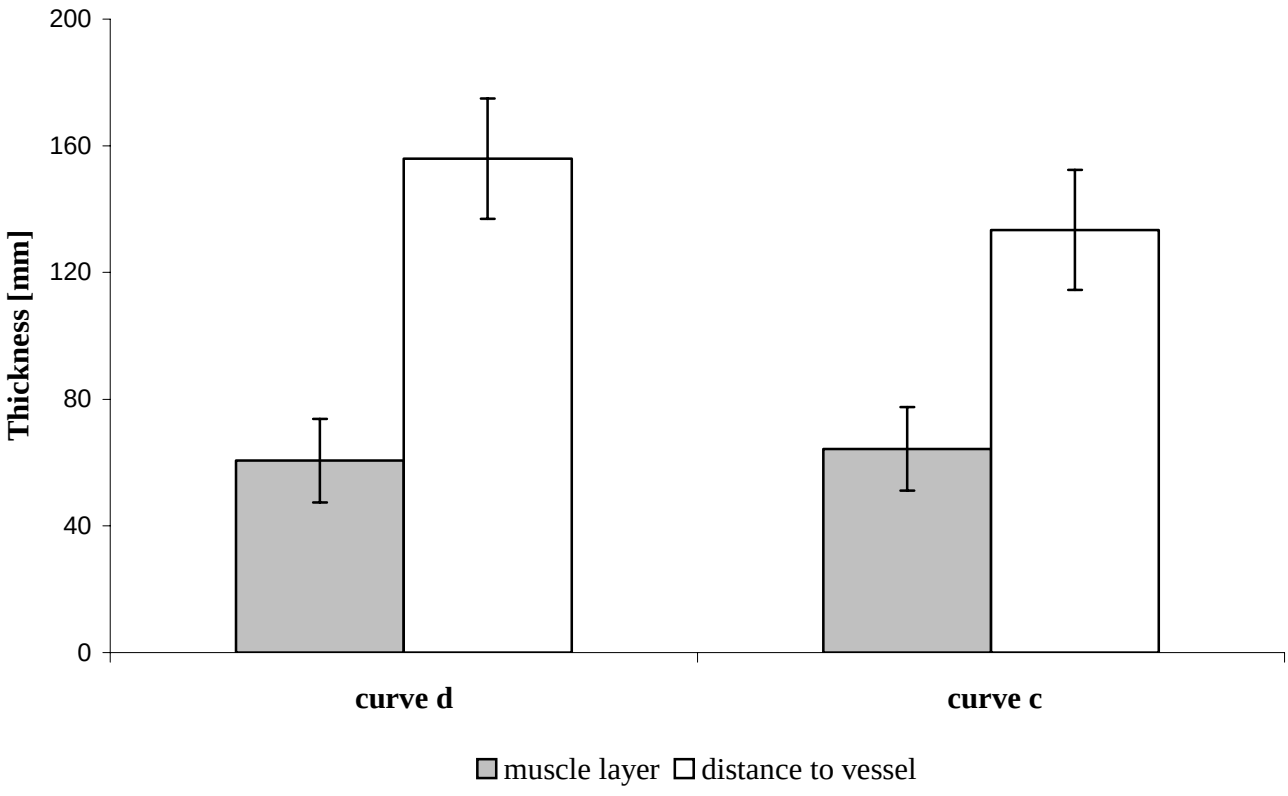

Figure 5: This picture shows the mean values of the tissue layers measurements on histological sample of the skinfold chamber of mice from the curves d and c shown in Figure 3.B., respectively corresponding to high and low leakage observed 2 hours after PDT. Measurements of the total muscle layer thickness showed no significant difference between the two groups (grey columns, 60.64µm ± 12.80µm and 64.34µm ± 13.18µm, respectively). Likewise, the distance between the inner surface covered by the glass and the treated vessels showed no significant difference between the groups d and c (white columns, 155.88µm ± 28.18µm and 133.42µm ± 19.00µm, respectively).

Chapitre 5

Tumour grafting in the skinfold chamber of nude mice observed by intravital microscopy

Introduction

The experiments exposed in the chapter 4 of this thesis work, entitled “Photodynamic selective drug delivery for combination therapy investigated in the skinfold chamber of nude mice observed by intravital microscopy” were performed in physiological mature blood vessels. This mammal model that allowed obtaining standard results could also be further developed to comprise neo -or tumoral- vasculature. The induction of neovessels in the skinfold chamber can be achieved by deposing an angiogenic factor (such as VEGF) a few days before PDT [1]. Tumoral blood vessels could also be induced by grafting angiogenic tumour cells in the chamber [2]. One of the techniques consists of deposing a solution comprising tumour cells on the optical chamber and to wait for the growth of the tumour until it induces tumoral neovessels. Actually, most quantitative information on tumour angiogenesis, microcirculation, and transport has been derived from tumours grown in transparent chamber preparations. Another technique consists of deposing a piece of tumour, already about 1 mm^3 in size, which should enhance the formation of neovessels in shorter time delay. This would allow reducing the time interval between the implantation of the optical chamber and the PDT experiments, thus shortening the overall time for the experiments, which is better for the mouse and for the integrity of its optical chamber. The immunodeficience of the nude mouse used in the chapter 4 and in the present chapter allows the implantation of human tumour xenograft in their skinfold chamber. The dorsal skinfold chamber can be used for the growth of human cancer cell lines. The growth for instance of angiogenic H-Meso-1 tumour cells in the optical chamber can and will be furthermore used for assessment of photodynamic drug delivery. Within this concept, this chapter consists of observing the evolution of this type of tumour graft.

Materials and Methods

The Swiss nude mice were provided by Charles River Laboratories (L'Arbresle, France). First, the tumour is formed by a subcutaneous injection of human mesothelioma tumour cells (H-Meso-1) on the shoulder, on top of the scapula of a first nude mouse. When the size of the tumour reaches a diameter of around 5 mm, the mouse is sacrificed by cervical dislocation and the tumour is carefully removed and dissected in pieces of about 1 mm^3 excluding necrotic tissues. These pieces of tumour can then be used for the implantation in the middle of the skinfold chamber of other nude mice. The experimental preparation of the skinfold chamber is the same as descrbied in the chapter 4 of this thesis, thus following the work of Lehr et al. [3, 4]. The experiments of tumour grafting were conducted in accordance with the national and institutional guides for the care and use of animals (cantonal veterinary authorisation n°1915).

Between the implantation of the observation chamber and the graft of the tumor, a recovery period of 24 hours was allowed to control the integrity and the good quality of the tissue after surgery. Trans-illumination microscopy and Achroplan objectives 2.5x and 4x (described in chapter 4) were used to observe the evolution of the tumour growth until the 9th days following the graft.

Fluorescein isothiocyanate (FITC) –dextran 2000 kDa was intravenously administered to observe the vasculature in the optical chamber and to assess if tumoral neovessels are being developed in the graft.

Results

The in vivo model of the skinfold chamber on the nude mouse can be used for the observation of tumour growth. This model could also be of great interest to further assess new treatment modalities such as the photodynamic drug delivery pathway and combination therapy. The

preliminary assessments exposed in this chapter show the development of a human tumour graft (H-Meso-I) and its neovascularisation. In this chapter, a typical sequence of pictures taken during the 9 days following the surgical grafting is shown. Figures A, B show pictures taken by white light trans-illumination, at day 1 following the deposit of a 1 mm^3 piece of tumour in the optical chamber. These pictures clearly show that the integrity of the blood vessels is well preserved. At day 2 (Figures C, D), one can note that the straightness of the blood vessels is perturbed by the graft, giving some tortuous shape to the main vasculature. The size of the tumour remains the same for the whole time of observation. During the 3 next days, no obvious change in shape, size, colour of the blood vessels and tumour graft was noted (data not show) but from the 6th day following the implant, a clear vascular reaction appears around the graft.

Two main phenomena were observed:

1) First, if we compare the junction of blood vessels encircled in Figures D and F, one can note that at day 2, the 2 branches of the vessel almost have similar diameters. On the opposite, four days later (Figures E, F) a clear vasodilation occurs in the branch situated in the neighbourhood of the graft (black arrow) showing a recruitment of the blood flow to help in the feeding of the tumour.
2) Secondly, Figure E shows small capillaries around the tumour that were absent before this day. These blood vessels are newly formed by angiogenesis, i.e. they bud perpendicularly from bigger pre-existing blood vessels (white arrows). The orientation of the pre-existing capillaries is also influenced by the graft, as we observed that they converge toward the tumour forming an almost parallel network. These different phenomena giving a reddish colour in Figure F around and inside the graft are signs of beginning of neovascularisation, together with a slight inflammation of the tissue.

Figure G gives an idea of the macroscopic aspect of the optical chamber at that stage of observation, when the graft and its surroundings present a reddish aspect.

From day 8, pictures were taken by mean of a new digital camera fixed to the objective of the microscope allowing variation the optical filters in order to improve the contrasts. Additionally, an intravenous injection of FITC 150 kDa allowed observing daily the evolution of the perfusion of the vasculature. These injections of a fluorescent dye should not be performed from the beginning of the observation (during 10 days) otherwise the accumulation of the residual fluorescence would dramatically decrease the contrast.

Figure H was taken with a white trans-illumination together with an epi-illumination at 470 nm. In this picture, we see that a dense vascular network surrounds the tumour and that the entire graft has blood spots both translating an evolution in the perfusion of the tumour. This neovascularisation around the tumour is confirmed by a hyperfluorescence around the graft observed after injection of FITC in Figure I. The observation of the intravascular FITC with a bigger magnification (4x instead of 2.5x for the other pictures), as illustrated in figure J, shows hypofluorescent blood spots, probably due to leaky vessels, giving a better contrast that allows observing some blood vessels passing through the tumour (see black arrows).

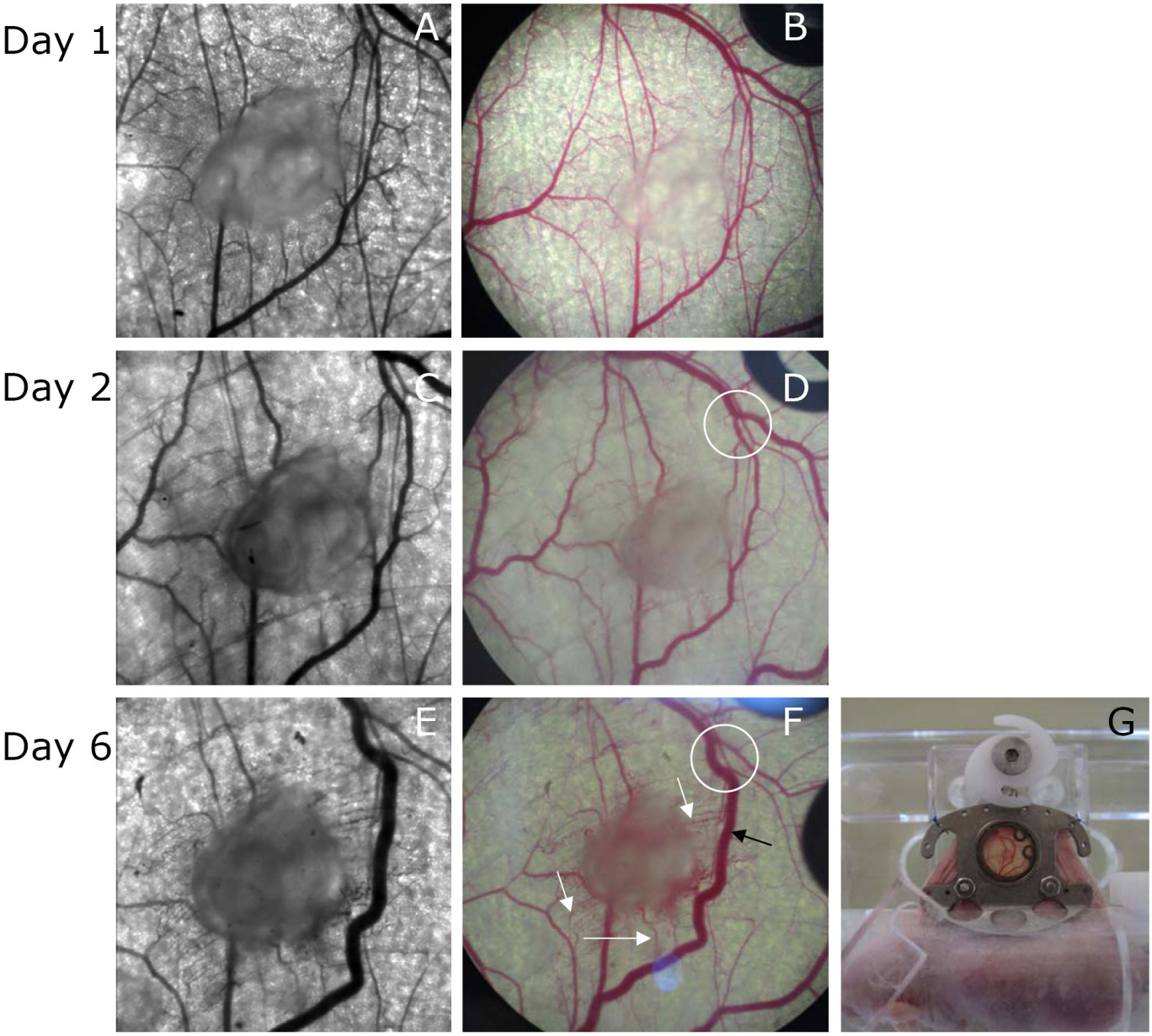
Day 1
A
B
Day 2
C
D
Day 6
E
F
G

Day 9

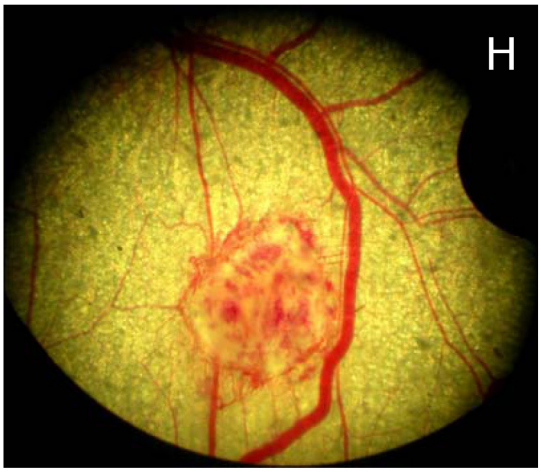

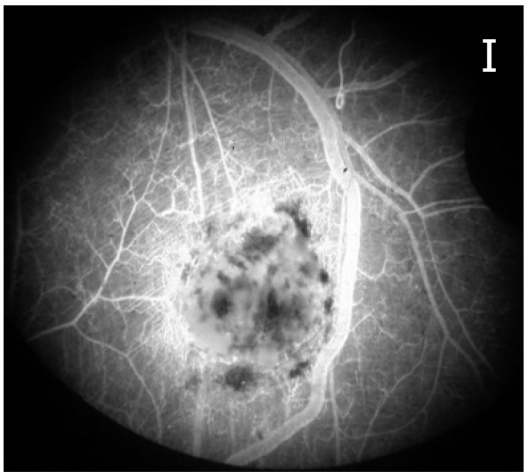

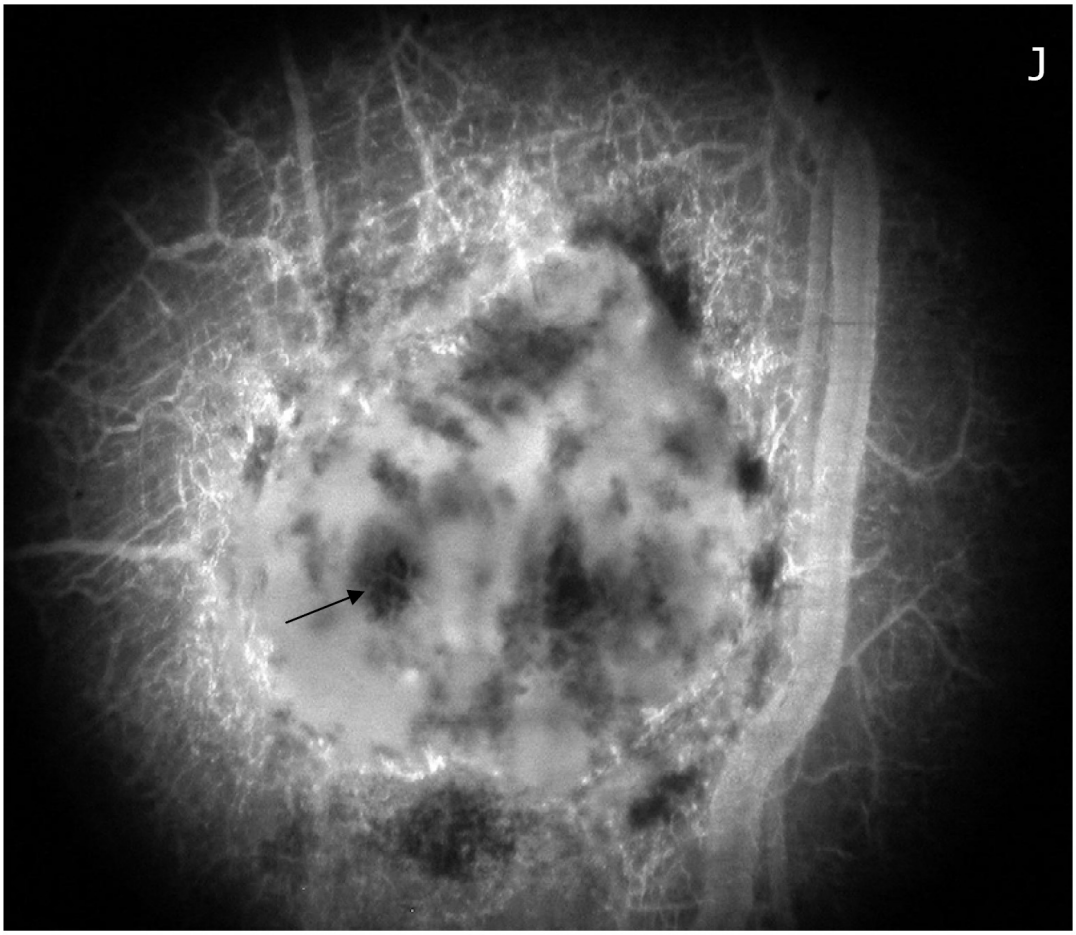

Conclusion

With all the observations of these preliminary assessments of tumour graft on the skinfold chamber of nude mice, we can conclude that the H-Meso-I can grow efficiently under the skin of a first host nude mouse in one week. A piece of this tumour can be efficiently transplanted and tolerated by another nude mouse carrying an optical skinfold chamber. This tumour graft develops some neovessels that are observable already 9 days after grafting. This model is the suitable to perform some experiments focusing on the vascular effects of photodynamic therapy.

References

1. Dellian, M., et al., *Quantitation and physiological characterization of angiogenic vessels in mice: Effect of basic fibroblast growth factor, vascular endothelial growth factor/vascular permeability factor, and host microenvironment.* American Journal of Pathology, 1996. **149**(1): p. 59-71.
2. Leunig, M., et al., *Angiogenesis, microvascular architecture, microhemodynamics, and interstitial fluid pressure during early growth of human adenocarcinoma LS174T in SCID mice.* Cancer Research, 1992. **52**(23): p. 6553-6560.
3. Lehr, H.A., et al., *Dorsal Skinfold Chamber Technique for Intravital Microscopy in Nude-Mice.* American Journal of Pathology, 1993. **143**(4): p. 1055-1062.
4. Schafer, S.C., et al., *Paradoxical attenuation of leukocyte rolling in response to ischemia-reperfusion and extracorporeal blood circulation in inflamed tissue.* American Journal of Physiology-Heart and Circulatory Physiology, 2005. **289**(1): p. H330-H335.

Chapitre 6
Discussion and conclusion

Conclusion and ideas for the future…

The experiments in the chorioallantoic membrane model (CAM) showed that modulation of the vascular PDT effects can lead to an enhanced local leakage (chapter 2). This modulation was achieved by administrating aspirin shortly before PDT treatment [1]. Aspirin acting principally as anti-aggregating factor delayed, but did not decrease, the PDT-induced formation of the thrombus. One of the advantages of this approach is its fast biochemical action after injection. One of its possible drawbacks is the irreversible activity on platelets [2, 3]. Furthermore, with a sufficient drug dose, acetylsalicylic acid also has an anti-inflammatory activity [4]. The haemostasis is thus difficult to quantitatively control in time. Delaying the vascular PDT effect to increase the local leakage before closure of the treated vessel requires a strictly controlled inhibition of platelet aggregation. Hence it is proposed here to use another anti-platelet drug acting exclusively at the level of platelet aggregation, thus avoiding other pharmacological activities. Integrilin® and Aggrastat® are possible candidates for this purpose. Integrilin® (Essex Chemie) [3] is an eptifibatidium speciality that acts by inhibiting the binding of fibrinogen and von Willebrand factor to the glycoprotein (Gp) IIb/IIIa receptor, which is the main receptor responsible for the platelet aggregation. Its activity on thrombocitar function is rapidly reversible and dose dependant. Aggrastat® (MSD) [3] is a triofiban derivative that acts as a non-peptidic antagonist of the Gp IIb/IIIa receptor, also inhibiting the thrombus formation with a reversible effect. Both of them should in further experiments be assessed and compared to aspirin in a combination therapy using Visudyne®-PDT in this model.

As observed in this thesis, the two main phenomena observed during and shortly after PDT are vasoconstriction and thrombus formation in the treated vessels (chapter 3). In the framework of this thesis, in order to delay the PDT-induced occlusion of the blood vessel to

allow the leakage of a fluorescent dye, we focused on the inhibition of platelet aggregation. The observed leakage may be optimized in a further study by temporary inhibiting not only the platelet aggregation but also the vasoconstriction induced by PDT. Delaying both these phenomena could be a possibility to optimize the photodynamic drug delivery. A drug acting as vasodilator is one possibility. Flolan® could be a better candidate for this purpose. Flolan® (Glaxo-SmithKline) [3] is an epoprostenol speciality that is a synthetic prostacyclin. It induces an inhibition of platelet function, combined with a vasodilator effect, both reversible.

In chapter 2 of the thesis, the model used was the chorioallantoic membrane model (CAM) of the chicken embryo where no leakage was observed during Visudyne®-PDT without aspirin, due to a sticking effect of the platelets. As described previously, to observe an increased leakage, before PDT, we must administrate a drug which delays thrombus formation. On the contrary, in chapter 4 of this thesis performed where we worked with the skinfold chamber of the nude mouse, an increase in leakage is shown and measured at two times (directly and 2h after PDT), even in the absence of aspirin or any other substance which delays clotting. In a further study, it would be interesting to assess in this mammal model the influence of aspirin or another inhibitor of the platelet function on the PDT-increased leakage.

One explaination for the absence of observable aspirin effect, is that with low doses of aspirin, an inhibition of the platelet aggregation is achieved, potentially increasing the leakage observed directly after PDT, when the thrombus formation is normally already initiated by Visudyne®-PDT in the skinfold chamber. If a sufficiently low dose of aspirin is used, it should not have any effect on the leukocyte kinetics. A high dose of aspirin could on the contrary interfere with the leukocytes activation by PDT, thus modulating their adhesion to the vessel wall of veins and maybe influencing the local leakage 2 hours after PDT. As the leukocytes are also involved in the increase in vessel permeability, their inhibition by a non steroidal anti-inflammatory drug, such as aspirin, could diminish the leakage. One could

imagine to “play” with all these parameters in order to optimise the control of the local dosage in time and quantity.

In the experiments performed in this thesis, fluorescein isothiocianate linked with different sizes of sugar was used as fluorescent leakage indicator. These fluorescent molecules have molecular weights between 10 kDa (chapters 2, 3) and 2000 kDa (chapter 4). Under the conditions chosen for these studies, the latter was able to extravasate from the blood vessel of the skinfold of the mouse. In a further study, one can imagine to assess a larger molecule or particle to find the steric limit of leakage induced under our PDT conditions. In another study of our group, biodegradable nanoparticles with different sizes ranging from 121 and 343 nm were tested into the CAM model for their leakage kinetics, demonstrating that the leakage is dependent on the size of nanoparticle drug carrier. Indeed, at the applied conditions, the large nanoparticles (300 nm) are apparently rapidely recognised by the reticulo-endothelial system decreasing their circulation time [5]. This study showed that the nanoparticle with a size around 100 nm had a longer circulation time than the larger particles. As the FITC-dextran 2000 kDa is in the same order of size, one could expect to have a similar vascular behaviour as observed for the nanoparticles of 100 nm. This mean size of nanoparticles allows the drug to keep circulating without leaking fast everywhere in the body, thus preventing adverse events due to the interactions with the non-targeted tissue. This type of biocompatible nanoparticles, as described by Konan *et al.* [6] offers the possibility of encapsulating an active drug that can be vehicled to the target tissue. If the leakage of these nanoparticles can be locally increased by PDT, the local delivery of a nano-encapsulated chemotherapeutic drug could be envisaged.

For all the experiments of this thesis, the photosensitiser used was Visudyne® that is well known for its vascular PDT efficacy [7]. Other photosensitisers with vascular PDT effects, such as Tookad [8] could also be tested for their ability to increase the vascular permeability

with and without delaying the blood clot formation. The pathway leading to the photo-occlusion could be somehow different than with Visudyne®. It would be interesting to evaluate if another pharmacodynamics of PDT occlusion could also lead to a local leakage.

A variation of the conditions of PDT, such as using a lower fluence rate [9] should be tested to evaluate its influence on the PDT-induced leakage, maybe with higher efficacy due to the renewal of oxygen needed for PDT reactions, which under our conditions may be somewhat limited by diffusion.

In the experiments exposed in chapter 4 of this thesis, we studied the influence of PDT on the vascular permeability in the skinfold chamber of nude mice observed by intravital microscopy (IVM). This mammal model allowed to assess the PDT-induced leakage in physiological mature blood vessels to obtain standard results but can also be further developed to comprise a tumoral vasculature. Different models comprising cancer cells have been developed [10] to assess the photodynamic delivery pathway in the tumoral vasculature. One of the possibilities is to graft a piece of tumour inside the skinfold chamber of the nude mouse. This is shown in the preliminary experiments of chapter 5 of this thesis. The induction of neovessels in tissue within the skinfold chamber might also be achieved by deposing an angiogenic factor (such as VEGF) a few days before PDT [11].

As explained in the discussion of the chapter 4, an induction of neovascularisation in the skinfold chamber model, by deposing an angiogenic factor or grafting angiogenic tumor cells (as explained in chapter 5), could increase the sensitivity of the endothelial cells to the Visudyne®-PDT, suggesting the use of lower drug/light doses to obtain the same level of vessel occlusion and maybe different kinetics of leakage.

Another study already begun, following the lines started in this thesis is being performed in mesothelioma bearing rats, (Methylcholanthrene-induced sarcoma (MCA)). This study is performed within of the collaboration between the EPFL and the CHUV of Lausanne to

evaluate if a pre-treatment by intraoperative photodynamic therapy of the chest cavity in malignant pleural mesothelioma bearing rats [12] inducing a vascular local leakage could increase the efficacy of cytostatic perfusion of the isolated lung (ILP) [13].

If this is the case, this new therapeutic approach offered by the photodynamic drug delivery could be a new opening for several cancers for which until now, there is no efficient curative treatment, such as mesothelioma [14, 15]. The incidence of malignant mesothelioma, principally due to contacts with asbestos, is still growing and is likely to do so beyond 2020 [16-18]. Mesothelioma is a serious form of cancer that occurs usually on the visceral pleura in the thorax. Until now, there's no efficient curative treatment. The treatment currently proposed includes surgery, followed by chimiotherapy and radiotherapy. In spite of these tri-therapies, the prognosis remains very poor because of the frequent local recurrence. Innovating therapies are consequently necessary in order to thwart this disease resistant to the therapies traditionally used in oncology. Cytostatic perfusion of the isolated lung (ILP) is already an attractive therapeutic concept because it allows to deliver a higher dose of cytostatic agent (such as doxorubicin) exclusively to the targeted organ, preserving systemic circulation and the adverse side effects [13, 19-21]. This ILP technique has been investigated in different studies in the Thoracic Surgery group of Professor Ris in the CHUV of Lausanne. Actually, doxorubicin is associated with important side effects, especially cardiotoxicity [3, 22] with high systemic doses. ILP based on doxorubicin (doxo-ILP) has been investigated in different phase I clinical studies and its feasibility has been demonstrated but up to now without any convincing efficacy [19-21]. Even if an amount of doxorubicin 10 times higher usual is accumulated in the lung compared to systemic circulation after ILP, space heterogeneity of the doxorubicin in the lung and a weak penetration of the substance in tumoral cells were observed. One does note an accumulation of doxorubicin in the tumoral vessel wall. This tumoral penetration was neither modified by the technique of perfusion

applied nor by the pegylation of the doxorubicin and its encapsulation in liposomes. Consequently, other innovating pre-treatments must be explored to overcome the accumulation of drug in the vessel wall in order increase the tumoral drug delivery and cellular uptake of the cytostatic agent during isolated lung perfusion based on doxorubicin (doxo-ILP). The goal of the future study, involving collaboration between EPFL and CHUV, is then to study the capacity of photodynamic therapy to specifically make the tumour vessels more permeable during the ILP in order to improve the tumoral penetration of doxorubicin and its liposomal/pegylated forms. A local leakage, as observed in the chorioallantoic membrane model and in the skinfold chamber of the nude mouse, could be promising for the treatment of cancers, by enhancing the drug delivery of chemotherapeutic agents. The fiber optic light delivered PDT will induce a local increase in leakage that will allow the local leakage of a chemotherapeutic. If this investigation which is under way in the rat model confirms our expectations, it will be used in clinical trials in the very near future.

Additionally to these two kinds of pre-clinical assessments of PDT-induced leakage into a skinfold chamber grafted with H-MESO-1 tumor cells, and in the MCA-induced sarcoma bearing rats, experiment could be performed to assess combination therapy for the treatment of age-related macular degeneration (AMD).

Many studies considered the use of Visudyne®-PDT in combination with intra-vitreous injection of anti-inflammatory or angiostatic agents as well as anti-VEGF antibodies. These therapies revealed promising outcomes [23, 24]. A PDT-induced enhancement in vascular permeability could allow avoiding the discomfort of the currently used repetitive intra-ocular administration by replacing it with a drug delivery from systemic circulation. This innovative drug delivery could also reduce the frequency of injection.

1. Debefve, E., et al., *Combination therapy using aspirin-enhanced photodynamic selective drug delivery.* Vascular Pharmacology, 2007. **46**(3): p. 171-180.
2. Rosenblum, W. and F. El-Sabban, *Platelet-aggregation in cerebral microcirculation-Effect of aspirin and other agents* Circulation Research 1977. **40**(3): p. 320-328.
3. Morant, J. and H. Ruppaner, *Compendium Suisse des Médicaments. Basel, Switzerland.* 2002.
4. Janka, H.U., *Inhibition of Platelet Adenylate-Cyclase by Aspirin - a Further Argument for a Low-Dose Regimen in Anti-Platelet Drug-Therapy.* Ircs Medical Science-Biochemistry, 1981. **9**(11): p. 1019-1019.
5. Pegaz, B., et al., *Effect of nanoparticle size on the extravasation and the photothrombic activity of meso(p-tetracarboxyphenyl)porphyrin.* Journal of Photochemistry and Photobiology B-Biology, 2006. **85**(3): p. 216-222.
6. Konan, Y.N., et al., *Preparation and characterization of sterile sub-200 nm meso-tetra(4-hydroxylphenyl)porphyrin-loaded nanoparticles for photodynamic therapy.* Eur J Pharm Biopharm, 2003. **55**(1): p. 115-24.
7. Fingar, V.H., et al., *Analysis of acute vascular damage after photodynamic therapy using benzoporphyrin derivative (BPD).* Br J Cancer, 1999. **79**(11-12): p. 1702-8.
8. Rück, A., A. Böhmler, and R. Steiner, *PDT with TOOKAD® studied in the chorioallantoic membrane of fertilized eggs.* Photodiagnosis and Photodynamic Therapy, 2005. **2**(1 SPEC. ISS.): p. 79-90.
9. Henderson, B.W., T.M. Busch, and J.W. Snyder, *Fluence rate as a modulator of PDT mechanisms.* Lasers in Surgery and Medicine, 2006. **38**(5): p. 489-493.
10. Leunig, M., et al., *Angiogenesis, microvascular architecture, microhemodynamics, and interstitial fluid pressure during early growth of human adenocarcinoma LS174T in SCID mice.* Cancer Research, 1992. **52**(23): p. 6553-6560.
11. Dellian, M., et al., *Quantitation and physiological characterization of angiogenic vessels in mice: Effect of basic fibroblast growth factor, vascular endothelial growth factor/vascular permeability factor, and host microenvironment.* American Journal of Pathology, 1996. **149**(1): p. 59-71.
12. Krueger, T., et al., *Intraoperative photodynamic therapy of the chest cavity in malignant pleural mesothelioma bearing rats.* Lasers in Surgery and Medicine, 2005. **37**(4): p. 271-277.
13. Krueger, T., et al., *Antegrade Versus Retrograde Isolated Lung Perfusion: Doxorubicin Uptake and Distribution in a Sarcoma Model.* Annals of Thoracic Surgery, 2006. **82**(6): p. 2024-2030.
14. Yusa, T., *Treatment of malignant pleural mesothelioma.* Gan to kagaku ryoho. Cancer & chemotherapy, 2007. **34**(4): p. 520-526.
15. Scagliotti, G.V. and G. Selvaggi, *Emerging drugs for mesothelioma.* Expert Opinion on Emerging Drugs, 2007. **12**(1): p. 127-137.
16. Ismail-Khan, R., et al., *Malignant pleural mesothelioma: A comprehensive review.* Cancer Control, 2006. **13**(4): p. 255-263.
17. Omura, Y., *Asbestos as a possible major cause of malignant lung tumors (including small cell carcinoma, Adenocarcinoma & Mesothelioma), brain tumors (i.e. astrocytoma & glioblastoma multiforme), many other malignant tumors, intractable pain including fibromyalgia, & some cardio-vascular pathology: Safe & effective methods of reducing asbestos from normal & pathological areas.* Acupuncture and Electro-Therapeutics Research, 2006. **31**(1-2): p. 61-125.
18. Purse, K., *Asbestos: A global epidemic in need of a global solution.* Journal of Occupational Health and Safety - Australia and New Zealand, 2006. **22**(1): p. 21-26.

19. Furrer, M., et al., *Cytostatic lung perfusion by use of an endovascular blood flow occlusion technique.* Annals of Thoracic Surgery, 1998. **65**(6): p. 1523-1528.
20. Kummerle, A., et al., *A validated assay for measuring doxorubicin in biological fluids and tissues in an isolated lung perfusion model: matrix effect and heparin interference strongly influence doxorubicin measurements.* Journal of Pharmaceutical and Biomedical Analysis, 2003. **33**(3): p. 475-494.
21. Pan, Y., et al., *Evaluation of tumour vascularisation in two rat sarcoma models for studying isolated lung perfusion - Injection route determines the origin of tumour vessels.* European Surgical Research, 2005. **37**(2): p. 92-99.
22. Kruger, A. and L. Wojnowski, *The cardiotoxicity of anthracyclines - A persistent problem.* Kardiotoxizita?t von anthrazyklinen - Ein ungelo?stes problem, 2006. **103**(37): p. A2393-2397.
23. Kaiser, P.K., *Verteporfin photodynamic therapy and anti-angiogenic drugs: Potential for combination therapy in exudative age-related macular degeneration.* Current Medical Research and Opinion, 2007. **23**(3): p. 477-487.
24. Kaiser, P.K., *Verteporfin therapy in combination with triamcinolone: Published studies investigating a potential synergistic effect.* Current Medical Research and Opinion, 2005. **21**(5): p. 705-713

Acknowledgements

First of all I want to thank the members of the jury for the careful reading of this manuscript and for their indulgence for my English writing and for the possible errors that would have been forgotten in this manuscript.

A few years ago, when I found with excitement an advertisement for a PhD student position at the EPFL, explaining that the candidate will work on a multidisciplinary research I was very enthusiastic to work in collaboration with chemists, physicists, biologists, physicians, with heterogeneous scientific education and furthermore coming from many different countries and cultures. I was not yet awake to what this meant in terms of wealth, scientifically as well as humanly. During this thesis work, many people crossed my way and many people contributed directly or indirectly to this research project. I would like to thank them all and I do apologize to those who are not personally mentioned below.

I am very grateful to Prof. Hubert van den Bergh for giving me the opportunity to be a PhD student in his laboratory and to become my director of thesis for my last 3 years of work (especially as I was honoured to be officially the last PhD student of his career!). I appreciate his encouragements and enthusiastic constructive discussions about my work and the perspectives of combination therapies. I also want to thank him for the freedom and confidence he has given me in my research, and for having offered to me the opportunity to take part in several international congresses.

I also want to thank Norbert Lange, who engaged me for this job and who became my first director of thesis. However, unfortunately for me, he left the laboratory a couple of months later, for an interesting job (fortunately) for him in the University of Geneva. Coming from this pharmacy faculty of Geneva, Yvette Konan entered the EPFL and became my second director of thesis for a year, before going back to her native country. I want to thank her for her help in writing reports, for our long discussions, for her advices and her spontaneity leading to great scientific ideas. Moreover, I want to thank her for the motivation she used to "insufflate" to Bernadette and me during her stay in Lausanne and after by international phone calls.

When I think about Jean-Pierre Ballini I hesitate between beginning with "I want to apologize for…" or "I want to thank him for…". I could say both, followed by a long list of things that he did to help me over this thesis work. He preferred not to have the official responsibility of being my new director of thesis upon Yvette's departure, but he finally supported much more than a director of thesis is supposed to do to help a PhD student. He was an adviser for almost all crucial questions concerning the research project; he is the expert for any problem about microscopy and optics, which was indeed sometimes very helpful for a student with a biomedical background like me; he played also the role of "buffer" to take many responsibilities and to "calm down the game" in bad situations. The list can be continued indefinitely, but again "merci Jean-Pierre". I also want to apologize to Thomas Glanzmann for disturbing him many times when running into the office when I was looking for Jean-Pierre.

My collegue and friend Bernadette Pegaz, needs my attention for her help in any question about chemistry. Our complementarities were obviously a key point in the realisation of this work. I thank her as well for having supported the sometimes endless discussions about life, for having to hear my singing (I have a terrible voice and I use to sing stupid songs).

My other fellow PhD students and other colleagues also need my attention for their infinite helpfulness (and cakes): Tanja Gabrecht, Blaise Lovisa, Filippo Piffaretti, Patrycja Nowak-Sliwinska, Pascal Uehlinger, Jerome Barge and the PhDs from the other groups for sharing our impressions about our thesis: Todor, Simone, Pascal, Federico…
I also want to thank Georges Wagnières, leader of the Photomedicine group, for his advices concerning scientific physical basics and all the hidden administrative work of such a group.

A special appreciation goes to Véronique Bauler and Carine Vagnières who makes the LPAS group running smoothly and who manage the more than 35 collaborators of the LPAS with ease together with the apprentice Stefania Tartaglia, the youngest of the group and maybe the craziest.

Much of my research work was performed in the Thoracic Surgery department of the CHUV (University Hospital in Lausanne). My deep gratitude goes to Prof. Hans-Beat Ris, the head of the Thoracic Surgery department, whose commitment solidified the collaboration between the CHUV and the EPFL group. I am very grateful to him for the equipment and infrastructure that he placed at disposal for the studies in the mice model. I had (and I am still having) a real pleasure to work with the people taking part in this collaboration. They displayed much patience, availability, tolerance and flexibility with our experiments. More particularly Cai Cheng, called Neo for "unpronounceability reason", who took care among other numerous things of the microsurgical preparation of the mice, with an incredible availability and flexibility. I thank him also for our long conversations (about the book that we should write…) and for introducing me to Chinese culture (within discussions and via his friends welcoming me in China). I want to thank also his compatriot, Hua Yan who initiated the experiments with mice for the leakage assessments.

Particular gratitude is addressed to Thorsten Krueger who could always manage to be available despite of his overbooked weeks and weekends. His motivation, enthusiasm and optimism concerning the project were of great importance for the collaboration.
Special thanks to Stephan Schäfer, for the histology work, the analysis of the samples followed by his excellent instruction on histopathology of inflamed tissue, his participation to brainstorming and constructive suggestions and remarks and his legendary patience and helpfulness. The same thanks go to Prof. Hans-Anton Lehr for his participation to our group meetings and his good advices concerning the skinfold chamber model.
I won't forget to thank Hélène Mottaz who welcomed and helped us for cells culture in her "cellar" laboratory at the CHUV, for the lunch times shared and for her good mood.

The whole work would not have been possible without the excellent handcraft skills of Flavio Comino who used to build the numerous un-commercialised equipments of microscope meticulously adapted to our exigent experiments on animal models. The same thank to André Studinski for his electronics engineering.

I also have to apologize for leaving my friends and family in Belgium, more particularly my grand-parents who could not visit me in Switzerland. Although he could not accompany me until the end of my thesis, my grand-father who would have loved to have the opportunity to go to the university. He showed me that he was proud of me. Thanks for his support and his internet installation, even if he was 90 years old, to keep in touch easily, to support me by mail and to share scientific and personal ideas. This was very important for me when I decided to put kilometres between us.

I would like to thank my family and friends for their support and their care. My deepest gratitude goes to my mother and my father who always encouraged me to make my plans become a reality and taking care of my happiness all along my life.
All the friends from Belgium with whom I discussed for hours by phone sharing the good and bad moments. My best friends for more than 15 years Philippe Genty and Nathalie van Aefferden, my sister Marie and Patochon. A particular excuse is addressed to my goddaughter Thelma, illustrated in the introduction, for spending her first year of life without seeing her enough. Moreover, I want to thank all the people who visited me so often here in Lausanne and who shared barbecues by the lake, as well as the friends who were or are still in Lausanne, more particularly Carla, Mathieu and Manon, Ermanno, Rainer, Pierre, Christian, Alexandra and Mathieu, Alex, Manu, Dominique and the others…

I also have to mention the people who rendered my life more comfortable during these last few months of work: Monsieur Ducret who sold me his nice car, Madame Desgraz who rent us the most beautiful house of the canton, General Li who provided me boxes of Chunghwa, my “small pig” Raziel for staying by my side during the last days of writing, Arcadie restaurant for the delicious “croissant au jambon” so rapidly eaten during the last stress days. A special thought for Coca Cola who could be my official sponsor over these years during which I drank litres and litres of diet coke.

I also want to apologize and to thanks all the chicken embryos and mice who independent of their will gave their body to science.

I can’t finish without thanking the EPFL and the National Foundation without what the project would not exist and people from Novartis for their enthusiasm and support for the further steps of the combination therapy studies.

The very last words of this manuscript are addressed to Bernard Berger. He changed my life and daily makes my dreams come true. The expression of my gratitude toward him was an entire chapter of this thesis, but I have decided to keep it personal.

Curriculum vitae

Elodie Debefve

Address:
Route des Tavernes, 13
1610 Châtillens
Switzerland

Personal information:
Date of Birth: 2 February 1976
Marital status: Single
Nationality: Belgian

Contacts :
Office : +41 21 693 31 80
+41 21 693 61 18
Home : +41 21 625 41 02
Mobile : +41 76 405 36 66

e-mail : elodie.debefve@epfl.ch
elodiedebefve@hotmail.ch

Studies

2002- July 2007	**PhD** in the group of **Photomedicine** at the « Ecole Polytechnique Fédérale Lausanne » (**EPFL**), Switzerland.
October 2005- February 2006	**Managment** course « Venture Challenge » organised by the EPFL by **Venturelab**.
1997-2001	**Four year degree in Biomedical Sciences,** options: 1) Nutrition 2) Biomedical Research + supplementary course: « Help to the developping countries » Diploma obtained with the mention "Grande Distinction" Medicine Faculty, **University of Liège, Belgium.**
1994-1997	**Tree year degree in Medical Sciences (3 years),** Medicine Faculty, **Université de Liège, Belgique.**
1988-1994	**High school** options "Latin, languages, mathematics", Institut Saint-Michel in **Verviers, Belgium**.

Work Experiences

Since March 2002	**Scientific Assistant and PhD student** in the group of **Photomedicine** at the « Ecole Polytechnique Fédérale Lausanne » (**EPFL**), Switzerland. Subject: "Characterizaition and Therapeutic Exploitation of the Vascular Leakage Induced by Photodynamic Therapy .» • In the framework of my thesis, I have been doing some pre-clinical assessments on the chorioallantoic membrane of chicken embryos (CAM). • In collaboration between EPFL, CHUV and Pathology Institute of UNIL, I'm doing some pre-clinical experiments on the skinfold chamber of nude mice. • In parallel with my thesis work, I have been working for different pharmaceutical industries in the evaluation of the pghotodynamic effect of new drugs. The results of these experiments were published (see list of publications).
June 2004	**Extrernal Expert** to the practical examination of the biology CFC at I**SREC, Lausanne.**
November 2000-August 2001	**Diploma work trainee** ending the Biomedical Sciences Diploma at the **Nestlé Research Centre,** Vers-chez-les-Blanc. Subjet: "Influence of natural plant extracts on the initiation of cancer and inflammation. M odulation of xenobiotics metabolizing enzymes." The results of these experiments were published (see list of publications).
1998-1999	**Student work** (nights and weekends) as **radiology technician** in the Emergency Room of the CHU of Liège, Belgium.

Languages	French (mother tongue) English (fluent written and spoken)
Computer Skills	Word, Excel, Access, Powerpoint, Outlook, Analysis, HiPic, Kaleidagraph, ImageJ, Capimage, Inkscape
Leisure Interests	Cello (since 1988; I took part in 4 different orchestra in Belgium), reading, Photo courses, travelling and discovering other cultures, scuba diving (PADI open water), hiking, snowboarding

Conferences

- Ocular Angiogenesis.
  Cambridge, MA, USA. February 2004.
- Controlled Release Society 32nd Annual Meeting & Exposition.
  Miami Beach, Floride, USA. June 2005.
- 6th International Symposium on Photodynamic Diagnosis and Therapy in Clinical Practice, Bressanone, Italie, October 2006
- 11th World Congress of the International Photodynamic Association,
  Shanghai, China, March 2007.

Publications

- Debefve E., Krueger T., Cheng C., Schäfer S.C., Yan H., Ballini J.-P., van den Bergh H., Lehr H.-A., Ris H.-B. Experimental Visudyne®-Mediated Photodynamic Therapy Affords Selective Drug Delivery: an Intravital Microscopy Study in Nude Mice. To be submitted to Microcirculation.
- Debefve E., Pegaz B., Ballini J-P and van den Bergh H. Leakage Induced by Combination of Photodynamic Therapy and Different Doses of Aspirin: Local Drug Delivery Observed in Arteries versus Veins. Submitted in Vascular Pharmacology.
- Debefve, E., Pegaz, B., Ballini, J.-P., Konan, Y.N. and van den Bergh, H. Combination therapy using aspirin-enhanced photodynamic selective drug delivery. Vascular Pharmacology (2007), 46 (3) : 171-180.
- Pegaz, B., Debefve, E., Ballini, J.-P., Konan-Kouakou, Y.N., van den Bergh, H. Effect of nanoparticle size on the extravasation and the photothrombic activity of meso(p-tetracarboxyphenyl)porphyrin. Journal of Photochemistry and Photobiology B: Biology (2006), 85 (3), 216-222C.
- Pegaz, B., Debefve, E., Borle, F., Ballini, J-P., Wagnières, G., Spaniol, S., Albrecht, V, Scheglmann, D., Nifantiev, N.E*, van den Bergh, H. and Konan, Y.N Photothrombic activity of m-THPC-loaded liposomal formulations: preclinicalassessment on chick chorioallantoic membrane model. Submitted in European Journal of Pharmaceutical Sciences.
- Pegaz, B., Debefve, E., Borle, F., Ballini, J-P., Wagnières, G., Spaniol, S., Albrecht, V, Scheglmann, D., Nifantiev, N.E*, van den Bergh, H. and Konan, Y.N. Pre-clinical evaluation of a novel water-soluble chlorin e_6 derivative (BLC 1010) as photosensitizer for the closure of the neovessels associated with age-related macular degeneration. Accepted for publication in the journal of Photochemistry and photobiology.
- B. Pegaz, E. Debefve, F. Borle, J.-P. Ballini, H. van den Bergh, Y.N. Kouakou-Konan. Encapsulation of porphyrins and chlorins in biodegradable nanoparticles: The effect of dye lipophilicity on the extravasation and the photothrombic activity. A comparative study. Journal of Photochemistry and Photobiology B: Biology (2005), 80 (1): 19-27.
- Cavin, M. Delannoy, A. Malnoe, E. Debefve, A. Touché, D. Courtois, B. Schilter. Inhibition of the expression and activity of cyclooxygenase-2 by chicory extract. Biochemical and Biophysical Research Communications (2005), 327 (3): 742-749.
- Angelica Vargas, Bernadette Pegaz, Elodie Debefve, Yvette Konan-Kouakou, Norbert Lange, Jean-Pierre Ballini, Hubert van den Bergh, Robert Gurny and Florence Delie. Improved photodynamic